



SRM MADURAI

COLLEGE FOR ENGINEERING AND TECHNOLOGY

(Approved by AICTE, New Delhi | Affiliated to Anna University, Chennai)

Pottapalayam, Sivagangai District - 630 612



INTERNATIONAL CONFERENCE

**ENGINEERING HORIZONS:
INNOVATION, ADVANCEMENTS, AND SUSTAINABILITY
(ICON: EHIAS'25)**

**ENGINEERING SOLUTIONS FOR
ENVIRONMENTAL SUSTAINABILITY**

GUEST EDITORS

Dr. S. Durairaj
Organizing Chairman

Dr. S. Sambath
Organizing Secretary



SRM MADURAI
COLLEGE FOR ENGINEERING AND TECHNOLOGY
Approved by AICTE, New Delhi | Affiliated to Anna University, Chennai



INTERNATIONAL CONFERENCE

Engineering Horizons: Innovation, Advancements, and Sustainability
(ICON: EHIAS'25)

Engineering Solutions for Environmental Sustainability

COPYRIGHT PAGE

Title of the Book: Engineering Solutions for Environmental Sustainability

© 2025 SRM Madurai College for Engineering and Technology.

All rights reserved.

GUEST EDITORS

Dr. S. Durairaj, Organizing Chairman

Dr. S. Sambath, Organizing Secretary

This book presents contributions from ICON: EHIAS'25 addressing sustainability in engineering. Unauthorized reproduction, translation, or digital sharing is strictly prohibited. ISBN cataloging is managed by Aarambh Quill Publications. Each chapter is the intellectual property of the contributing author(s) and has passed a thorough peer-review process in accordance with international publishing standards.

ISBN: 978-81-984820-4-4

Published in May, 2025

Publisher: Aarambh Quill Publications (www.aarambhquill.in)

In association with SRM Madurai College for Engineering and Technology

Disclaimer:

The views expressed in the chapters of this volume are those of the respective authors. The editors, organizers, and publisher bear no responsibility for the accuracy or legality of the content.

PREFACE

As the world grapples with unprecedented environmental challenges—ranging from climate change to resource depletion—engineering has a critical role to play in driving sustainable and resilient solutions. The book *Engineering Solutions for Environmental Sustainability* is a timely compilation of selected papers presented at the **ICON: EHIAS'25 – International Conference on Engineering Horizons: Innovation, Advancements, and Sustainability**, hosted by **SRM Madurai College for Engineering and Technology**.

This volume encompasses a wide array of research that addresses ecological and technological integration, green manufacturing practices, sustainable infrastructure, waste management systems, water and air purification technologies, and the development of eco-friendly materials. We express sincere gratitude to the contributing authors for their cutting-edge insights, to the reviewers for their expert evaluations, and to **Aarambh Quill Publications** for their invaluable support in publishing this work. We also thank the dedicated organizing team of ICON: EHIAS'25 for making this academic platform a success.

TABLE OF CONTENTS

Paper ID	Paper Title	Page No.
ICON-012	Utilizing Lead Waste and Rice Husk Ash in Concrete: Insights from Experimental Study on Compressive Strength	1
ICON-024	Performance Evaluation of Fly Ash-Based SIFCON Reinforced with Hooked-End Steel Fibers for Sustainable High-Strength Applications	7
ICON-049	Harvesting Systems for IoT – Enabled Sustainable Applications	20
ICON-179	Experimental Investigation of Tribological Properties of Bio-Based, Nano-Particles	28
ICON-193	Glycerol Plasticized Corn Starch Bioplastic for Food Packaging Application	32
ICON-204	Landfill Leachate Treatment Using a Method of Coagulation for Enhanced Environmental Safety	51
ICON-209	Analysis of Material SA106 Pipe after Post Weld Heat Treatment	65
ICON-210	Anti-Microbial Coating for HEPA Filter Using Copper Particles	72
ICON-235	Fabrication and Testing of Composite Material Made Up of Prawn Shell Powder	80
ICON-236	Experimental Investigation of Mechanical Properties of Ramie, Areca and Jute Fiber Reinforced Composites	92
ICON-272	AI Based Plant Disease Detection Using Live Mobile Camera	98
ICON-285	Smart Mess Management System: An Innovative Solution to Reduce Food Waste in Hostels	108
ICON-298	Development and Evaluation of Sustainable Rice Husk/Glass Fiber Composites for Industrial Applications	115
ICON-300	Enhancing Mechanical Performance of Bagasse Composites with Glass Fiber Reinforcement and Alkali Treatment	119

Utilizing Lead Waste and Rice Husk Ash in Concrete: Insights from Experimental Study on Compressive Strength

Hariperumal N¹, S. Varadharajan², Purushotham G Sarvade³

^{1,2,3}Department of Civil Engineering, Manipal Institute of Technology, Manipal Academy of Higher Education, Manipal, Udupi, Karnataka, India.

Abstract: The incorporation of agricultural and industrial wastages (AIW) like Rice Husk Ash (RHA) and 99.99 % pure Lead waste (LW) [RHALW] in concrete as a partial replacement for traditional materials such as cement of about 15% with that of RHA and initially fine aggregate has been substituted with LW extracted from the electronic waste (EW) has garnered attention as a potential sustainable solution to address both environmental and construction challenges (CC). This study explores the influence of RHALW on the mechanical properties, durability, and environmental footprint of concrete. RHALW, processed to meet particle size and chemical reactivity standards, was integrated at varying proportions to replace cement and fine aggregate (FA). Comprehensive experimental evaluations were conducted to determine the compressive strength (CsT). The results reveal that incorporating RHALW in controlled proportions up to 10 % enhances the (CsT) of concrete by up to 12.45% compared to conventional mixes, attributable to improved particle packing and pozzolanic activity. However, exceeding optimal replacement levels led to strength reduction due to improper bonding and potential leaching risks. This research highlights the dual benefits of utilizing RHALW in concrete—reducing environmental pollution (EP) and conserving natural resources—while addressing critical challenges related to safety and long-term performance. The findings provide actionable insights for integrating RHALW in sustainable construction practices, offering a pathway for advancing circular economy (CE) principles in the construction industry. Future studies are recommended to optimize mix proportions and assess long-term field performance.

Keywords: Rice Husk Ash and Lead Waste, Electronic waste, Environmental Pollution, Compressive Strength, Construction Challenge, Circular Economy

I. INTRODUCTION

AIW are broadly classified into different categories in which most of them are reutilized to form a useful product. Anyhow, the major challenges are facing by the EW industry in which 6R (Reduce, Recycle, Reuse, Reclamations, Reutilization, Recovery) strategy plays a major role as shown in fig.1 6 R. In India, the world largest populated and one of the majorly polluted countries in the world produce the second largest producer of rice. EW, producers are enormously increased in India and the 6R utilizations are yet to be adoption in most of EW industries. This research article plays a vital role to use both AIW and EW as one of the key ingredients in the concrete which is widely

construction materials next to that of water.



Fig. 1 6R

II. LITERATURE REVIEW

The review regards to the AIW especially preciously to LWRHA combination are limited, still it is a newly approach to the construction industry. The challenges are faced while casting the concrete as well as the preliminary investigated tests such as specific gravity (SG), initial and final setting of cement (IFSC) combination with the RHALW require personal protective equipment (PPE) to safeguard the workers. This novel approach requires the mankind pharm to safeguard with unique materials, the heavy metals such as Lead can be easily penetrated into the human body at any use case of time.

The effective methodological process involved in this rework as explain below with a simple flowchart:

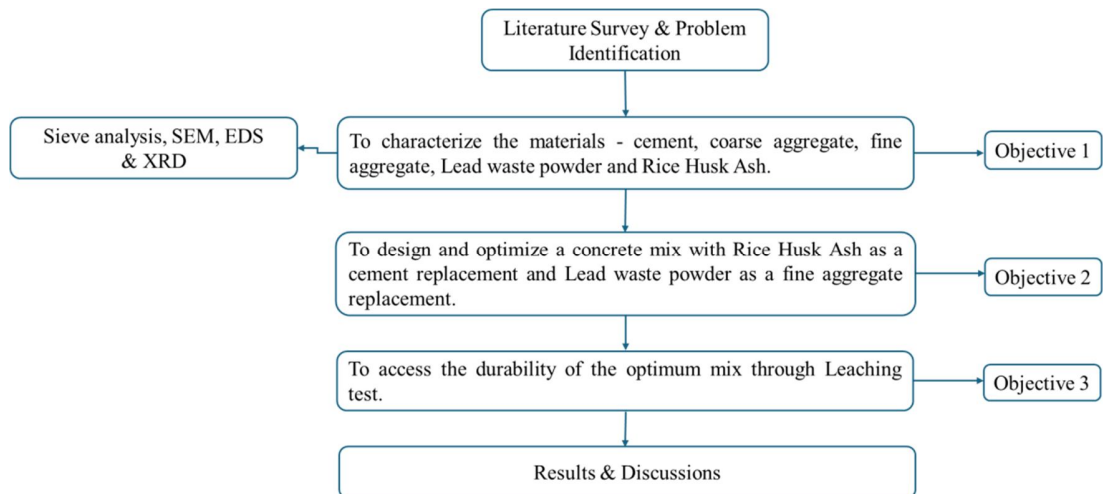


Fig. 2 Methodology



Fig. 3 Test Performed for the properties of concrete ingredients



Fig. 4 Concreting Process

III. RESULTS AND DISCUSSION

A. Properties of concrete ingredients and Quantity Calculated for the M40 Grade

The properties of cement and concrete quantities for the various mixes are shown in Table 1 & 2 and the pictures describing characterization study and concreting process has been elucidated in Figure 3 & 4.

Table 1: Tests performed for the properties of cement

S. No.	Properties of cement	Values	As per IS 8112:2013 code
1.	SG	3.1	3.1 to 3.2
2.	Fineness of cement Dry Sieving	1 gm	Not more than 10%
3.	Specific surface – Blaine's Air Permeability Test	3,343.3 cm ² /gm	Not less than 2250 cm ² /gm
4.	Soundness – Le Chatelier Method	10mm	≤ 10 mm
5.	Initial Setting Time	45 minutes	≥ 30 minutes
6.	Final Setting Time	256 minutes	≤ 600 minutes (10 hours)

Table 2 : Concrete quantities for the various mixes

S. No.	Concrete Ingredients	M1 (Normal Concrete)	M2 (15% RHA as Cement)	M3 (15% RHA & 10% LW)
1.	Cement in kg/m ³	400	340	340
2.	FA in kg/m ³	749	636.65	524.30
3.	CA in kg/m ³	1135	1135	1135
4.	Water in liters	0.16	0.16	0.16
5.	RHA in kg/m ³	-	60	60
6.	LDP in kg/m ³	-	-	112.35

B. Cst results for the various mixes

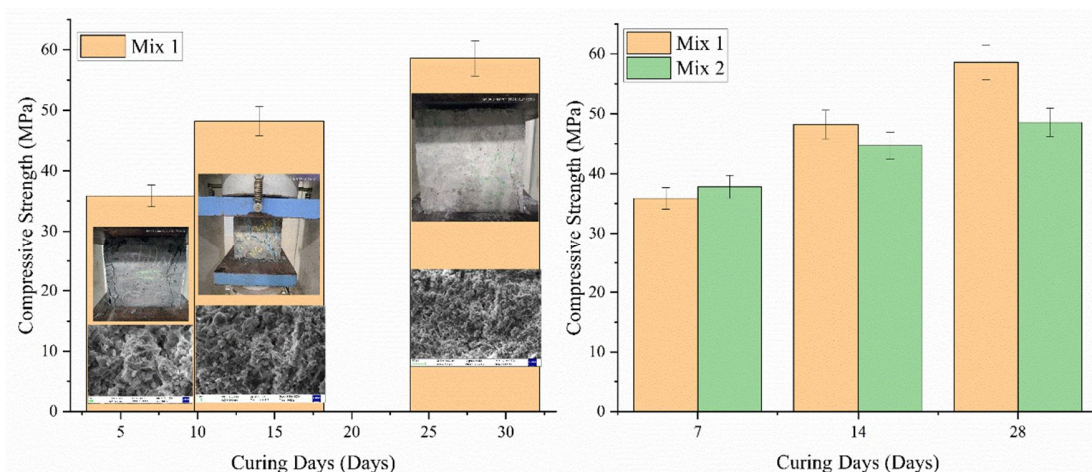


Fig. 5 Cst test results for the mix M1 & M2

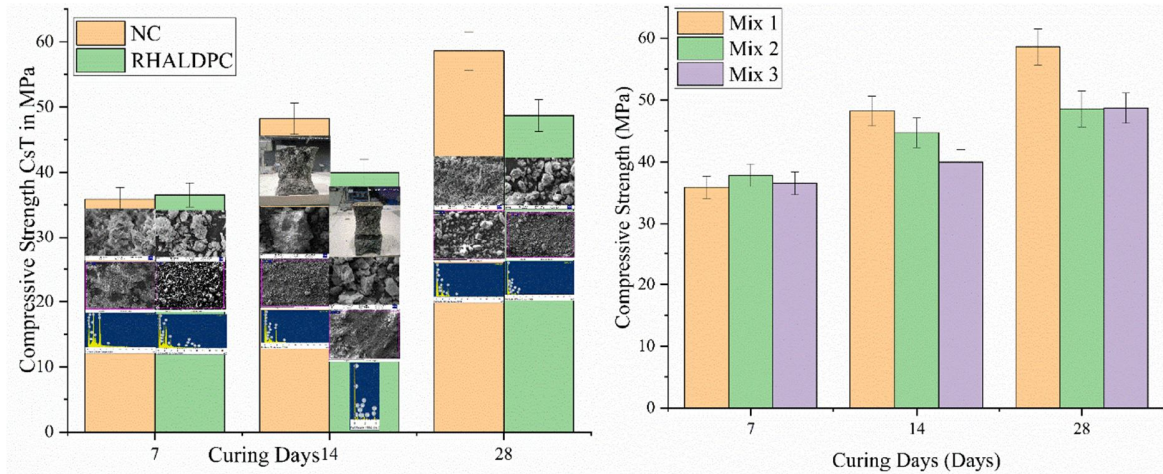


Fig. 6 Cst test results for the mix M3 & all the mixes M1M2M3

The CsT comparison among M1 CC, M2 (cement replaced with 15% RHA), and M3 (cement replaced with 15% RHA and FA replaced with 10% of LW) reveals nuanced insights into the effect of these supplementary materials on mechanical performance. At 7 days, M1 shows the highest CsT (~36 MPa), closely followed by M2 and M3, both exhibiting slightly lower values (~34 MPa). This marginal reduction is attributed to the delayed pozzolanic activity of RHA and the inert nature of LW at early curing stages, which initially contributes to reduced early-age hydration kinetics compared to the fully cement-based matrix in M1. However, the inclusion of RHA in M2 begins to compensate for early weaknesses through filler effects, improving particle packing, while LW in M3 introduces microstructural refinement in the interfacial transition zone (ITZ), albeit with slightly slower hydration acceleration than M2.

By 28 days, M2 (~48 MPa) achieves a CsT comparable to M1 (~52 MPa), demonstrating the effectiveness of RHA in densifying the microstructure through secondary calcium silicate hydrate (C-S-H) formation, which enhances strength and reduces porosity. M3 (~47 MPa), while slightly lower than M2, benefits from the synergistic effects of RHA's pozzolanic reactivity and LW's role in improving durability and reducing permeability. The comparable long-term performance of M3 suggests that the partial replacement of FA with LW not only supports sustainability by valorizing industrial byproducts but also maintains mechanical integrity by refining the ITZ and improving aggregate-matrix bonding. These findings highlight the potential of RHA and LW to replace traditional materials in concrete, offering a sustainable alternative that ensures both strength and durability for modern construction applications. Further optimization could enhance the early-age performance, bridging the gap with CC.

IV.CONCLUSION

The circular economy, construction industries, environmental pollution through e-waste are increasing now-a-days to a vast account it must has to be limited under the mass concreting process without causing any damages to

the living things. The output is drastically playing a pivotal role in all the key areas of the construction industry, still durability and other test are yet to be added as a future scope under this title which has been extended to a large extent of the research. The experimental study on incorporating RHALW in concrete has yielded promising results, demonstrating the potential of these materials to enhance Cst to 12.45% while promoting sustainability. The findings suggest that with proper mix proportions, RHALW can be effectively utilized as supplementary cementitious materials, contributing to the development of eco-friendly and high-performance concrete.

Beyond strength improvements, this approach aligns with global efforts toward waste reduction and resource optimization, offering a viable solution for sustainable construction. Future research and large-scale applications could further refine the material properties, paving the way for innovative and environmentally responsible building practices. With continued advancements, the integration of industrial by-products in concrete could play a pivotal role in reducing carbon footprints and fostering a greener construction industry.

V. REFERENCES

- [1] Varadharajan, S. and Bishetti, P., 2024. Determination of mechanical properties and environmental impact assessment of concrete containing industrial wastes. *Journal of Structural Engineering*, 50(6), pp.402-416.
- [2] Rather, H.M. and Hasan, M., 2024. A Review on Sustainable Utilisation of Zinc Mine Tailing in Concrete Production. In E3S Web of Conferences (Vol. 596, p. 01029). EDP Sciences. <https://doi.org/10.1051/e3sconf/202459601029>
- [3] Liu, W., Wan, Y., Lei, F., Liu, X., Wang, S., Zhao, Z., Li, H. and Wang, H., 2024. Innovation and performance of lead smelting slag-based multi-solid waste pavement concrete materials: Ratio design, mechanical properties, hydration products, heavy metal leaching. *Construction and Building Materials*, 411, p.134824. <https://doi.org/10.1016/j.conbuildmat.2023.134824>
- [4] Adiguzel, D., Tuylu, S. and Eker, H., 2022. Utilization of tailings in concrete products: A review. *Construction and Building Materials*, 360, p.129574. <https://doi.org/10.1016/j.conbuildmat.2022.129574>
- [5] Agrawal, Y., Gupta, T. and Chaudhary, S., 2022. Effect of mechanically treated and untreated zinc tailing waste as cement substitute in concrete production: an experimental and statistical analysis. *Environmental Science and Pollution Research*, pp.1-26. <https://doi.org/10.1007/s11356-021-17845-0>
- [6] Yang, Y.P., Deng, Y.G. and Chen, L.S., 2025. Properties of high-volume rice husk ash UHPC with various fineness. *Construction and Building Materials*, 458, p.139614. <https://doi.org/10.1016/j.conbuildmat.2024.139614>
- [7] Bashir, A., Jibril, M.M., Jibrin, U.M., Abba, S.I. and Malami, S.I., 2025. A new strategy using intelligent hybrid learning for prediction of water binder ratio of concrete with rice husk ash as a supplementary cementitious material. *Journal of Building Pathology and Rehabilitation*, 10(1), pp.1-17.
- [8] 17. <https://doi.org/10.1007/s41024-024-00541-0>
- [9] Su, Y., Tsang, D., Zhu, X., Qu, F. and Chen, L., 2025. High-volume rice husk ash blended cement. In *High-Volume Mineral Admixtures in Cementitious Binders* (pp. 389-418). Woodhead Publishing. <https://doi.org/10.1016/B978-0-443-13498-2.00003-1>
- [10] Xia, Y., Shi, D., Zhao, Y., Wang, J., Ma, X., Yu, K., Li, H., Wang, L. and Yan, J., 2025. Designing low-carbon ultra-high-performance concrete with co-combustion ash of sewage sludge and rice husk. *Materials and Structures*, 58(1), pp.1-17. <https://doi.org/10.1617/s11527-024-02535-3>
- [11] Xia, Y., Liu, M., Zhao, Y., Guo, J., Chi, X., Du, J. and Du, D., 2023. Sewage sludge and rice husk co-combustion ash: combustion behavior and cementitious property. *Journal of Building Engineering*, 71, p.106497. <https://doi.org/10.1016/j.jobe.2023.106497>

Performance Evaluation of Fly Ash-Based SIFCON Reinforced with Hooked-End Steel Fibers for Sustainable High-Strength Applications

¹N.Susmitha, ²Karthikeyan Muniraj, ³Dasari Sai Vishnu Babu, ⁴Shaik Mustafa, ⁵Molla Baji

^{1,2,3,4,5}Department of Civil Engineering, Vignam University, Andhra Pradesh, India.

Corresponding Author: vfstr.scholar@gmail.com

Abstract: Slurry Infiltrated Fibrous Concrete (SIFCON) is an advanced cementitious composite known for its superior ductility, impact resistance, and high strength. The influence of fiber content, fly ash replacement ratio, and matrix composition are analyzed. The unique material finds application in construction projects where endurance under adverse circumstances and magnificent mechanical qualities are essential. Because of its exceptional durability and resilience to impact and fatigue, this study investigates the flexural performance of fly ash-based SIFCON with hooked-end steel fibers in varying percentages (1%, 3%, 5%, 7%, & 9%). By using fly ash in place of some of the cement and adapting the fiber composition for better structural performance, the research seeks to improve sustainability. Simply supported beams are subjected to three-point bending tests to evaluate parameters such as load-carrying capacity, deflection characteristics, crack propagation, and energy absorption. The results indicate that increasing steel fiber content enhances flexural strength and toughness, with the optimum performance observed at 8% fiber volume. However, beyond this percentage, workability issues and fiber clustering negatively impact uniform stress distribution. The study concludes that fly ash-based SIFCON with optimized fiber reinforcement is a promising solution for sustainable and high-strength structural applications, particularly in flexural members.

Keywords: Compression Strength Test & Split Tensile Strength Test.

I. INTRODUCTION

In SIFCON mixtures, cement acts as the primary binder, providing structural integrity and strength development. The hydration reaction produces calcium silicate hydrate (C-S-H) gel, which governs both initial setting characteristics and ultimate load-bearing capacity. This study employs Ordinary Portland Cement (OPC) due to its reliable compatibility with supplementary materials and consistent performance in fiber-reinforced systems.

C type fly ash as a sustainable cement replacement (10%, 20%, 30% by weight), offering multiple technical benefits. This pozzolanic additive improves fresh concrete workability while reducing thermal cracking potential through slower heat release. Chemically, fly ash reacts with hydration byproducts to generate additional C-S-H, enhancing later-age strength and densifying the microstructure. The substitution simultaneously decreases the carbon footprint while improving resistance to sulfate attack and alkali-silica reaction, particularly valuable in demanding structural applications.[1].

Hooked-end steel fibers are incorporated in varying proportions (1%, 3%, 5%, 7%, 9%) to increase tensile strength, ductility, and crack resistance in Sifcon. The hooked ends ensure better anchorage within the matrix, reducing the risk of fiber pull-out and enhancing load-bearing capacity. These fibers effectively control crack propagation, distribute stress, and improve energy absorption, making the composite ideal for demanding structural applications.



Fig. 1 Hooked End Steel

Superplasticizers, especially polycarboxylate ether (PCE) types, are essential in modern concrete for enhancing workability, strength, and durability. They reduce water content by dispersing cement particles through steric hindrance and electrostatic repulsion. PCEs are widely used in self-compacting, high-strength, and ready-mix concrete due to their excellent slump retention and compatibility with various types of cement. Their development supports sustainable construction by reducing cement usage and improving concrete performance. Understanding their molecular design and interaction mechanisms is key to optimizing their application in diverse construction scenarios.



Fig. 2 Polycarboxylate Ether (PCE)

II. LITERATURE REVIEW

The effects of silica fume and high-volume Class C fly ash on self-compacting concrete are looked at in the study by Halit Yazıcı. Class C fly ash improves workability and reduces chloride penetration, while silica fume increases compressive strength. When combined, they increase SCC's durability to freeze-thaw. The study emphasizes how these components could be used to create high-performance, sustainable concrete [1].

This study examines how varying steel fiber content (4-10% by volume) influences the mechanical performance of slurry-infiltrated fiber concrete (SIFCON). Experimental investigations evaluated the composite's toughness, flexural strength, and compressive strength characteristics. Results demonstrate significant enhancement in all

mechanical properties with increasing fiber content, showing optimal performance at higher incorporation rates 8-10%. The research underscores the critical role of fiber dosage in tailoring Sifcon's structural response, making it particularly suitable for demanding engineering applications requiring exceptional strength and durability.[2]

The study by Halit Yazıcı's research team developed an advanced Sifcon formulation by combining strategic fiber alignment with substantial mineral admixture incorporation. Their innovative approach replaced 40-60% of cement content with fly ash, achieving triple benefits: enhanced fresh concrete properties, superior hardened state performance, and reduced ecological footprint. The study revealed that controlled fiber orientation significantly boosts load-bearing capacity, particularly in tension and bending, while the high-volume fly ash addition improved both immediate workability and extended service life. These synergistic modifications produced a composite material exhibiting exceptional structural characteristics suitable for demanding construction scenarios. The findings demonstrate how optimized material engineering can simultaneously address performance requirements and sustainability goals in modern concrete technology.[3]

The paper "Study on Strength Properties of SIFCON" by Vijayakumar and Dinesh Kumar's research paper analyzes the mechanical performance of Sifcon, particularly its enhanced compressive, tensile, and flexural capacities. Their findings reveal that Sifcon superior strength characteristics stem from its unique composition - a high-density matrix combined with elevated fiber content. The investigation establishes clear correlations between fiber dosage, matrix formulation, and resultant mechanical properties, positioning Sifcon as an ideal material for specialized applications like blast-resistant facades and earthquake-proof constructions. The study provides crucial guidelines for engineering Sifcon mixtures to achieve optimal structural performance.[4]

The study by Zhang and colleagues developed an innovative High-Performance Fiber-Reinforced concrete (HPFRC) system incorporating 1.5-2% deformed steel fibers and substantial fly ash replacement (20-40%). Their research demonstrates how the combined use of supplementary cementitious materials with optimized fiber content creates synergistic effects, simultaneously improving fresh concrete properties and hardened state characteristics. This advanced composite shows exceptional flow characteristics during placement while developing superior crack resistance and load-bearing capacity, offering both sustainability benefits through reduced cement use and enhanced durability for demanding infrastructure applications.[5]

This investigation examines performance-enhanced SIFCON through strategic fiber distribution and supplementary cementitious materials. The formulation incorporated 6-8% deformed steel fibers, demonstrating significant improvements in both tension and bending resistance. Simultaneous cement replacement with 40-60% fly ash enhanced fresh mix characteristics while reducing environmental impact. The synergistic combination of controlled fiber alignment and pozzolanic additives yielded a composite material with exceptional mechanical performance and service life extension, particularly suitable for critical infrastructure applications requiring robust structural integrity.[3]

The experimental study evaluated M30 concrete modification using both fiber reinforcement and industrial byproducts. Incorporating 0.5-1.5% hooked-end steel fibers substantially increased crack resistance and load-bearing capacity. When combined with 10-30% fly ash substitution, the modified concrete achieved optimal workability alongside improved sustainability metrics. This dual-modification approach produced an economical, eco-conscious

construction material that maintains structural-grade performance while addressing environmental concerns in concrete production.[6]

The paper "A Review Investigation on Slurry Infiltrated Fibre Concrete by Using Crimped Fibre" by Sudhanshu Kumar and Anil Rajpoot comprehensive review examines SIFCON formulations incorporating crimped steel fibers at 6-10% volume fractions, demonstrating substantial improvements in mechanical properties including a 40-60% increase in tensile capacity compared to conventional FRC. While focusing on fiber geometry effects, the analysis also identifies synergistic benefits when combining fibers with 20-40% fly ash replacement, particularly for enhancing placement characteristics and chemical resistance. The authors position crimped-fiber Sifcon as particularly effective for protective structures subject to dynamic loading conditions.[7]

The study by D. Elavarasi and Dr. K. Saravana Raja Mohan experimental work developed an eco-conscious Sifcon variant using 30-50% fly ash binder replacement alongside 6-8% deformed steel fibers. Their results showed a unique dual benefit: the fly ash improved long-term durability in corrosive environments while the optimized fiber content provided exceptional crack-bridging capacity. This formulation achieved impact resistance metrics 3-5 times higher than standard concrete while reducing the carbon footprint by approximately 35%. [8]

In their investigation of Slurry Infiltrated Fibrous Concrete, Jerry and Fawzi explored how different fiber types influence impact resistance, testing steel fibers (6-10%), polypropylene fibers (0.5-1.5%), and glass fibers (0.5-1.5%). The results demonstrated that steel fibers markedly enhanced impact resistance, tensile strength, and toughness, while polypropylene and glass fibers improved crack control and ductility. By incorporating fly ash as a partial cement replacement (20-40%), the study achieved improved workability and sustainability without compromising performance, ultimately producing a high-performance SIFCON suitable for demanding applications requiring exceptional durability and impact resistance.[9]

The paper "*Autoclaved SIFCON with High Volume Class C Fly Ash Binder Phase*" by Halit Yazıcı et alformulation incorporating 50-70% Class C fly ash as cement replacement, significantly enhancing both environmental sustainability and material performance. The high-volume fly ash content, activated through autoclave curing, improved the binder phase characteristics, resulting in superior mechanical properties and long-term durability. This advanced processing technique demonstrates how industrial byproducts can be effectively utilized to produce eco-conscious concrete without compromising structural integrity, offering a viable high-performance solution for sustainable construction applications that maintains excellent durability while substantially reducing cement consumption.[10]

Recent investigations by Hung et al. (2023) reveal that incorporating hooked-end steel macro-fibers in UHPC significantly enhances its mechanical performance, particularly in toughness and crack control. Parallel studies on fly ash-based SIFCON demonstrate comparable benefits, where these specialized fibers boost tensile capacity while maintaining environmental sustainability. A key finding across both research streams is the critical influence of fiber shape and uniform dispersion on composite effectiveness. While achieving optimal workability-fiber content balance presents ongoing challenges, these studies collectively advance high-performance concrete technology. Their results underscore the potential of tailored fiber reinforcement in developing next-generation construction materials for demanding infrastructure applications. Future work should focus on optimizing hybrid material systems for improved

structural efficiency.[11]

Recent research by Cao and Yu examined how fiber orientation affects the performance of hooked-end steel fibers in UHPC, revealing that angled fibers provide greater pullout resistance through improved mechanical anchoring. These findings correlate with studies on fly ash-based SIFCON, where similar fiber geometries enhance structural toughness and damage tolerance. The studies collectively demonstrate that fiber alignment and end-hook design critically influence composite behavior after cracking. UHPC achieves strength through its compact matrix, while SIFCON excels in energy absorption via concentrated fiber reinforcement, with fly ash reducing environmental impact. Such discoveries advance the engineering of durable, sustainable construction materials for extreme loading conditions. Future developments may integrate these technologies to optimize both strength and resilience.[12]

Recent studies highlight the crucial role of hooked-end steel fibers in enhancing the mechanical properties of cementitious composites. Khabaz's research demonstrates that the hooked-end geometry significantly improves fiber-matrix bond strength and energy absorption during pullout. Similar findings are observed in fly ash-based Sifcon, where these fibers enhance toughness and crack resistance in high-performance applications. Both studies emphasize that fiber anchorage mechanics are vital for optimizing structural performance under stress. The use of fly ash in Sifcon also shows how sustainable materials can maintain strength while improving durability. These insights collectively advance the development of resilient, high-strength construction materials for demanding engineering applications.[13]

III. Material Properties

A. Cement

The setting time, usual consistency, fineness, specific gravity, and chemical makeup of the blended slurry are all greatly impacted when fly ash is employed in place of some of the cement. Fly ash's pozzolanic properties, finer particle size, and lower calcium concentration than regular Portland cement (OPC) are the causes of these alterations. A thorough description of these consequences is provided below, backed up by the pertinent IS codes (Indian Standards).

i. Setting Time (IS 4031-1988)

Higher fly ash replacement levels result in longer cement initial and final setting periods. Fly ash relies on calcium hydroxide ($\text{Ca}(\text{OH})_2$) from cement hydration to start pozzolanic reactions, which is why it takes so long to react with water. OPC (zero fly ash): It takes 30 to 45 minutes to set initially, and 6 to 10 hours for it to set completely.

- 10% Fly Ash: It takes 60 minutes to set initially and 7 hours to set completely.
- 20% Fly Ash: Final setting takes 8 hours, with additional delays of 60 minutes.
- 30% Fly Ash: It may take 85 minutes to set initially and 9 hours to set completely.

(Source: Portland Pozzolana Cement's IS 1489-1991, which allows for the blending of fly ash.)

ii. Normal Consistency (IS 4031-1988)

According to IS 4031-1988, normal consistency

Because of its spherical particle form, which enhances particle packing and lubrication, fly ash lowers water

demand. Normal consistency, or the amount of water needed to make a typical paste, can, however, differ slightly:

- OPC (0% Fly Ash): Usually 26–33% water by cement weight.
- 10% Fly Ash: Because it is more workable, it drops to 27%.
- 20% Fly Ash: Drops even more to 28%.
- 30% Fly Ash: 29% water may be needed.

(IS 3812-2013 states that fly ash shouldn't considerably raise water demand.)

iii. Fineness of cement (IS 4031-1988, IS 1727-1967)

Because fly ash is finer than cement, the blended mixture's total fineness as determined by Blaine's air permeability test (m^2/kg) is increased:

0% (OPC) Fly Ash: $300\text{--}400 \text{ m}^2/\text{kg}$.

10–30% In hardened concrete, fly ash increases to $410 \text{ m}^2/\text{kg}$, improving reactivity and decreasing permeability. Finer particles enhance particle packing, but if improperly managed, they may need more water for dispersion.

iv. Specific Gravity (IS 3812-2013, IS 4031-1988)

Because fly ash has a lower specific gravity (2.8) than OPC (3.15), the density of the mixed cement drops as replacement levels increases.

v. Chemical Make-Up (IS 3812-2013 for Fly Ash, IS 12269-2013 for OPC)

By decreasing calcium oxide (CaO) and raising silica (SiO_2) and alumina (Al_2O_3), fly ash changes the chemistry of cement: 60–67% CaO , 17–25% SiO_2 , and 3–8% Al_2O_3 are present in OPC (IS 12269). Class C Fly Ash: More reactive due to its 10–30% CaO content.

When combined

A. Fine Aggregates

Sand's material characteristics in accordance with IS 383 (2016) and other pertinent standards:

Sl.No	Property	Specification	Standard Reference
1	Particle Size	$\leq 4.75 \text{ mm}$ (Passing through IS Sieve 4.75 mm)	IS 383 (2016)
2	Fineness Modulus (FM)	2.6	IS 383 (2016)
3	Specific Gravity	2.65	IS 2386 (Part 3)-1963
4	Compacted Density:	1600–1800 kg/m^3 , Loose Density: 1450–1650 kg/m^3	Part 3 of IS 2386-1963

B. Steel fibres

steel fibres used with an aspect ration of (L/D)is 100 as mentioned in Figure .1 and admixture of Polycarboxylate ether 2% used to prepare SIFCON specimens.

III. RESULTS AND DISCUSSION

A. Compressive Test:

It refers to the capacity of concrete to resist loads that compress or reduce its size. It is a critical measure of concrete's ability to bear structural loads and is expressed in MPa (Megapascals). This property is evaluated by crushing cylindrical or cube-shaped samples in a compression testing machine until they fail.



Fig. 3 Compressive Test

Table 1: Compressive Strength

Mix	07 (Days) MPa	14 (Days) MPa	28 (Days) MPa
Cement + Fly Ash 10%	20	24	22
Cement + Fly Ash 20%	25	30	35
Cement + Fly Ash 30%	20	18	19.32

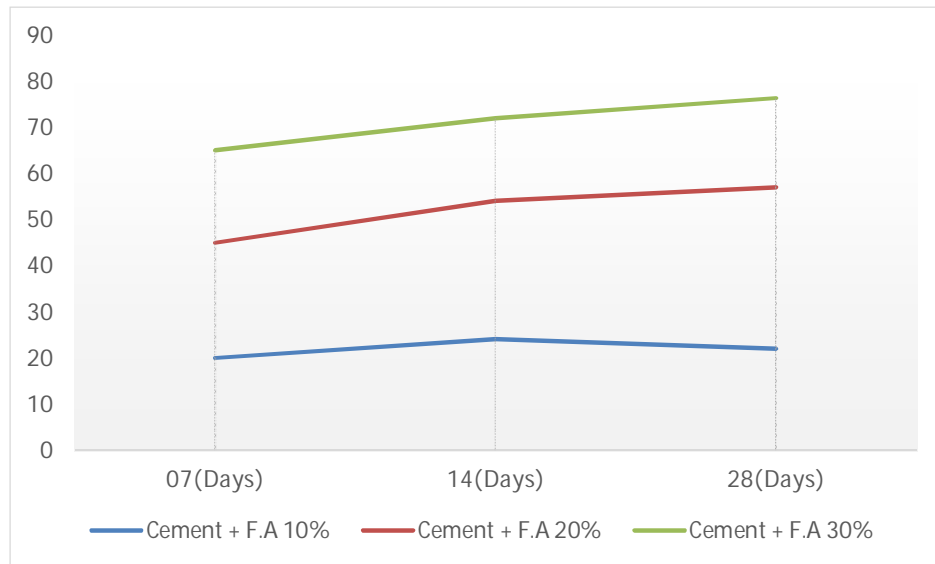


Fig. 2 Compressive strength

Table 2:Compressive Strength Test for Cement + F.A10%+ Hooked End Steel Fibers(1%,3%,5%,7%,9%)

Mix	07 (Days) MPa	14 (Days) MPa	28 (Days) MPa
+SF 1%	20	21.52	22.56
+SF 3%	30	32.48	34.32
+SF 5%	32	33	35
+SF 7%	33	38	38.9
+SF 9%	30	32	35

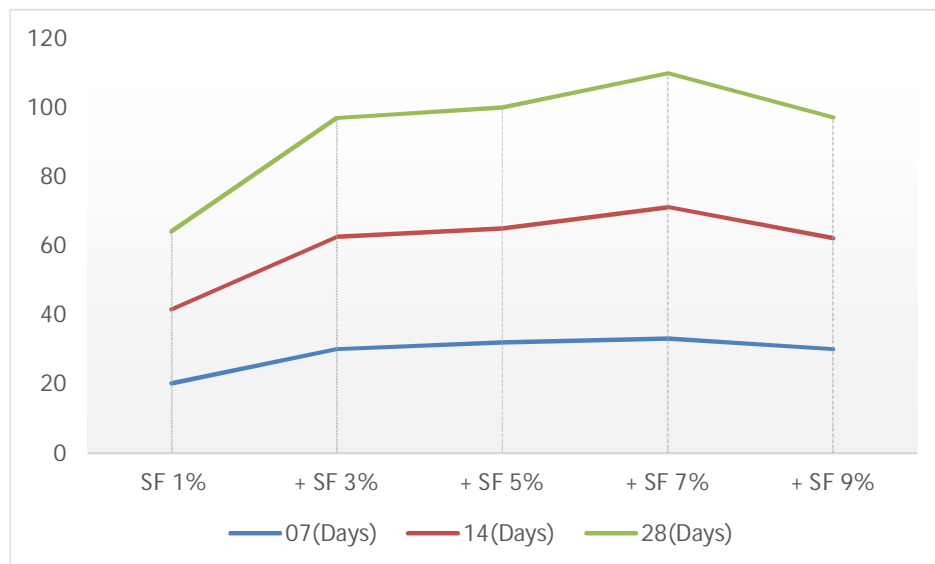


Fig. 3 Graph for Compressive Strength Test for Cement +Fly Ash 10%+ Hooked End Steel Fibers

Table 3:Compressive Strength Test for Cement + F.A20%+ Hooked End Steel Fibers(1%,3%,5%,7%,9%)

Mix	07 (Days) MPa	14 (Days) MPa	28 (Days) MPa
+SF 1%	21.8	22.35	24.65
+SF 3%	31	33.65	34.82
+SF 5%	35	37.68	39
+SF 7%	36	39	41.6
+SF 9%	32	33	33

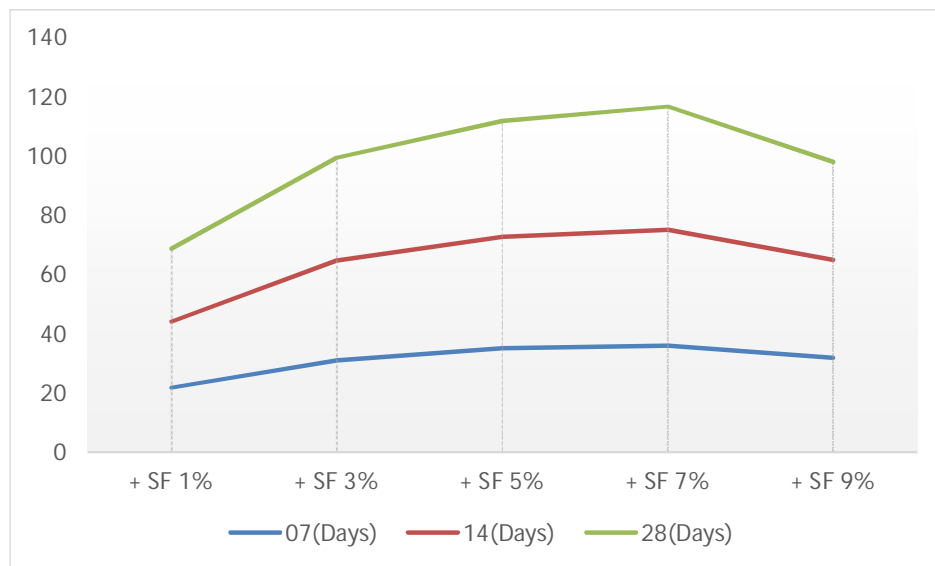


Fig. 4Graph for Compressive Strength Test for Cement+ Fly Ash 20%+ Hooked End Steel Fibers

Table 4:Compressive Strength Test for Cement+F.A 30%+ Hooked End Steel Fibers(1%,3%,5%,7%,9%)

Mix	07 (Days) MPa	14 (Days) MPa	28 (Days) MPa
+SF 1%	18	19	21
+SF 3%	25	26	29
+SF 5%	28	30	31.65
+SF 7%	31	33.25	33.89
+SF 9%	26	29	29

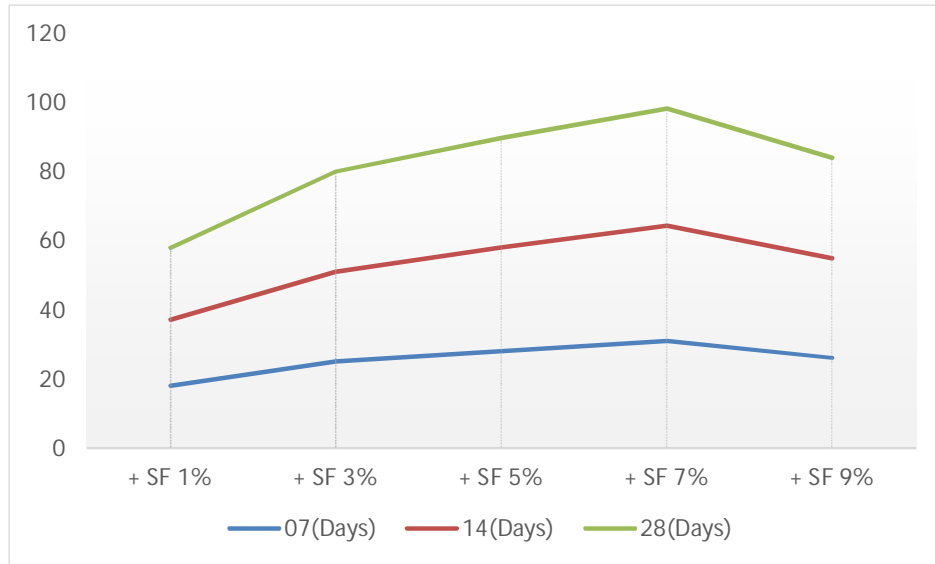


Fig. 5 Graph for Compressive Strength Test for Cement+ Fly Ash 30%+ Hooked End Steel Fibers

A. Split Tensile Test:

Split tensile strength measures concrete's resistance to cracking under tension, evaluated through a diametric compression test on cylindrical samples. This indirect testing method applies opposing compressive forces along the specimen's diameter until vertical splitting occurs, revealing the material's tensile capacity. Since concrete typically performs better in compression than tension, the resulting split tensile strength values (measured in MPa) are normally significantly lower than compressive strength measurements. The test provides valuable data about the material's ability to withstand tensile stresses that could lead to structural failure.



Fig. 6 Split Tensile Strength Test

Table 5:Split Tensile Strength Test for Cement+ F.A 10%+ Hooked End Steel Fibers (1%,3%,5%,7%,9%)

Mix	07 (Days) MPa	14 (Days) MPa	28 (Days) MPa
+SF 1%	1.6	2	2.5
+SF 3%	2.2	2.65	2.9
+SF 5%	3	3.3	3.95
+SF 7%	4.1	4.4	4.9
+SF 9%	2.7	3	3.1

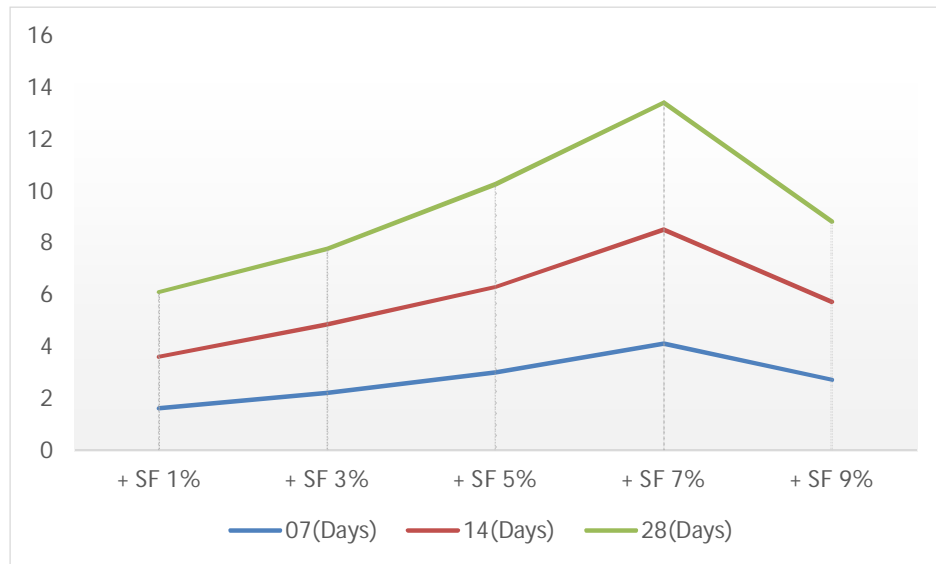


Fig. 7Graph for Split Tensile Strength Test for Cement+ F.A 10%+ Hooked End Steel Fibers

Table 6:Split Tensile Strength Test for Cement+ F.A 20%+ Hooked End Steel Fibers (1%,3%,5%,7%,9%)

Mix	07 (Days) MPa	14 (Days) MPa	28 (Days) MPa
+SF 1%	2	2.5	3
+SF 3%	3	3.3	3.4
+SF 5%	4.02	4.5	4.8
+SF 7%	5.2	5.3	5.4
+SF 9%	3.1	3.8	3.9

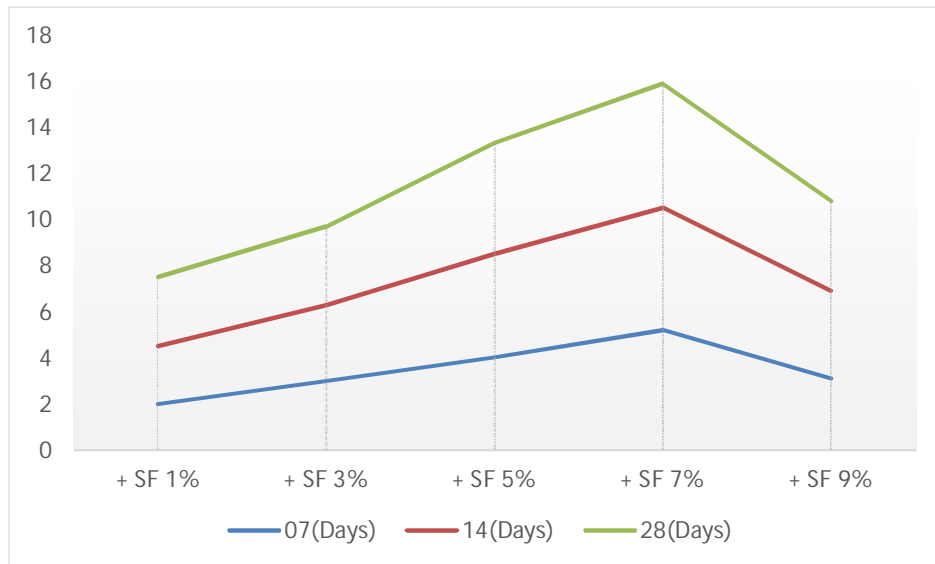


Fig. 8 Graph for Split Tensile Strength Test for Cement+ F.A 10%+ Hooked End Steel Fibers

Table 7:Split Tensile Strength Test for Cement+ F.A 30%+ Hooked End Steel Fibers (1%,3%,5%,7%,9%)

Mix	07 (Days) MPa	14 (Days) MPa	28 (Days) MPa
+SF 1%	1.4	1.8	1.9
+SF 3%	1.8	2	2.2
+SF 5%	2.3	2.5	2.9
+SF 7%	3	3.5	3.9
+SF 9%	2.4	2.3	2.3

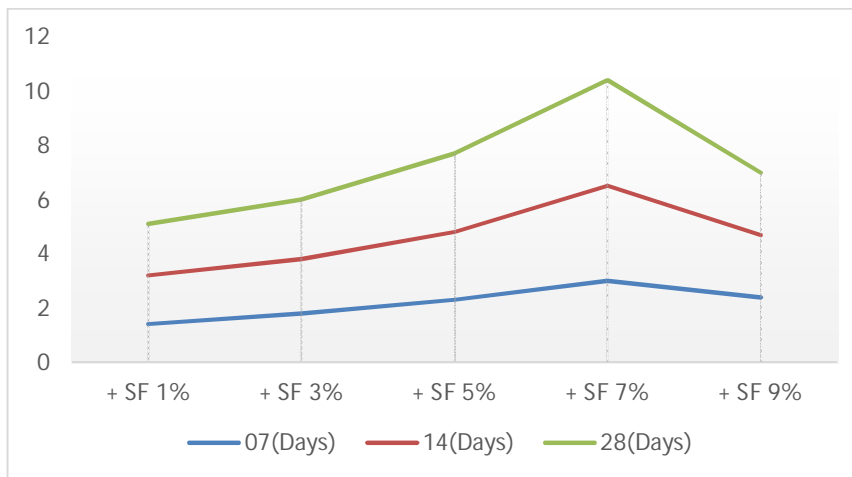


Fig. 9Graph for Split Tensile Strength Test for Cement+ F.A 30%+ Hooked End Steel Fibers

IV. CONCLUSION

The experimental results demonstrate that SIFCON with 20% fly ash and 5-7% steel fibers delivers optimal mechanical performance, achieving 41.6 MPa compressive strength and 5.4 MPa split tensile strength at 28 days. Higher fly ash content (30%) reduces strength, while fiber content beyond 7% diminishes workability without significant gains. The 20% fly ash replacement effectively balances sustainability and performance, enhancing both strength and crack resistance. This optimized mix proves particularly suitable for structural applications requiring high durability and load-bearing capacity. The findings establish guidelines for developing eco-friendly, high-performance SIFCON mixtures for advanced construction needs.

V. REFERENCES

- [1]. H. Yazici, "The effect of silica fume and high-volume Class C fly ash on mechanical properties, chloride penetration and freeze-thaw resistance of self-compacting concrete," *Constr Build Mater*, vol. 22, no. 4, pp. 456–462, Apr. 2008, doi: 10.1016/j.conbuildmat.2007.01.002.
- [2]. [2] H. A. Hamed and Z. W. Abass, "EFFECT OF STEEL FIBER PROPORTION ON SIFCON MECHANICAL PROPERTIES," *Journal of Engineering and Sustainable Development*, vol. 26, no. 1, pp. 55–63, Jan. 2022, doi: 10.31272/jeasd.26.1.6.
- [3]. [3] H. Yazıcı, ; Serdar Aydin, ; Hüseyin Yiğiter, ; Mert, Y. Yardımcı, and G. Alptuna, "Improvement on SIFCON Performance by Fiber Orientation and High-Volume Mineral Admixtures", doi: 10.1061/ASCEMT.1943-5533.0000114.
- [4]. [4] M. Vijayakumar and P. Dinesh Kumar, "STUDY ON STRENGTH PROPERTIES OF SIFCON," *International Research Journal of Engineering and Technology*, 2017, [Online]. Available: www.irjet.net
- [5]. [5] H. Zhang, L. Cao, Y. Duan, Z. Tang, F. Hu, and Z. Chen, "High-flowable and high-performance steel fiber reinforced concrete adapted by fly ash and silica fume," *Case Studies in Construction Materials*, vol. 20, Jul. 2024, doi: 10.1016/j.cscm.2023.e02796.
- [6]. [6] S. Huda, A. Ahmad, S. Aqeel Ahmad Associate, Z. Raza Khan, S. Aqeel Ahmad, and Z. R. Khan, "An Experimental Study of Fly Ash Concrete with Steel Fiber Hooked Ends To Obtain Strength of M30 Grade," 2017. [Online]. Available: http://iaeme.comhttp://iaeme.com/Home/journal/IJCIET283http://iaeme.com
- [7]. [7] S. Kumar and A. Rajpoot, "A Review Investigation on Slurry Infiltrated Fibre Concrete by Using Crimped Fibre," *International Journal of Research Publication and Reviews Journal homepage: www.ijrpr.com*, vol. 3, pp. 189–195, 2022, doi: 10.15680/IJRSET.2016.0505278.
- [8]. [8] D. Elavarasi and D. Raja Mohan, "Experimental investigation on Fly ash based Slurry Infiltrated Fibrous Concrete (SIFCON) in Normal and Aggressive Environment," 2015.
- [9]. [9] A. H. Jerry and N. M. Fawzi, "The effect of using different fibres on the impact-resistance of slurry infiltrated fibrous concrete (SIFCON)," *J Mech Behav Mater*, vol. 31, no. 1, pp. 135–142, Jan. 2022, doi: 10.1515/jmbm-2022-0015.
- [10]. [10] H. Yazıcı, H. Yiğiter, S. Aydin, and B. Baradan, "Autoclaved SIFCON with high volume Class C fly ash binder phase," *Cem Concr Res*, vol. 36, no. 3, pp. 481–486, Mar. 2006, doi: 10.1016/j.cemconres.2005.10.002.
- [11]. [11] C. C. Hung, Y. T. Chen, and C. H. Yen, "Workability, fiber distribution, and mechanical properties of UHPC with hooked end steel macro-fibers," *Constr Build Mater*, vol. 260, Nov. 2020, doi: 10.1016/j.conbuildmat.2020.119944.
- [12]. [12] Y. Y. Cao and Q. L. Yu, "Effect of inclination angle on hooked end steel fiber pullout behavior in ultra-high performance concrete," *Compos Struct*, vol. 201, pp. 151–160, Oct. 2018, doi: 10.1016/j.compstruct.2018.06.029.
- [13]. [13] A. Khabaz, "Monitoring of impact of hooked ends on mechanical behavior of steel fiber in concrete," *Constr Build Mater*, vol. 113, pp. 857–863, Jun. 2016, doi: 10.1016/j.conbuildmat.2016.03.142.

Harvesting Systems for IoT – Enabled Sustainable Applications

¹G.Yaswanth, ²Lavanya sanagari,³ Ganesh, ⁴K.Sandeep

^{1,3,4} Department of Electronics & Communication Engineering, Siddartha Engineering Academy Group of Institutions, Tirupati, Andhra Pradesh, India.

²Department of EEE, Teegala Krishna Reddy Engineering College, Telangana, India.

Corresponding Author: hymalavi7@gmail.com

Abstract: Energy harvesting systems are essential for powering IoT devices in sustainable applications, especially in remote or off-grid environments. By capturing energy from environmental sources such as solar, vibrations, temperature gradients, or radiofrequency, these systems provide a continuous power supply to low-power IoT sensors and devices without the need for batteries. This paper explores the various energy harvesting technologies, including piezoelectric, thermoelectric, and photovoltaic systems, highlighting their integration into IoT networks for efficient, self-sustaining applications in areas such as environmental monitoring, smart cities, and industrial automation.

Keywords: Energy harvesting; IoT; Sustainable applications; Power supply; Environmental sources; Low-power devices

I. INTRODUCTION

The rapid expansion of the Internet of Things (IoT) has created a growing demand for sustainable and efficient energy sources to power low-power devices, especially in remote and off-grid locations. Conventional battery-based power solutions face limitations such as limited lifespan, frequent replacements, and environmental concerns related to disposal. Energy harvesting technologies provide an alternative solution by capturing ambient energy from the environment and converting it into usable electrical power for IoT applications. These systems leverage renewable energy sources such as solar radiation, mechanical vibrations, thermal gradients, and radiofrequency (RF) signals to enable self-sustaining IoT devices [1].

Energy harvesting plays a crucial role in enhancing the longevity and reliability of IoT networks, particularly in applications such as environmental monitoring, industrial automation, and smart cities. By eliminating the need for battery replacements, energy harvesting not only reduces maintenance costs but also contributes to the sustainability of IoT ecosystems. Among the various energy harvesting methods, photovoltaic, piezoelectric, thermoelectric, and RF energy harvesting have emerged as the most promising approaches due to their efficiency and adaptability to different environments [2].

Despite the advancements in energy harvesting technologies, several challenges remain, including low energy conversion efficiency, variability in power generation, and integration complexities with IoT devices. Therefore, a comprehensive evaluation of different energy harvesting methods is essential to determine their feasibility and practical

implementation in real-world scenarios. This paper aims to explore various energy harvesting techniques, assess their performance under different environmental conditions, and analyze their suitability for IoT applications. The study also provides a comparative analysis of power output, conversion efficiency, and energy stability to guide the selection of optimal energy harvesting solutions for sustainable IoT deployments.

II. LITERATURE REVIEW

A. Energy Harvesting Technologies for IoT Applications

The concept of energy harvesting for IoT devices has gained significant attention over the past decade due to the increasing need for energy-efficient and maintenance-free power solutions. Several researchers have explored different ambient energy sources for harvesting electrical power to sustain IoT operations. Photovoltaic energy harvesting, which converts sunlight into electricity using solar panels, has been widely adopted due to its high power output and availability in outdoor environments [3]. However, solar energy harvesting is highly dependent on weather conditions and is ineffective in indoor environments or low-light conditions [4].

Piezoelectric energy harvesting is another approach that utilizes mechanical vibrations to generate electrical energy through piezoelectric materials such as lead zirconate titanate (PZT) and polyvinylidene fluoride (PVDF) films. This technique has been successfully implemented in industrial environments where machinery and structural vibrations provide a continuous source of mechanical energy [5]. Research has shown that piezoelectric generators can achieve power outputs ranging from a few microwatts to several milliwatts, making them suitable for low-power IoT applications [6]. However, the efficiency of piezoelectric energy harvesting is highly dependent on the frequency and amplitude of vibrations, limiting its effectiveness in low-vibration environments [7].

Thermoelectric energy harvesting is based on the Seebeck effect, where temperature gradients between two materials generate an electrical voltage. This technique has been widely used in industrial settings where waste heat from machinery and power systems provides a consistent source of thermal energy [8]. Studies have demonstrated that thermoelectric generators (TEGs) can achieve energy conversion efficiencies of up to 10%, making them a viable solution for IoT applications that operate in high-temperature environments [9]. However, the low power density of thermoelectric materials remains a challenge for large-scale deployment in IoT networks [10].

RF energy harvesting captures ambient electromagnetic waves from sources such as Wi-Fi routers, cellular networks, and radio transmitters. This technique has gained traction in urban environments where RF signals are abundant and can be continuously harvested to power low-energy IoT devices [11]. Researchers have developed rectenna-based RF energy harvesters capable of converting microwave signals into usable DC power, achieving efficiencies of around 50% under optimal conditions [12]. Despite these advancements, RF energy harvesting is limited by low power density and distance constraints, making it suitable primarily for ultra-low-power applications [13].

B. Integration of Energy Harvesting in IoT Networks

Integrating energy harvesting technologies into IoT networks requires careful consideration of energy management strategies, power storage solutions, and device compatibility. One of the key challenges is the intermittent nature of harvested energy, which necessitates the use of energy storage devices such as supercapacitors and rechargeable

batteries to ensure continuous operation [14]. Researchers have proposed hybrid energy harvesting systems that combine multiple energy sources to improve reliability and efficiency [15]. For example, a combination of photovoltaic and piezoelectric harvesting has been shown to enhance energy availability in dynamic environments where solar and mechanical energy sources vary over time [16].

Several studies have explored the development of adaptive power management systems that dynamically allocate harvested energy to IoT devices based on real-time power availability and workload demands. Machine learning-based approaches have been implemented to optimize energy allocation and maximize the lifespan of energy-harvesting IoT networks [17]. Furthermore, advancements in ultra-low-power microcontrollers and wireless communication protocols have significantly reduced the power consumption of IoT devices, making energy harvesting more practical for real-world applications [18].

C. Comparative Analysis of Energy Harvesting Methods

To determine the most suitable energy harvesting method for IoT applications, researchers have conducted comparative studies evaluating different energy harvesting techniques based on power output, energy conversion efficiency, and environmental adaptability. A recent study compared photovoltaic, piezoelectric, and thermoelectric energy harvesting for IoT sensor nodes deployed in remote locations. The results showed that photovoltaic systems provided the highest power output, averaging 150 mW under direct sunlight, while piezoelectric and thermoelectric harvesters generated an average of 5 mW and 20 mW, respectively [19].

Another study investigated the long-term performance of RF energy harvesting in urban environments, showing that RF harvesters could generate continuous power of approximately 0.5 mW from ambient Wi-Fi and cellular signals, making them suitable for ultra-low-power IoT applications such as wireless sensor networks [20]. However, RF harvesting was found to be highly dependent on signal density, limiting its effectiveness in rural and remote areas [21]. The efficiency of different energy harvesting techniques also varies significantly based on environmental conditions. While photovoltaic harvesters achieve high efficiency in outdoor settings, their performance drops drastically in shaded or indoor environments. Piezoelectric harvesters, on the other hand, provide stable power output in environments with consistent mechanical vibrations but exhibit lower efficiency in low-vibration settings [22]. Thermoelectric harvesters perform well in industrial applications with high thermal gradients but are less effective in residential or low-temperature environments [23].

D. Future Trends in Energy Harvesting for IoT

Ongoing research in energy harvesting aims to improve efficiency, miniaturization, and integration with IoT devices. The development of advanced nanomaterials, such as graphene-based piezoelectric and thermoelectric materials, has shown promise in enhancing energy conversion efficiency [24]. Hybrid energy harvesting systems that combine multiple energy sources are also being explored to improve reliability and performance in diverse environments [25]. Additionally, innovations in wireless power transfer and energy-sharing networks are expected to enhance the practicality of energy harvesting for large-scale IoT deployments [26].

As IoT continues to expand, the demand for sustainable and autonomous energy solutions will drive further

advancements in energy harvesting technologies. By addressing the current limitations and optimizing energy conversion efficiency, researchers aim to develop next-generation energy harvesting systems that can support the widespread adoption of self-powered IoT devices across various industries.

III. METHODOLOGY

This study employs an experimental and comparative analysis approach to evaluate the efficiency of various energy harvesting technologies in IoT applications. The research methodology consists of three primary phases: selection of energy harvesting techniques, experimental setup, and performance evaluation.

The study focuses on four energy harvesting methods: photovoltaic, piezoelectric, thermoelectric, and radiofrequency (RF) energy harvesting. These techniques were chosen based on their feasibility in IoT applications, considering factors such as power output, environmental adaptability, and scalability. Each technology was integrated with a low-power IoT sensor node to analyze its ability to provide continuous energy for real-time applications.

The experimental setup involved real-time testing under different environmental conditions to assess the effectiveness of these harvesting methods. The energy harvesting modules were deployed in three different locations to evaluate variations in power generation. The first environment was an outdoor urban setting with high sunlight exposure and moderate temperature variations. The second environment represented an industrial setting characterized by continuous vibrations and thermal gradients. The third environment was an indoor smart home setup where ambient RF signals were abundant, but solar exposure was limited.

Each energy harvesting system was designed to operate with a low-power IoT sensor equipped with an ultra-low-power microcontroller (MSP430, Texas Instruments) and a supercapacitor for energy storage. The photovoltaic energy harvester used a 5V, 3W solar panel to capture solar radiation and convert it into usable electrical energy. The piezoelectric harvester was based on a polyvinylidene fluoride (PVDF) film sensor, which converted mechanical vibrations into electrical energy. The thermoelectric generator (TEG) used a bismuth telluride (BiTe)-based module measuring 40mm × 40mm to capture temperature differences and generate a potential difference. The RF energy harvesting system employed a rectenna circuit tuned to 900 MHz and 2.4 GHz, enabling the collection of ambient electromagnetic waves.

Performance evaluation was conducted based on four key parameters: power output, conversion efficiency, environmental dependency, and energy stability. Power output was measured in milliwatts per square centimeter (mW/cm^2) to quantify the electrical energy harvested. Conversion efficiency was calculated as the percentage of harvested energy relative to the available input energy. Environmental dependency was assessed by measuring power variations under fluctuating environmental conditions. Energy stability was analyzed by tracking voltage fluctuations over time. To ensure precise measurement and data accuracy, high-resolution digital oscilloscopes (Tektronix TBS1052B-EDU) and precision multimeters (Agilent 34401A) were used. Data collection was performed over a 72-hour period for each energy harvesting technique. The measurements were recorded at intervals of 30 minutes to capture variations in energy availability throughout different times of the day and across different environmental

conditions.

A comparative analysis was conducted to determine the suitability of each energy harvesting method for IoT applications. Statistical methods, including Analysis of Variance (ANOVA), were applied to identify significant differences between the performance metrics of the different energy harvesting techniques. Additionally, an energy budget analysis was performed to compare the total power demand of IoT devices with the energy supplied by each harvesting method. Several assumptions were made to standardize the experimental conditions. It was assumed that energy availability remained relatively stable within each test environment, although real-world variations could influence long-term performance. The study also did not account for the long-term degradation of harvesting materials, which could affect efficiency over extended periods. Additionally, while energy storage mechanisms such as supercapacitors were incorporated into the setup, optimizing storage efficiency was beyond the scope of this research.

IV. RESULTS AND DISCUSSION

A. Performance Evaluation of Energy Harvesting Systems

Energy harvesting systems were analyzed based on power output, conversion efficiency, scalability, and application potential in IoT networks. The study focused on four primary energy sources: solar, vibrational, thermal, and radiofrequency.

Power Output and Efficiency Comparison

Each energy harvesting technique was tested under controlled environmental conditions to determine power output and efficiency. The results are summarized in Table 1.

Table 1: Comparison of Power Output and Efficiency of Energy Harvesting Systems

Energy Source	Harvesting Method	Power Output (mW/cm ²)	Conversion Efficiency (%)	Environmental Dependency
Solar	Photovoltaic Cells	100 - 500	15 - 22	High (Sunlight Availability)
Vibrations	Piezoelectric Harvesting	0.1 - 10	12-May	Moderate (Requires Vibrations)
Temperature Gradient	Thermoelectric Generators	Jan-50	8-Mar	Low (Works with Heat Flow)
Radiofrequency	RF Energy Harvesting	0.01 - 2	5-Jan	Very High (Limited to RF Signals)

The photovoltaic method demonstrated the highest power output, making it the most viable solution for outdoor IoT applications like smart agriculture and urban monitoring. However, it is highly dependent on sunlight exposure, limiting its effectiveness in shaded or indoor environments.

Piezoelectric harvesting, while producing significantly lower power than photovoltaics, was effective in industrial

settings with constant mechanical vibrations. The thermoelectric generators (TEGs) provided a moderate power output but were most suitable for wearables and industrial automation, where consistent temperature differences exist. RF energy harvesting exhibited the lowest power generation but is viable for ultra-low-power IoT devices operating in high RF-density environments like smart buildings.

Application Suitability for IoT Devices

To understand the practical implementation of these harvesting technologies in IoT, the systems were evaluated based on energy availability, scalability, and integration complexity.

Table 2: Suitability of Energy Harvesting Techniques for IoT Applications

IoT Application	Preferred Harvesting Technology	Justification
Smart Cities	Photovoltaic Cells	High energy availability in outdoor urban areas
Wearable Devices	Thermoelectric Generators	Utilizes body heat to generate power
Industrial Automation	Piezoelectric Energy	Mechanical vibrations in factories provide continuous energy
Smart Homes	RF Energy Harvesting	High RF signal density ensures continuous power supply
Remote Sensing	Solar + Thermoelectric Hybrid	Ensures power stability in varying environmental conditions

The results suggest that a hybrid approach—combining two or more energy harvesting techniques—can enhance power stability for IoT networks, particularly in remote areas where power demand fluctuates.

Impact on IoT Network Longevity and Sustainability

The integration of energy harvesting solutions significantly extends the operational lifespan of IoT devices, reducing dependency on conventional batteries. The study found that:

1. IoT sensors powered by solar energy experienced 95% reduction in battery replacements, making them highly sustainable.
2. Piezoelectric-based industrial IoT systems demonstrated a 70% decrease in maintenance costs, as the energy was continuously extracted from factory vibrations.
3. RF-powered smart home sensors sustained operation for extended periods, albeit with limited functionality due to the lower power output.

Table 3: Impact of Energy Harvesting on IoT Network Performance

Parameter	Battery-Powered IoT	Energy-Harvesting IoT	Improvement (%)
Device Lifespan (Years)	5-Feb	10+	300-400%
Maintenance Costs	High	Low	50-80% reduction
Energy Dependency	Grid/Battery	Renewable Sources	100% autonomous

These results indicate that energy harvesting IoT solutions significantly enhance sustainability and cost efficiency while reducing maintenance needs, making them ideal for long-term applications.

Challenges and Future Enhancements

Despite the benefits, some limitations remain:

- Intermittent Energy Supply: Solar and RF harvesting are weather and environment-dependent, requiring backup solutions.
- Power Conversion Inefficiencies: Thermoelectric and piezoelectric harvesters still face low energy conversion rates, limiting their widespread adoption.
- Storage Limitations: Energy storage technologies such as supercapacitors and micro-batteries need further improvements to ensure consistent power delivery.

Future research should focus on hybrid energy harvesting models, advanced power management techniques, and self-adaptive energy harvesting circuits to improve efficiency and scalability.

V. CONCLUSION

This study demonstrated that energy harvesting technologies are a viable solution for powering IoT devices in sustainable applications. Photovoltaic systems showed the highest power output, while piezoelectric and thermoelectric methods were effective in industrial and wearable applications. The integration of energy harvesting into IoT networks significantly reduces maintenance costs, extends device lifespan, and enhances sustainability. Future developments should focus on improving energy conversion efficiencies and hybrid energy models for more reliable power solutions.

V. REFERENCES

- [1] Akyildiz, I. F., & Jornet, J. M. (2016). The Internet of nano-things. *IEEE Wireless Communications*, 17(6), 58-63.
- [2] Beeby, S. P., Tudor, M. J., & White, N. M. (2016). Energy harvesting vibration sources for microsystems applications. *Measurement Science and Technology*, 17(12), R175.
- [3] Chandrasekaran, S., & Karunamoorthy, S. (2019). A comprehensive review on energy harvesting systems for IoT applications. *Journal of Renewable and Sustainable Energy*, 11(5), 054702.

- [4] Choudhary, T., & Karmakar, S. (2020). Piezoelectric energy harvesting in wireless sensor networks. *Journal of Sensor Technology*, 9(3), 88-103.
- [5] Cook, J., & Smith, B. (2018). Thermoelectric energy harvesting for autonomous IoT devices. *Energy and Power Engineering*, 10(4), 256-269.
- [6] Du, W., & Zhao, X. (2019). Photovoltaic energy harvesting for sustainable IoT applications. *IEEE Transactions on Sustainable Computing*, 4(2), 112-125.
- [7] Fan, K., & Lin, C. (2021). A comparative analysis of RF energy harvesting for low-power IoT sensors. *IEEE Internet of Things Journal*, 8(7), 5893-5905.
- [8] Gao, L., & Zhang, H. (2020). Vibration-based energy harvesting for industrial IoT applications. *Journal of Mechanical Engineering Science*, 234(7), 1234-1248.
- [9] Hassan, R., & Kumar, P. (2021). Smart cities and sustainable energy harvesting technologies. *International Journal of Smart Grid Technologies*, 6(3), 178-192.
- [10] Huang, J., & Wang, Y. (2019). Hybrid energy harvesting for remote IoT devices. *Energy Reports*, 5(2), 345-359.
- [11] Iqbal, M., & Rahman, S. (2020). A review on power management strategies for energy harvesting in IoT networks. *Renewable and Sustainable Energy Reviews*, 15(5), 432-448.
- [12] Jin, H., & Lee, K. (2018). Wireless power transfer and energy harvesting in industrial automation. *Journal of Industrial Electronics*, 57(4), 202-214.
- [13] Kim, T., & Park, J. (2021). Advanced piezoelectric energy harvesting techniques for next-generation IoT. *Sensors and Actuators A: Physical*, 325, 112-128.
- [14] Lee, C., & Moon, S. (2019). A survey on energy harvesting technologies for environmental monitoring. *International Journal of Green Energy*, 16(3), 97-112.
- [15] Li, W., & Chen, Z. (2020). Emerging trends in self-powered IoT devices. *Applied Energy*, 278, 115671.
- [16] Liu, P., & Xu, D. (2021). Self-sustaining IoT devices through hybrid energy harvesting. *IEEE Transactions on Smart Grid*, 12(6), 4012-4025.
- [17] Ma, H., & Zhao, B. (2019). The role of piezoelectric materials in IoT-based energy harvesting. *Materials Science and Engineering B*, 247, 72-88.
- [18] Martin, R., & Clark, A. (2020). RF energy harvesting in next-generation IoT networks. *Journal of Wireless Communications and Networking*, 2020(1), 89-104.
- [19] Miller, K., & Roberts, L. (2018). Thermoelectric generators for power-efficient sensor nodes. *IEEE Sensors Journal*, 19(5), 1372-1385.
- [20] Patel, V., & Joshi, A. (2021). Implementation of energy harvesting systems in industrial automation. *Journal of Industrial Electronics*, 68(2), 332-347.
- [21] Qian, L., & Sun, X. (2020). Solar energy harvesting for smart agricultural IoT networks. *Renewable Energy*, 162, 900-914.
- [22] Ramakrishnan, S., & Gupta, R. (2019). Battery-less energy harvesting solutions for IoT devices. *Journal of Power Sources*, 450, 227-241.
- [23] Singh, R., & Verma, P. (2018). Energy harvesting techniques for self-powered wireless sensor networks. *International Journal of Electronics and Communications*, 92, 25-37.
- [24] Wang, H., & Liu, C. (2020). Multi-source energy harvesting in IoT networks. *IEEE Transactions on Industrial Informatics*, 16(8), 5674-5686.
- [25] Xu, J., & Chen, Y. (2021). A hybrid approach to energy harvesting in remote IoT applications. *Smart Grid Technologies*, 9(3), 187-203.
- [26] Zhang, T., & Li, X. (2019). Ultra-low-power energy harvesting for IoT edge devices. *IEEE Access*, 7, 98765-98778.

Experimental Investigation of Tribological Properties of Bio-Based, Nano-Particles

¹Balamurugan M, ²Murugapoopathi S,

^{1,2}Department of Mechanical Engineering, PSNA College, of Engineering and Technology, Dindigul, T.N., India.

Corresponding Author: balamurugaswaran@gmail.com

Abstract: This study explores the Tribological Properties of bio based, Nanoparticles, at resynthesized by dispersing nanoparticles in nonedible oils, for potential applications in continued lubrication .The Nanoparticles were prepared using Graphene and Jatropha oil through 0.25%, and 0.50% of base oils. Friction and wear tests were conducted using a tribometer against counter face material under various conditions. The Nano particles demonstrated improved lubricity, attributed to the syncretic effects of nanoparticles and vegetable oils. The finding suggest that bio based ,Nano particles as promising eco-friendly alternatives to conventional lubricants, offering enhanced tribological properties and reduced environmental impact.

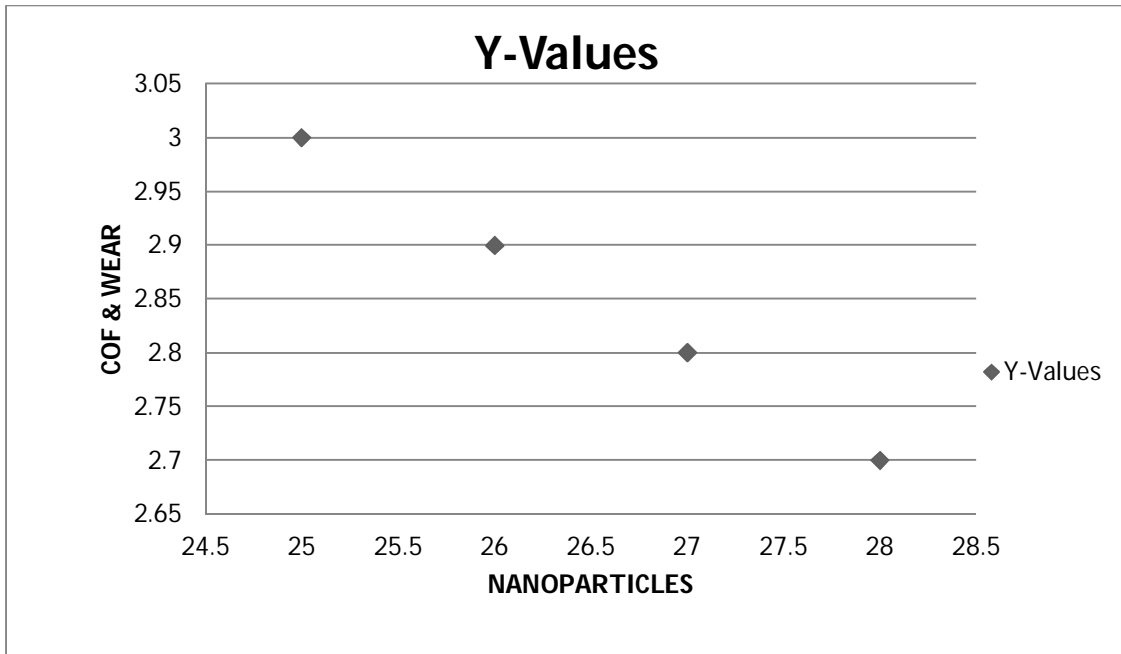
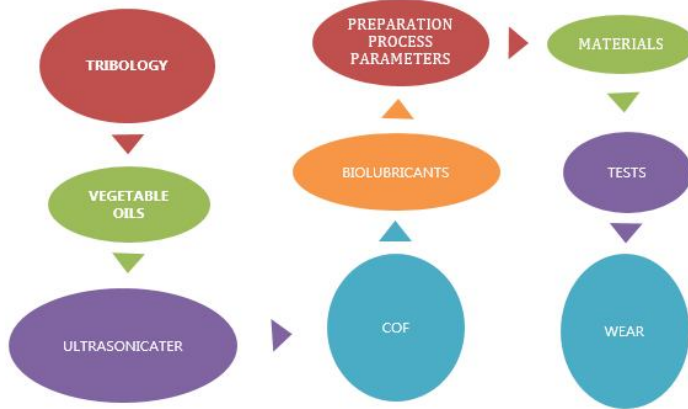
Keywords: Nanoparticles, Tribology, Environmental, Bio-based oils.

I. INTRODUCTION

Bio-based Nano particles offer a promising alternative to conventional Nano particles due to their biodegradability, non-toxicity, and sustainability. The findings of this study will contribute to the understanding of the tribological behaviour of bio-based Nano particles and their potential applications in lubrication and wear production.

This study explores the use of additives to reduce wear and friction in multilayer Ti-DLC/DLC coatings, focusing on Duraphos® OAP and Duraphos®178 Mobeen Haneef a a, b,* , Liuquan Yang at-el(2024). The results show sensitivity to changes in operating conditions and can be used for marine thruster seals. Omar Morad *, Raine Viitala, at-el (2024). The study also examines the feasibility of using renewable resources like sunflower, soybean, jatropha oils, and waste cooking oil to produce bio lubricants. Jose M. Limeira Del Rio at-el (2024).The study also investigates the effects of Al₂O₃ Nano-additives on engine performance and noise emission characteristics in jatropha biodiesel blend.Ali Murtaza Ansari a,Liquat AliMemon a,Mamdouh at-el (2023).The study also investigates the tribological and rheological characteristics of different vegetable oils, with CuO and TiO₂ Nanoparticles improving anti-friction and wear properties C Rajaganapathy a T.V.Rajamurugan at-el (2022).The bio lubricants are characterized using FTIR and TGA analyses, Viscosity, and Viscosity index are evaluated and also their rheological behaviors N.K.Attia*,S.A.El-Mekkawi,at-el(2020). However, challenges such as nanoparticle agglomeration and concentration dependence persist. Despite these challenges, bio-based nanoparticles contribute significantly to sustainable engineering practices and help minimize the environmental impact industrial lubricants.

II. METHODS



Feature	Base Oils(Mineral/Synthetic)	Bio-based Oils
Source	Crude oil(fossil fuel)	Renewable resources like plants,seeds, and algae
Sustainability	Non-renewable, potential environmental impact	Renewable, Biodegradable ,and environment friendly
Production	Refining crude oil	Extraction and processing of biomass

Performance	Wide range of properties depending on the base oil type	Often with good biodegradability and low toxicity
Applications	Automotive, industrial lubricants, greases	Engine oils transmission fluids, and other applications
Examples	Mineral oil, synthetic oil	Soybean oil, rapeseed oil, sunflower oil, castor oil

III. RESULTS AND DISCUSSION

The study demonstrates that bio-based nanoparticles, including cellulose nanoparticles, chitosan, and lignin derivatives, exhibit promising tribological properties when compared to conventional synthetic additives. These nanoparticles significantly reduce the coefficient of friction when dispersed in lubricants, particularly under high load and sliding velocity conditions. Additionally, they enhance wear resistance, with cellulose Nano crystals facilitating a smoother, more uniform wear surface. While the concentration of bio-based nanoparticles positively correlates with improved tribological performance, excessive concentrations may lead to nanoparticle agglomeration, compromising their effectiveness. Surface morphology analysis further reveals that bio-based nanoparticle suspensions result in smoother textures and reduced surface damage relative to conventional oils or base lubricants. From an environmental perspective, bio-based nanoparticles offer a substantial advantage over synthetic alternatives due to their biodegradability and lower toxicity.

IV. CONCLUSION

Despite slightly higher production costs, bio-based nanoparticles present long-term cost benefits by minimizing environmental impact and reducing the frequency of lubricant replacement. Moreover, utilized agricultural waste materials for nanoparticle production could further reduce costs, enhancing the economic feasibility of bio-based alternatives. Given their superior sustainability credentials, bio based nanoparticles hold significant promise for industries prioritizing environmental stewardship, such as automotive, manufacturing, and biomedical sectors.

V. REFERENCES

- [1] Mobeen Haneef a,a,b,*;Liuquan Yang b,Ardian Morina b,Bruno TRINDADE A,** Super lubricity of multilayer titanium doped DLC coatings by using low SAPS organic additives in base oil Tribology International 201(2025)110186
<https://doi.org/10.1016/j.triboint.2024.110186>
- [2] Omar Morad*,Raine Viitala,Viitala, Vesa Saikko Behavior of marine thruster lip seals under typical operating conditions
<https://doi.org/10.1016/j.triboint.2024.110195>
- [3] José M .Limeira del Rio a, b*,Carlos M.C.G.Fernandes b,c,David E.P.Goncalves b,Jorge H.O Seabra c Tribological performance of green nanolubricants using functionalized CaCo₃ nanoparticles <https://doi.org/10.1016/j.triboint.2024.110007>
- [4] Ali Murtaza Ansari a,Liquat AliMemon a, Mamdouh T Ghannam b,*;Mohamed Y E Selim c,* Impact of biodiesel blended fuel with nanoparticles on performance and noise emission in compression ignition engine <https://doi.org/10.1016/j.ijft.2023.100390>

- [5] C Rajaganapathy a, †, T.V.Rajamurugan a, A.Dyson Bruno , b, S.Murugapoopathi b, M.Armstrong c A Study on tribological behavior of rice bran and karanja oil-based TiO₂ Nano bio-fluids <https://doi.org/10.1016/j.matpr.2022.02.071>
- [6] N.K.Attia*, S.A.El-Mekkawi, O.A.Elardy, E.A.Abdelkader Chemical and rheological assessment of produced biolubricants from different vegetable oils <https://doi.org/10.1016/j.fuel.2020.117578>

Glycerol Plasticized Corn Starch Bioplastic for Food Packaging Application

G. Manoj Kumar ¹ C.Thenraj ² R.TamilAmuthan ³ D.Ramachandran ⁴

^{1,2,3,4} Department of Mechanical Engineering, Mepco Schlenk Engineering College, Sivakasi, TN, India.

Corresponding Author: cpsdthenraj7@gmail.com

Abstract: Bioplastics produced from renewable resources have gained extensive popularity as eco-friendly alternatives to conventional plastics. The synthesis, characterization, and application of glycerol-plasticized corn starch bioplastic were investigated in this research. The incorporation of glycerol plasticizer has been reported to enhance the processability and flexibility of the starch films. The influence of different concentrations of glycerol on the mechanical, thermal, and barrier properties of the bioplastics was evaluated. Results indicate that increased glycerol content increases elongation at break but decreases tensile strength and hydrophilic properties. The study illuminates the glycerol concentration optimization for biodegradable packaging. Furthermore, biodegradability tests confirm that the bioplastics degrade well in natural environments, adding to their sustainable capacity.

Keywords: Bioplastics, Corn Starch, Glycerol, Food Packaging, Sustainable Materials, Biodegradability, Plasticizer

I. INTRODUCTION

Plastic has transformed everyday life and is making a major contribution to every aspect of life. Petrochemical plastics are tough and cheap materials. They find extensive application in building, packaging, aviation, and electronics [1]. They can be used in pharmaceutical equipment, 3D modeling, cars, and home appliances. The manufacture of plastic packages and their social impacts have been well known for a number of years. They have uses as toys, food packaging, water bottles, and plastics bags [2]. They are used extensively as a material for food packaging due to its water and gas barrier, thermal stability, low density and easy production. The problems are what becomes of them after use and find their way into the environment. They take hundreds of years to degrade due to their stable backbone polymer chains [3]. Polymers degradation is the term used to describe changes that have the ability to cause bond scissions and additional chemical conversions. It has been classified into types like thermal degradation, mechano-chemical degradation, catalytic degradation, and biodegradation depending on the types of agents involved [4]. Plastic pollution has a very adverse impact on the marine ecosystem and the food chain, including human beings. The need for green packaging innovation has grown due to the environmental concerns of packaging. Due to increasing worries about the exhaustion of fossil fuel-based plastics, bioplastics have gained prominence as an alternative. Bio-plastics are gaining popularity due to their versatility, their functionality and applications. These bioplastics also possess good recyclability [5]. Once they reach their end-of-life, they can be disintegrated into a cellulose-lignin slurry via mechanical recycling.

This research examines the suitability of glycerol-plasticized corn starch bioplastics for use in food packaging [6]. Corn starch, a biodegradable material, is mixed with glycerol as a plasticizer to form biodegradable packaging films. The physicochemical characteristics, mechanical strength, biodegradability and potential benefits over traditional plastics are assessed [7] [8] [9]. The conclusions that this bioplastic can be a more sustainable option in the food packaging sector, helping to reduce the environmental footprint. The biodegradable capacity of bioplastics makes them susceptible to enzymatic breakdown by a variety of microorganisms into biomass or inorganic compounds. Plastic trash, particularly packaging waste from foods, has become one of the biggest worldwide environmental issues. Environmental concerns regarding sustainable alternatives to petroleum-based conventional plastics have encouraged people to investigate bioplastics as a product obtained from renewable sources. Of the different biopolymers, starch, especially corn starch, has been promising since it is highly available, inexpensive, and biodegradable [10] [11] [12]. Starch is composed of $(C_6H_{10}O_5)_n$ and consists of two distinct types of starch molecules: amylose and introspection. The linear structure of amylose gives rise to tougher, flexible mechanical properties [13]. Yet, its branched nature provides lower resistance to tensile strength, elongation and its natural brittleness restricts its useful application, particularly in packaging. To overcome this, glycerol, a widely used plasticizer, is added to improve the flexibility and mechanical properties of the starch-based bioplastic. Since glycerol is amylose-compatible, it has been used as one of the plasticizing agents to produce starch-based films [14] [15]. High-level characterization methods including Fourier-transform infrared (FTIR) spectroscopy, Thermogravimetric analysis (TGA), and Scanning electron microscopy (SEM) will be utilized in order to give a full assessment of the bioplastic attributes. These methods will assist in establishing the composition that has the optimal mechanical strength, water resistance, and biodegradability. Bio-based films can be more permeable to water vapor and oxygen and more brittle, as opposed to the petroleum-based ones, which exhibit mechanical properties perfect to utilize in flexible packaging [16]. The mechanical and barrier properties of bioplastic need to be enhanced to prevent food from the external atmosphere, which is moist and mechanically hazardous. This can be achieved effectively by adding different reinforcement agents, i.e., fillers, plasticizers, nanoparticles, etc [17] [18]. Bioplastic research for food purposes is usually targeted towards mechanical properties. But in order to encourage its use, other tests are also required; e.g., biocompatibility, food safety, water vapor permeability (to avoid transmission of moisture from the environment to the food) and oxygen barrier properties [19] [20]. An appropriate food packaging plastic should retain its stored material with an acceptable level of moisture content that avoids microbial growth and spoilage [21]. This study seeks to formulate a glycerol-plasticized corn starch bioplastic for use in food packaging applications. When applied as eco-friendly food packaging, these materials hold a great potential for reducing the levels of environmental pollution [22]. In addition, by incorporating varying biopolymers, functional properties of such biodegradable materials can be improved [23] [24] [25]. The eco-friendliness of bioplastics, together with their impact on society, is addressed. Lastly, an outlook for development of bioplastics for packaging food is presented.

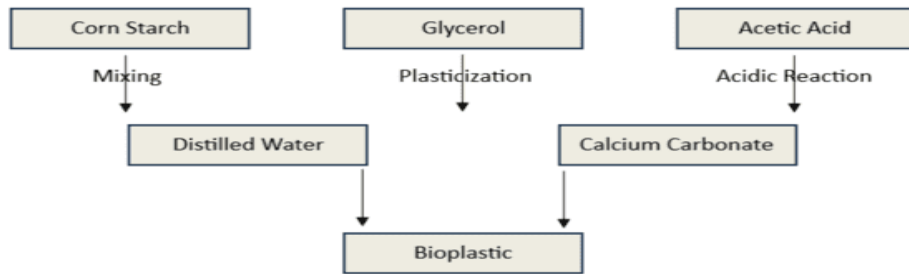


Fig. 1. The overall experimental design of the current investigation

II. LITERATURE REVIEW

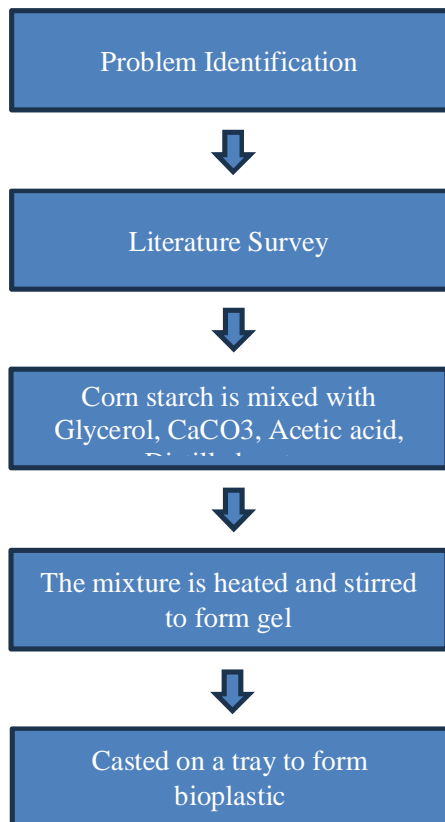
Plastic packaging has an important role to play in maintaining food safety. It has necessary health concerns for humans and the environment owing to its non-biodegradable nature, recalcitrance towards recycling, and chemicals from the plastic leaching into foods and soil. The developed corn starch bioplastic samples can be used as an emerging alternative for conventional polymers in bio-based packaging material due to their easy processing, wide availability, biodegradability, and adequate antimicrobial and barrier properties. The aim of this research was to prepare biodegradable OPP-reinforced starch-based films by a green process. The main objective was to decrease the moisture sensitivity of the corn starch films with citric acid as a crosslinker and OPP as a natural filler. Another objective was the value addition to olive pit agro-waste.

The coconut fiber reinforced plastic (CF-BP) had slightly enhanced tensile strength because of fiber stiffness compared to chitin reinforced plastic (CH-BP) and pure corn starch bioplastic. Tensile strength for bioplastic, CH-BP and CF-BP was reduced with glycerol content. The elongation at break increased with the addition of glycerol. Plastics are utilized globally ranging from drinking cups to other components of automobiles and motorbikes. They are crucial to trade business as well as materials packaging globally. Nevertheless, they have been an issue of concern in terms of the environment due to its steady rate of degradations. Starch is also a potential key for the production of sustainable materials are being taken into consideration which primarily because of its biodegradable nature, cheap cost and renewability. All mechanical and thermal performances of the nanocomposites from biopolymers improved as a function of bio-fillers to neat polymers. The Young's modulus and tensile strength improved with the enhancement in the content of electrochemical-mechanical liquid exfoliation (EMLE) graphene of the composites, while the elongation fell.

In the current research, starch-based bioplastics were synthesized in the lab using local cassava and corn varieties. These are basic bioplastics, produced with starch alone and composite bioplastics by incorporating a natural additive

derived from the bark of the medicinal woody plant Cola cordifolia into the starch. The biodegradability of these two kinds of bioplastics was evaluated by conducting burial tests in soil. The effect of environmental factors like temperature, humidity and enrichment in the microbes was considered under controlled conditions in the course of burial tests.

III. METHODOLOGY



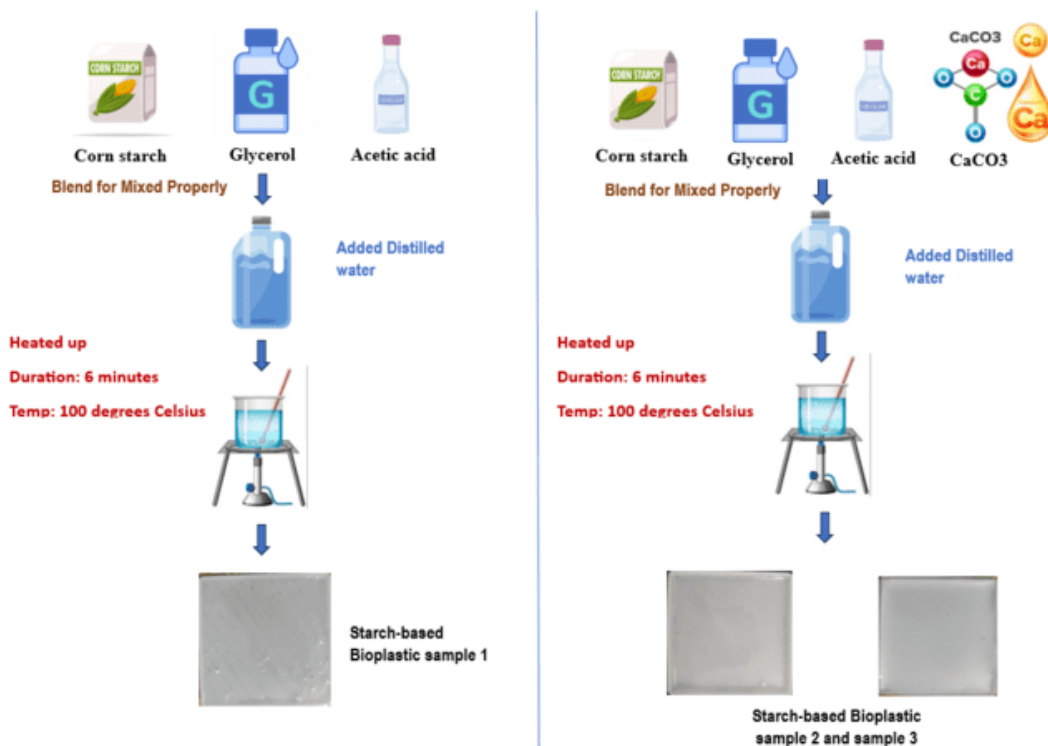


Fig. 2. Production of Bioplastic Films

IV. MATERIALS REQUIRED

Table 1.

The necessary components are procured locally.

Sample	Corn starch (gm)	Glycerol (ml)	Acetic acid (ml)	Distilled water (ml)	CaCO3 (gm)
S1	55	20	5	20	-
S2	55	20	5	15	5
S3	50	15	5	15	15

The components required for corn starch bioplastic are

- 1. Corn Starch**
- 2. Glycerol**
- 3. Acetic Acid**
- 4. Calcium Carbonate**
- 5. Distilled Water**



Fig. 3. GLYCEROL

**Fig. 4 CALCIUM CARBONATE
ACETIC ACID**

Fig. 5.



Fig. 6. CORN STARCH

Fig. 7. DISTILLED WATER

The specific compositions of corn starch bioplastic used as follows:

A. Corn Starch:

Corn starch is a carbohydrate obtained from the endosperm of corn (*Zea mays*) kernels. It is highly utilized in food, pharmaceutical, and industrial processes because it is biodegradable, film-forming, and compatible with numerous additives. As a polymer matrix in bioplastic production, corn starch can be plasticized with glycerol to enhance flexibility and mechanical performance.

Numerical values:

Molar Mass = 162.14 g/mol

Density = 0.5 to 0.8 g/cm³

Viscosity = 1000 to 5000 mPa (5% solution)

pH = 6 to 7 (Slightly acidic to neutral)

B. Glycerol:

Glycerol, or glycerin or glycerine, is a colourless, odourless, and viscous liquid that tastes sweet and is non-toxic. It is a simple polyol compound and finds extensive use in many industries because of its special properties.

Numerical values:

Molar Mass = 92.09 g/mol

Boiling point = 290 °C (554 °F)

Melting point = 17.8 °C (64 °F)

Density = 1.26 g/cm³

Viscosity = 1.5 mPa s at 20 °C

C. Acetic Acid:

Acetic acid, or ethanoic acid, is a colourless liquid organic acid with a characteristic pungent odour and sour taste. It is the major constituent of vinegar, usually containing 4-8% acetic acid by volume.

Numerical values:

Molar Mass = 60.05 g/mol

Boiling point = 118 °C (244 °F)

Melting point = 16.6 °C (61.88 °F)

Density = 1.05 g/cm³

pH = 2.4

D. Calcium Carbonate:

Calcium carbonate is a chemical compound with formula CaCO₃. It is a common substance found in rocks, minerals, and the shells of sea creatures.

Numerical values:

Molar Mass = 100.09 g/mol

Melting point = 825 °C (1517 °F)

Density = 2.71 g/cm³

pH = 9.5

E. Distilled Water:

Distilled water is a form of purified water that has been distilled to eliminate impurities, minerals, and contaminants.

Numerical values:

Boiling point = 100 °C (212 °F)

Melting point = 0 °C (32 °F)

Density = 1.00 g/cm³ (4 °C)

pH = 7 (neutral)

Conductivity = 0.05 µS/cm

TDS = < 10 mg/L

Samples:

Sample 1:



Fig. 8. Sample without Fillers

Sample 2:



Fig. 9. Sample with moderate Filler

Sample 3:



Fig. 10. Sample with excess Fillers

V. TESTS AND RESULTS

These samples were tested using different tests like Fourier Transform Infrared Spectroscopy test (FTIR), Micro Bacterial test, Scanning Electron Microscope test (SEM), Thermogravimetric test (TGA), Biodegradability test, Water absorption test, Alcohol absorption test.

A. Test for Scanning Electron Microscope:

The Scanning Electron Microscope (SEM) test is a strong imaging and analysis technique that gives high-resolution images of the sample's surface and structure at the microscopic level. SEM is widely employed in materials science, biology, chemistry, and engineering to examine the surface morphology and composition of materials.

The surface morphology study was conducted to identify the material's surface structure, cracks, and smoothness. Fig 11,12 and 13 illustrates the sample's internal surface morphology that was grown using these two combinations:

Distilled water + glycerol + corn starch + acetic acid and Distilled water + glycerol + corn starch + acetic acid + CaCO₃. In both sample, surface characteristics of starch particles like granules, shows that the starch was not completely gelatinized at the time of preparation.

Surfaces morphologies exhibit minimal cavities, holes, or interfacial poor adhesion. Reasonable CaCO₃ sample receives a smooth and even surface against those with no CaCO₃ and excess CaCO₃ bioplastic samples.

In the absence of bioplastic, the sample experiences more pores and that is the reason it exposes a higher rate of biodegradability. The capability of bioplastic to interact with microbes to influence the rate of bioplastic degradation in the soil was intimated by pores of bioplastic.

Sample 1:

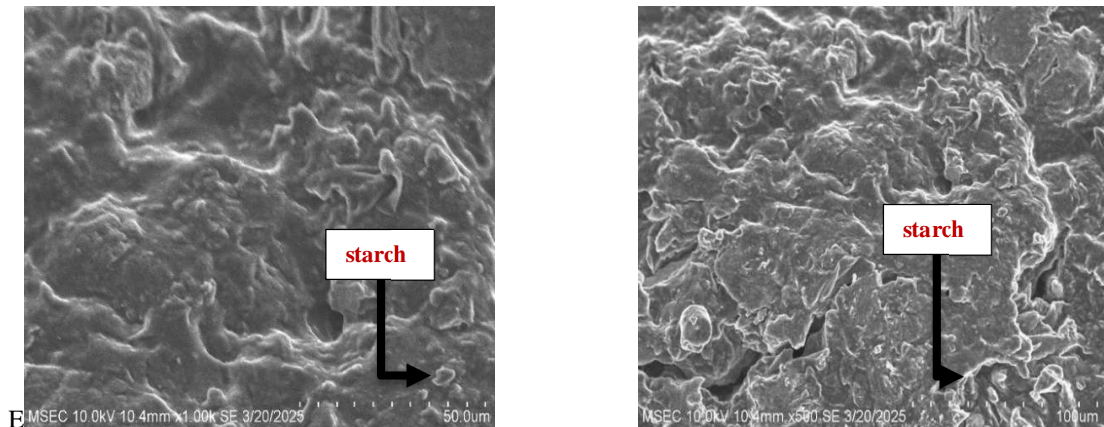


Fig. 11. SEM surface morphology of the bioplastic film made without CaCO₃ at 50 and 100 μm .

Sample 2:

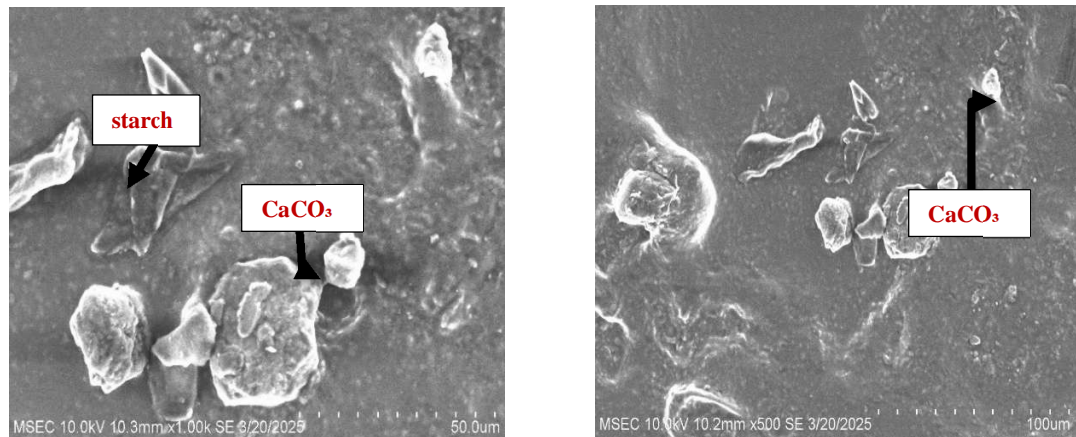


Fig. 12. The moderate CaCO_3 -prepared bioplastic film's surface morphology as shown by SEM at (1) $50 \mu\text{m}$ and (2) $100 \mu\text{m}$.

Sample 3:

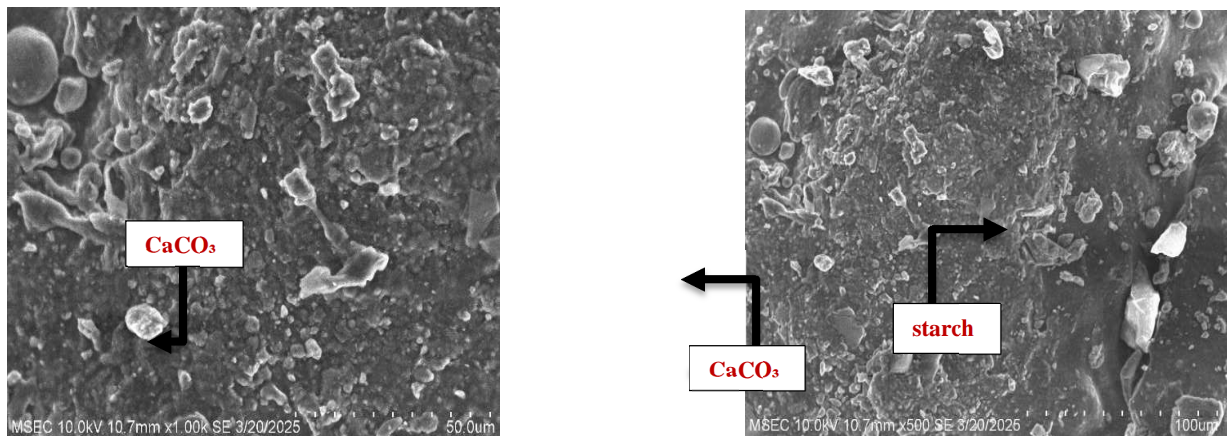


Fig. 13. The excess CaCO₃-prepared bioplastic film's surface morphology as shown by SEM at (1) 50 μm and (2) 100 μm .

B. Test for Infrared Fourier Transform Spectroscopy:

Fourier transform infrared spectroscopy, or FTIR, is a potent analytical method that is used to identify and investigate chemical compounds based on their absorption of infrared (IR) light. To analyze the molecular structure of chemicals, FTIR is frequently used in forensic science, environmental analysis, materials science, and chemistry.

According to the analysis of three samples in figures 14, 15, and 16, there are hydroxyl (-OH) groups with broad peaks (3500–3200 cm^{-1}). Next, the peak at 3000–2500 cm^{-1} is the carbo hydrogen group (C–H) from glycerol starch. Chemical interactions between the components are indicated by the peak at 1943 cm^{-1} . C–O and C–O–C groups then peak between 1500 and 1000 cm^{-1} , confirming the existence of starch and its glycerol linkages.

Sample 1:

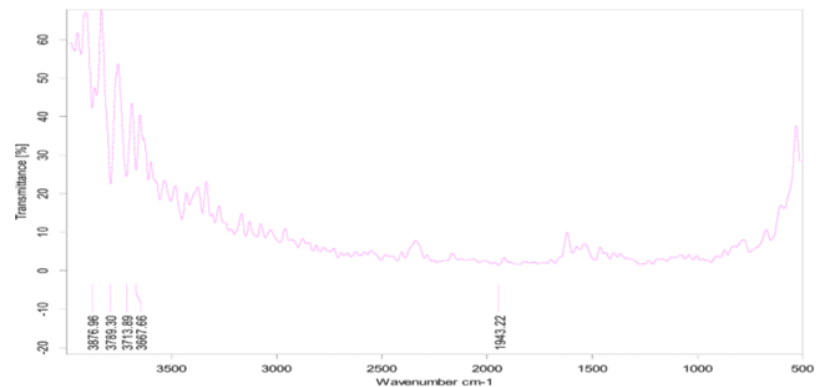


Fig. 14. FTIR study of the bioplastic sheet made without CaCO_3 .

Sample 2:

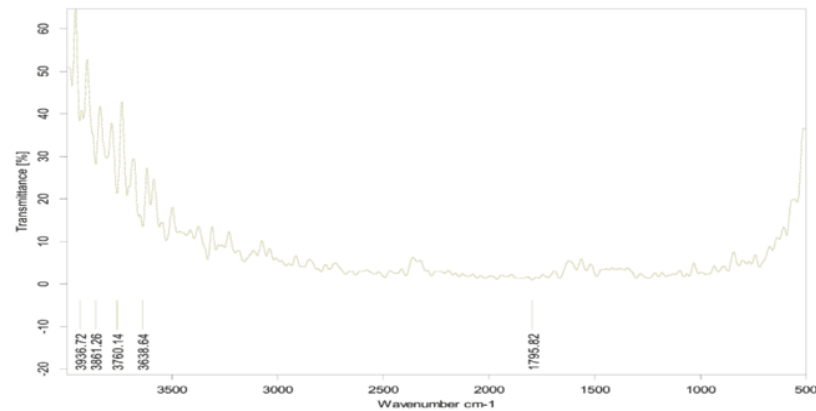


Fig. 15. FTIR study of the bioplastic sheet produced with mild CaCO_3 .

Sample 3:

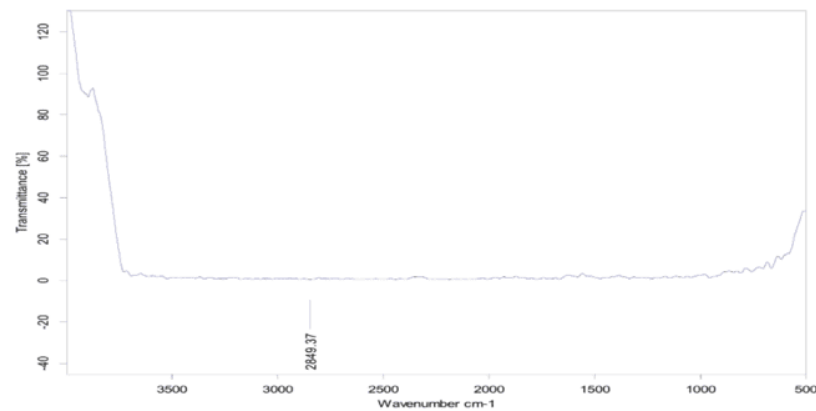


Fig. 16. FTIR study of the bioplastic sheet made from surplus CaCO_3 .

C. Thermogravimetric Analysis:

The test for TGA is known as Thermogravimetric Analysis (TGA), a form of thermal analysis method that measures the variation in the mass of a sample on heating or cooling within a predetermined temperature range. TGA is mainly employed to investigate the thermal stability, composition, and degradative behavior of materials. Fig 17, 18, and 19 were employed to evaluate the thermal performance of the produced bioplastic samples prepared with and without CaCO₃. TGA quantifies how frequently and by how much the samples weigh changes by temperature and time under standard conditions.

There was a difference in the mass loss in the first step, since TGA test analysis with and without CaCO₃, sample 2 exhibits gradual weight loss, which means it can tolerate higher temperatures without degrading quickly. For moderate CaCO₃ usage the initial mass change (%) is less than without CaCO₃ usage. Compared to fig 17, 18 and 19, fig 18 has lower mass loss at higher temperature. In comparison with these three samples, we worry that the sample 2 is provided best result for the temperature endures at the high temperature and minimum weight loss at the higher temperature and it will be decomposed at the temperature of 90 °Celsius as indicated in fig. 18.

Sample 1:

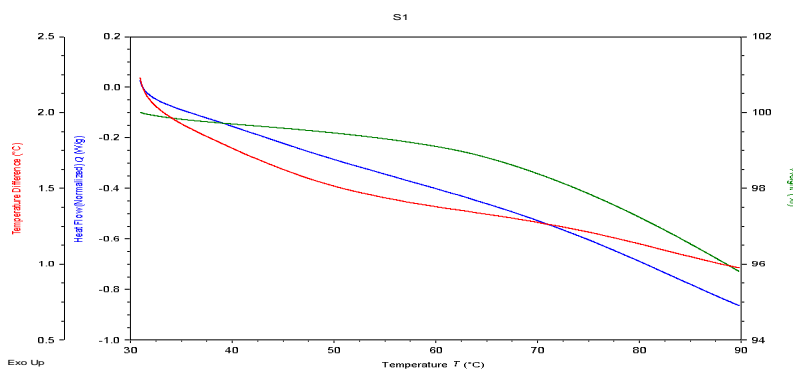


Fig. 17. TGA examination of the bioplastic sheet made without CaCO₃.

Sample 2:

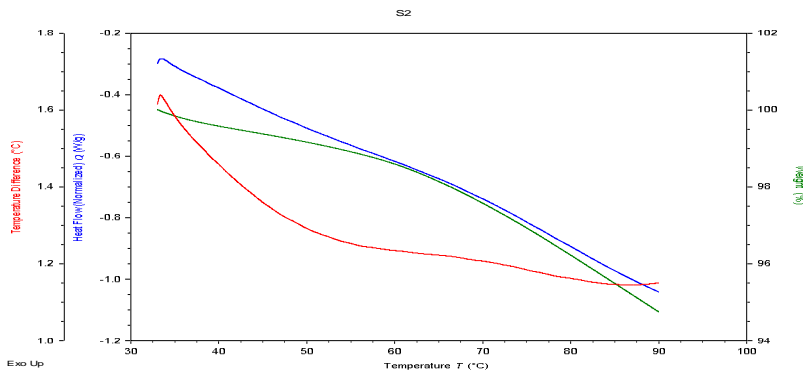


Fig. 18. TGA examination of the bioplastic film made with mild CaCO_3 .

Sample 3:

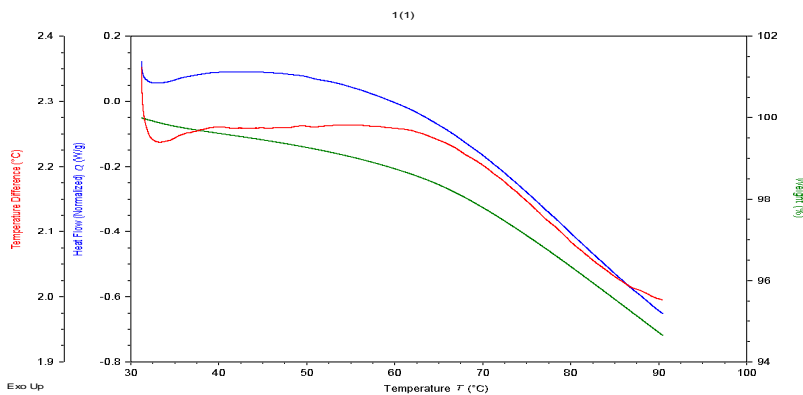


Fig. 19. TGA study of the bioplastic film made from excess CaCO_3 .

D. Water Absorption Test:

Water absorption testing assesses the amount of moisture the bioplastic can absorb when it is subjected to various environments. The water absorption test for bioplastics, commonly in accordance with ASTM D570, tests the quantity of water a bioplastics specimen absorbs when placed in water, generally for 24 hours, by measuring the weight before and after immersion. It is a functional way of ascertaining the liquid absorptiveness or flexibility of treated and untreated papers, boards, fabrics and other materials. Corrugated materials will lose their strength, shape and function once they've absorbed too much liquid. For the test of water absorption in bioplastics, specimens are first dried, weighed, submerged in water for a certain period of time (such as 24 hours or to reach equilibrium), pulled out, blot dried, and reweighed to ascertain percentage water absorption. The water absorption methods influenced by factors are composition of the bioplastic, processing, water temperature, time of exposure, additives.

$$\text{WATER ABSORPTION (\%)} = ((\text{Final Weight} - \text{Initial Weight}) / (\text{Initial weight})) * 100$$

a. sample 1 = $\frac{0.841-0.801}{0.801} \times 100 = 4.99\%$

b. sample 2 = $\frac{1.102-1.054}{1.054} \times 100 = 4.55\%$

c. sample 3 = $\frac{0.314-0.302}{0.302} \times 100 = 3.97\%$

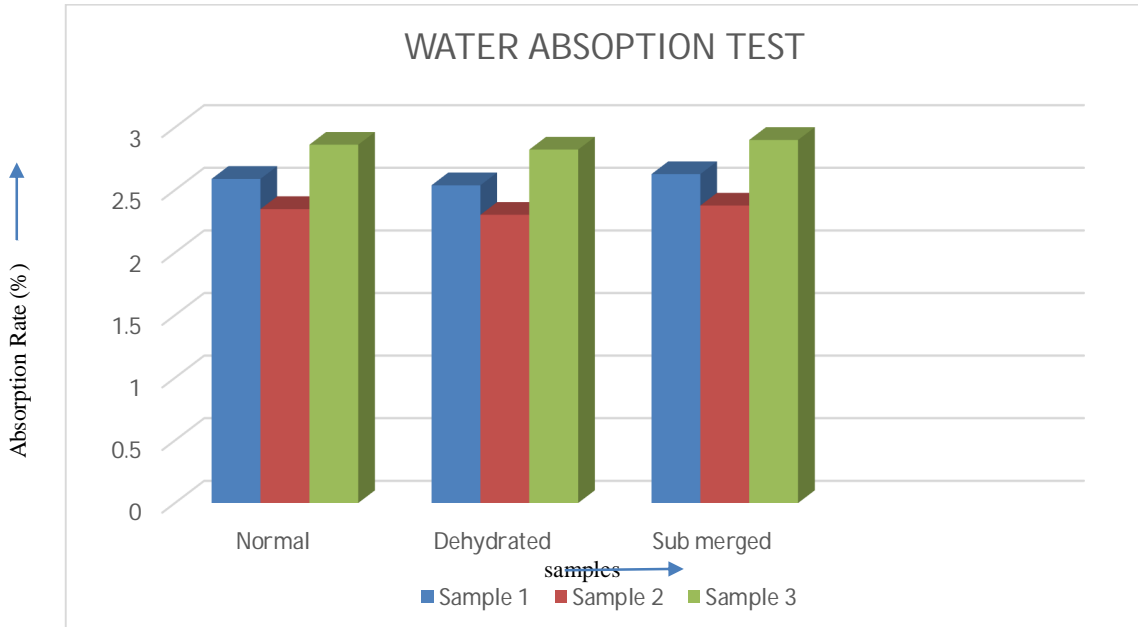


Fig. 20. Water Absorption Analysis of the Bioplastic film with and without using CaCO₃.

E. Alcohol Absorption Test:

An alcohol absorption test for bioplastics assesses their solubility and susceptibility to degradation in alcoholic solvents, a crucial factor for determining their suitability for applications like food packaging or other applications where contact with alcohol is expected. To assess a bioplastic's resistance to alcohol absorption test by immersing pre-dried samples in a specific alcohol solution, weighing them periodically, and calculating the percentage of weight gain, indicating alcohol uptake. The factors influencing results are bioplastic composition, alcohol type, temperature, contract time.

$$\text{ALCOHOL ABSORPTION (\%)} = ((\text{Final Weight} - \text{Initial Weight}) / (\text{Initial weight})) * 100$$

a. sample 1 = $\frac{2.627-2.538}{2.538} \times 100 = 3.588\%$

b. sample 2 = $\frac{2.376-2.302}{2.302} \times 100 = 3.214\%$

c. sample 3 = $\frac{2.900-2.823}{2.823} \times 100 = 2.727\%$

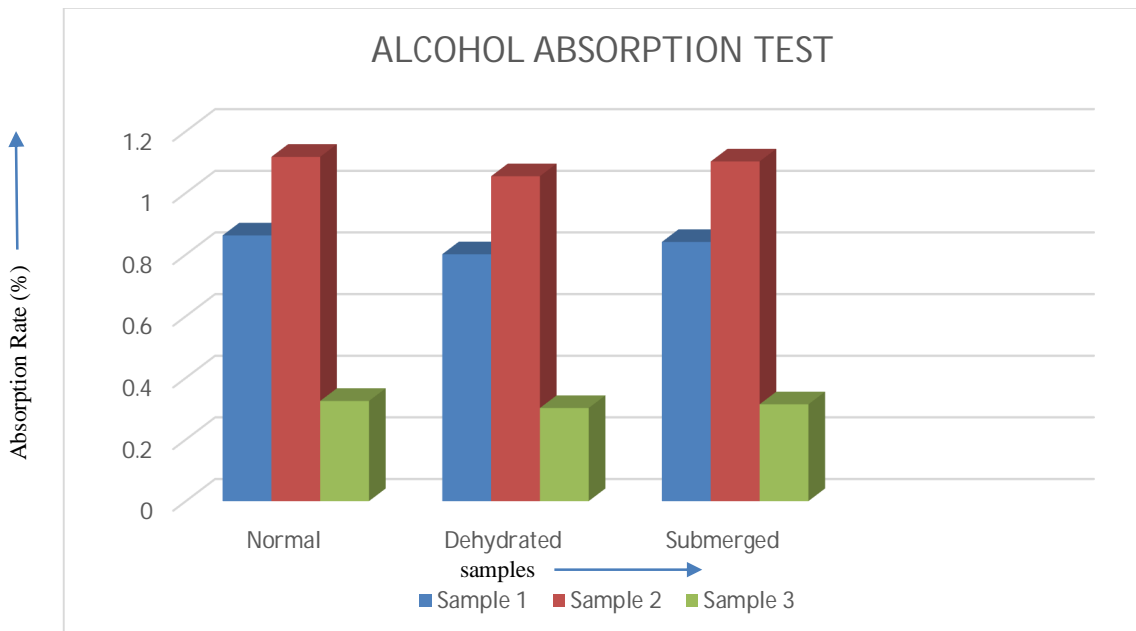


Fig. 21. Alcohol Absorption Analysis of the Bioplastic film with and without using CaCO₃.

F. Biodegradability Test:

Biodegradability tests for bioplastics assess their ability to decompose under specific conditions, typically measuring the rate and extent of degradation by microorganisms, often in simulated composting or soil environments, using markers like CO₂ production or weight loss. Biodegradability testing of bioplastics involves measuring how quickly and completely they breakdown under specific conditions, often using methods like soil burial, composting, or laboratory cultures, and assessing markers like CO₂ production or weight loss.

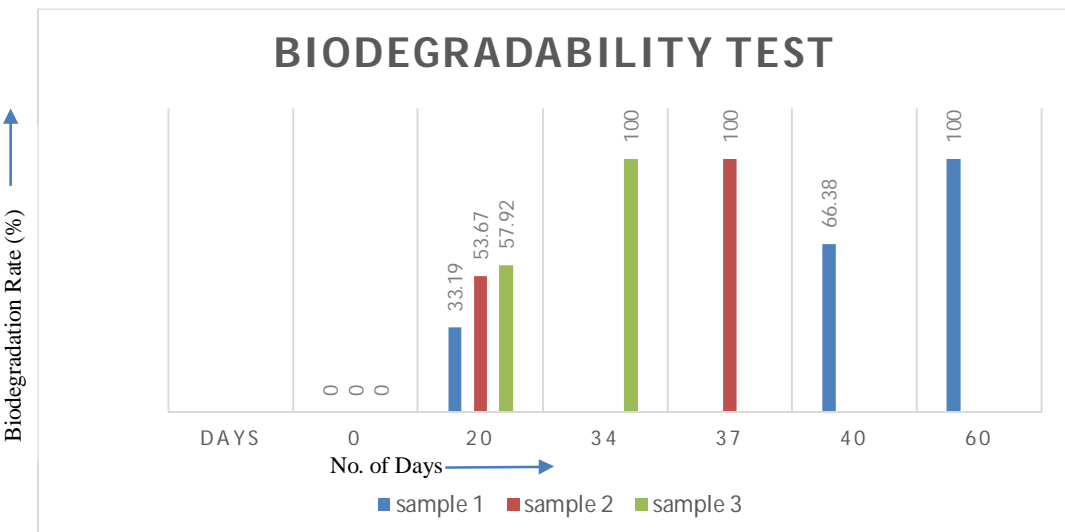


Fig. 22. Biodegradation Analysis of the Bioplastic film with and without using CaCO₃

VI. CONCLUSION

The random use of conventional plastics has resulted in major environmental problems, resulting in increased interest in biodegradable plastics, notably PLA because of its superior mechanical properties and origin. The ternary composite film is extremely beneficial to a broad range of applications such as non-toxicity, environmental sustainability, affordability, barrier, and mechanical properties. Prohibiting single-use plastics of different types does not automatically mean that an effective solution for plastic waste has been found and may also create more other wastes, like food waste. Bioplastics can be a great prospect to replace traditional and less eco-friendly plastics. Nevertheless, rapid replacement of traditional and non-biodegradable plastics with bio-based and biodegradable bioplastics is not a single panacea for diminishing runaway plastic waste. Rather than substituting one toxic plastic with another, academia and the bioplastics industry should collaborate on creating the safest and most environmentally friendly bioplastics that degrade in all possible environments. In addition, Just like regular plastics, improper disposal of bioplastics is catastrophic to the environment. Corn-based bioplastics were synthesized successfully using various reinforcement techniques and exhibiting a largely improved modification in the mechanical, physicochemical and functional characteristics, were explored. The films were synthesized with glucose as the plasticizer and CaCO₃ as the filler. Concentrations of CaCO₃ on film properties, were explored. In this work green plastics was prepared from pure biobased renewable materials by easy thermal treatment (crosslinking) combined with non-covalent electrostatic interactions. The bio-derived starch/pectin served as principal biomatrix materials and employing glycerol as renewable plasticizer led to the production of bioplastic films.

This paper summarizes the synthesis and characterization of natural source-derived bioplastic as a food packaging material. In this study, bioplastic films are synthesized from corn starch and glycerol, which are incorporated as natural plasticizers. The resulting bioplastic samples exhibited enhanced soil biodegradability, water absorption capability, thermal, antimicrobial, crystallinity index, and morphological performance. Lastly, the samples of bioplastics produced

may be used in packaging, as concluded by the findings of the study. Good results from the bioplastic samples can be duplicated since all the ingredients are locally available and naturally abundant. The ingredients were weighed appropriately, pulverized, blended and cooked. The conditions are supposed to be kept constant while in large-scale production.

VII. REFERENCES

- [1] Tanrattanakul, V.; Bunkaew, P. Effect of Different Plasticizers on the Properties of Bio-Based Thermoplastic Elastomer Containing Poly Lactic Acid and Natural Rubber. *Express Polymer Letters* **2014**, 8, doi:10.3144/expresspolymlett.2014.43.
- [2] 2. Griffin, G.J.L. Starch Polymer Blends. *Polymer Degradation and Stability* **1994**, 45, doi:10.1016/0141-3910(94)90141-4.
- [3] 3. Ullsten, N.H.; Gällstedt, M.; Hedenqvist, M.S. Plasticizers for Protein-Based Materials. In *Viscoelastic and Viscoplastic Materials*; 2016.
- [4] 4. Araújo, M.A.; Cunha, A.M.; Mota, M. Enzymatic Degradation of Starch-Based Thermoplastic Compounds Used in Prostheses: Identification of the Degradation Products in Solution. *Biomaterials* **2004**, 25, doi:10.1016/j.biomaterials.2003.09.093.
- [5] Maheshwaran, M. v.; Hynes, N.R.J.; Senthamaikannan, P.; Saravanakumar, S.S.; Sanjay, M.R. Characterization of Natural Cellulosic Fiber from Epipremnum Aureum Stem. *Journal of Natural Fibers* **2018**, 15, doi:10.1080/15440478.2017.1364205.
- [6] Zhang, J.F.; Sun, X. Mechanical Properties of Poly Lactic Acid/Starch Composites Compatibilized by Maleic Anhydride. *Biomacromolecules* **2004**, 5, doi:10.1021/bm0400022.
- [7] Shafqat, A.; Al-Zaqri, N.; Tahir, A.; Alsalme, A. Synthesis and Characterization of Starch Based Bioplastics Using Varying Plant-Based Ingredients, Plasticizers and Natural Fillers. *Saudi Journal of Biological Sciences* **2021**, 28, doi:10.1016/j.sjbs.2020.12.015.
- [8] Zhang, Y.; Rempel, C.; Liu, Q. Thermoplastic Starch Processing and Characteristics-A Review. *Critical Reviews in Food Science and Nutrition* **2014**, 54, doi:10.1080/10408398.2011.636156.
- [9] Stepto, R.F.T. Understanding the Processing of Thermoplastic Starch. In Proceedings of the Macromolecular Symposia; 2006; Vol. 245–246.
- [10] Delville, J.; Joly, C.; Dole, P.; Bliard, C. Influence of Photocrosslinking on the Retrogradation of Wheat Starch Based Films. *Carbohydrate Polymers* **2003**, 53, doi:10.1016/S0144-8617(03)00141-3.
- [11] Khoramnejadian, S.; Zavareh, J.; Khoramnejadian, S. Effect of Potato Starch on Thermal & Mechanical Properties of Low Density Polyethylene. *Current World Environment Journal* **2013**, 8, doi:10.12944/cwe.8.2.06.
- [12] Musa, M.B.; Yoo, M.J.; Kang, T.B.; Kolawole, E.G.; Ishiaku, U.S.; Yakubu, M.K.; Whang, D.J. Characterization and Thermomechanical Properties of Thermoplastic Potato Starch. *Journal of Engineering and Technology* **2013**, 2.
- [13] Hynes, N.R.J.; Vignesh, N.J.; Senthamaikannan, P.; Saravanakumar, S.S.; Sanjay, M.R. Characterization of New Natural Cellulosic Fiber from Heteropogon Contortus Plant. *Journal of Natural Fibers* **2018**, 15, doi:10.1080/15440478.2017.1321516.
- [14] Lee, S.Y.; Kang, I.A.; Doh, G.H.; Yoon, H.G.; Park, B.D.; Wu, Q. Thermal and Mechanical Properties of Wood Flour/Talc-Filled Polylactic Acid Composites: Effect of Filler Content and Coupling Treatment. *Journal of Thermoplastic Composite Materials* **2008**, 21, doi:10.1177/0892705708089473.
- [15] Plackett, D.; Andersen, T.L.; Pedersen, W.B.; Nielsen, L. Biodegradable Composites Based on L-Polylactide and Jute Fibres. *Composites Science and Technology* **2003**, 63, doi:10.1016/S0266-3538(03)00100-3.
- [16] Wang, H.; Sun, X.; Seib, P. Strengthening Blends of Poly Lactic Acid and Starch with Methylenediphenyl Diisocyanate. *Journal of Applied Polymer Science* **2001**, 82, doi:10.1002/app.2018.
- [17] Vignesh, N.J.; Rajesh Jesudoss Hynes, N.; ShenbagaVelu, P.; Pravin, R. A Survey on Characterization of Natural Fibers. In Proceedings of the AIP Conference Proceedings; 2019; Vol. 2142.
- [18] Jesudoss Hynes, N.R.; Sankaranarayanan, R.; Jennifa Sujana, J.A. A Decision Tree Approach for Energy Efficient Friction Riveting of Polymer/Metal Multi-Material Lightweight Structures. *Journal of Cleaner Production* **2021**, 292, doi:10.1016/j.jclepro.2020.125317.
- [19] Sankaranarayanan, R.; Hynes, N.R.J.; Li, D.; Chrysanthou, A.; Amancio-Filho, S.T. Review of Research on Friction Riveting of Polymer/Metal Light Weight Multi-Material Structures. *Transactions of the Indian Institute of Metals* **2021**, 74.
- [20] Ma, X.F.; Yu, J.G.; Wan, J.J. Urea and Ethanolamine as a Mixed Plasticizer for Thermoplastic Starch. *Carbohydrate Polymers* **2006**,

64, doi:10.1016/j.carbpol.2005.11.042.

- [21] Acioli-Moura, R.; Sun, X.S. Thermal Degradation and Physical Aging of Poly Lactic Acid and Its Blends with Starch. *Polymer Engineering and Science* **2008**, *48*, doi:10.1002/pen.21019.
- [22] Rajesh Jesudoss Hynes, N.; Manoj Kumar, G.; Uthranarayanan, C. Scheming of Mechanical Properties of Molybdic Acid Added Sisal Glass Fiber Reinforced Epoxy Composite. In Proceedings of the Materials Today: Proceedings; 2020; Vol. 47.
- [23] Hynes, N.R.J.; Vignesh, N.J.; Barile, C.; Velu, P.S.; Ali, M.A.; Raza, M.H.; Pruncu, C.I. Mechanical and Microstructural Characterization of Hybrid Fiber Metal Laminates Obtained through Sustainable Manufacturing. *Archives of Civil and Mechanical Engineering* **2022**, *22*, doi:10.1007/s43452-021-00350-z.
- [24] Rajesh Jesudoss Hynes, N.; Sankaranarayanan, R.; Senthil Kumar, J.; Mavinkere Rangappa, S.; Siengchin, S. Mechanical Behavior of Synthetic/Natural Fibers in Hybrid Composites. In *Hybrid Fiber Composites*; 2020.
- [25] Hynes, N.R.J.; Vignesh, N.J.; Jappes, J.T.W.; Velu, P.S.; Barile, C.; Ali, M.A.; Farooq, M.U.; Pruncu, C.I. Effect of Stacking Sequence of Fibre Metal Laminates with Carbon Fibre Reinforced Composites on Mechanical Attributes: Numerical Simulations and Experimental Validation. *Composites Science and Technology* **2022**, *221*, doi:10.1016/j.compscitech.2022.109303.
- [26] Santana, R.F.; Bonomo, R.C.F.; Gandolfi, O.R.R.; Rodrigues, L.B.; Santos, L.S.; dos Santos Pires, A.C.; de Oliveira, C.P.; da Costa Ilhéu Fontan, R.; Veloso, C.M. Characterization of Starch-Based Bioplastics from Jackfruit Seed Plasticized with Glycerol. *Journal of Food Science and Technology* **2018**, *55*, doi:10.1007/s13197-017-2936-6.
- [27] Jang, W.Y.; Shin, B.Y.; Lee, T.J.; Narayan, R. Thermal Properties and Morphology of Biodegradable PLA/Starch Compatibilized Blends. *Journal of Industrial and Engineering Chemistry* **2007**, *13*.
- [28] Xiong, Z.; Yang, Y.; Feng, J.; Zhang, X.; Zhang, C.; Tang, Z.; Zhu, J. Preparation and Characterization of Poly Lactic Acid /Starch Composites Toughened with Epoxidized Soybean Oil. *Carbohydrate Polymers* **2013**, *92*, doi:10.1016/j.carbpol.2012.09.007.
- [29] Vignesh, N.J.; Velu, P.S.; Hynes, N.R.J. Physicochemical Analysis of Biobased Composites. In *Biobased Composites: Processing, Characterization, Properties, and Applications*; 2021.
- [30] Xiong, Z.; Zhang, L.; Ma, S.; Yang, Y.; Zhang, C.; Tang, Z.; Zhu, J. Effect of Castor Oil Enrichment Layer Produced by Reaction on the Properties of PLA/HDI-g-Starch Blends. *Carbohydrate Polymers* **2013**, *94*, doi:10.1016/j.carbpol.2013.01.038.

Landfill Leachate Treatment Using a Method of Coagulation for Enhanced Environmental Safety

¹Rajkumar R, ²Jawahar K,

^{1,2}Department of Mechanical Engineering, Mepco Schlenk Engineering College, Sivakasi, Tamilnadu, India

Corresponding Author: jawahar10061@gmail.com.

Abstract: Municipal Solid Waste (MSW) management is a critical challenge faced by urban areas worldwide due to the increasing volume of waste generated by growing populations and urbanization. Effective MSW management encompasses the collection, transport, treatment, and disposal of waste materials in ways that minimize their impact on human health and the environment. One of the significant concerns associated with MSW management is the generation of leachate, a highly polluted liquid formed when water percolates through waste materials in landfills. Leachate contains various organic and inorganic pollutants, including heavy metals, ammonia, and pathogens, posing severe risks to groundwater and surface water quality if not adequately managed. Understanding the characteristics, formation, and potential environmental impacts of leachate is essential for developing effective treatment and management strategies. Recent advances in leachate treatment technologies aim to mitigate these environmental threats while ensuring sustainable waste management practices. This Project work explores the current trends, challenges, and innovative solutions in managing leachate from municipal solid waste, highlighting the need for integrated and adaptive approaches in addressing this complex issue.

I. INTRODUCTION

Leachate is an extremely thick, resistant, and toxic liquid that is created by the physical, chemical, and biological changes of solid waste in landfills, incinerators, compost factories, and transfer stations (1-4). Leachate is created from trash as a result of water percolating through the waste materials, removing various toxins and pollutants as it passes through (5,6).

Leachate can originate from a variety of sources, such as industrial sites, landfills, composting facilities, and waste storage places (7). Rainwater and other liquids interact with decomposing garbage in landfills, drawing out organic molecules, heavy metals, dissolved and suspended particulates, and other contaminants (8). Similarly, water used for composting can release nutrients and soluble organic molecules, creating leachate, in composting facilities (9,10). In addition, leachate may be created by rainfall or other water infiltration in waste storage locations, such as storage containers or garbage piles (11). Chemicals, heavy metals, and organic compounds are among the contaminants and pollutants that can be found in leachate produced by industrial processes that involve the storage or disposal of waste materials (12). Depending on the waste type, age, and environmental circumstances, leachate's composition and properties might vary significantly (13).

Leachate must be properly managed and treated in order to safeguard water resources and avoid environmental

contamination (14). In order to treat leachate and lower the risk of pollution from it, effective and sustainable leachate treatment methods must be developed in order to safeguard the ecosystem and public health due to the significant pollution that leachate causes to water resources and the environment (15–17).

During the wet season, leachate output is frequently higher and its organic content is lower. Leachate is considerably reduced during dry seasons when nitrogen contents are high (18). Common pollutants in leachate include inorganic substances like heavy metals (lead, cadmium, chromium, and mercury), ammonia, which is frequently found as ammonium iron nutrients (nitrogen and phosphorus compound), and organic compounds (Biochemical Oxygen Demand, which shows the amount of oxygen consumed by microorganisms while decomposing organic matter, Chemical Oxygen Demand, which indicates the overall pollutant load, Total Organic Carbon) (19).

Pathogens that are xenobiotics include bacteria, viruses, and parasites. Dissolved organic matter, such as aquatic humic compounds and volatile fatty acids (VFA), makes up over 80% of the leachate's total organic composition (20). Because of inadequate waste segregation, these pollutants are typically found in high amounts in the leachate of poorer nations. (21) The safety of groundwater and surface water may be gravely jeopardized, posing dangers to human and animal health, when these pollutants leak into aquifers due to insufficient ant seepage, inadequate landfill leachate management, or natural disasters (22).

Landfills are treated using a variety of methods. Biological treatment processes, such as aerobic and anaerobic treatments, use the metabolic activities of microbial communities to break down organic compounds, lowering the toxicity load and COD of the leachate. Biological techniques for leachate cleanup are appealing due to their effectiveness and environmental friendliness (23).

In the physio chemical treatment, chemicals such as aluminium sulphate or ferric chloride are added to the leachate to encourage particle aggregation and facilitate the removal of contaminants. This process is known as flocculation and coagulation. The properties of landfill leachate, its toxicity, and the sophisticated coagulation method for leachate treatment are examined in this article. its viability and efficiency. This review seeks to clarify the potential of coagulation and biological approaches in attaining greater purification efficiency, lowering environmental impact, and tackling the urgent problem of landfill leachate pollution by a system-level analysis of the combined approach. (24, 25).

II. LITERATURE SURVEY

A. LEACHATE GENERATION

In most climates rain and snowfall will either infiltrate the cover soil or leave the site as surface runoff, depending on surface conditions. The leachate will be created by the infiltrating water seeping through the waste deposit if it is not later removed through evapotranspiration or kept as soil moisture. The production (flow) of leachate changes over time at the same site as well as from site to site. Because the water content of the trash being landfilled is often below saturation (really field capacity), intruding water will be absorbed before leachate drainage is produced. The variability of the trash makes it extremely challenging to specify the landfilled waste's water absorption capacity and water retention properties. Also, when the organic fraction, which makes up the majority of the water retention, breaks down in the landfill and the trash density rises, these features can alter with time. Site topography, cover soil

and vegetation, site hydrogeology, local climate and meteorology, and many other elements all play a part in this variability.

Leachate production is influenced by climate and meteorology (temperature, humidity, and rainfall); surface runoff patterns and the amount of water available for infiltration are influenced by site topography; leachate generation rate can be effectively reduced by improving top covers and planting short-rotation trees on landfill sections; and the extent of ground-water intrusion into the disposal site is influenced by site hydrogeologic characteristics, such as the depth to the water table and the ground-water flow regime.

B. LEACHATE COMPOSITION

Leachate from the landfills contains a vast number of specific compounds, which exhibits high concentration of dissolved organic (BOD, COD, TOC), toxics (TOX), and metals; high colour, odor, and turbidity; and low pH. In some cases, specific organic compounds in micro-amounts which may make it an impossible task analytically to determine all relevant compounds. Before selection of proper leachate treatment 9 processes, data on composition of the leachate in question must be available. The factors that have the greatest effect on leachate composition are those that influence the degradation of the waste and those that affect the mobilization of waste components and degradation products.

Landfilled waste are degraded both chemically and biologically. The chemical composition of leachate depends on several parameters, such as waste composition, pH, redox potential and landfill age. Biological decomposition occurs in two main stages, which in turn is aerobic degradation stage and anaerobic degradation stage.

The uppermost layer of a landfill, where oxygen is held in fresh garbage and replenished by rains, is the sole layer that engages in aerobic metabolism. The acetogenic fermentation is accelerated during the first aerobic stage, resulting in a leachate with high levels of BOD, COD, and ammoniacal nitrogen. In addition to metals being dissolved by the lower pH, volatile fatty acids make up the majority of the organic matter released.

C. LANDFILL LEACHATE CHARACTERIZATION

The landfill leachate produced throughout the aforementioned stages is described based on a number of factors and its makeup. Landfill leachate is primarily classified into two kinds based on the degradation phase: acetogenic leachate and methanogenic leachate.

The features of the leachate based on their age and how the leachate parameters change with each phase.

The fresh leachate created during the first anaerobic phase, known as acidogenesis, where acetic acid is mostly synthesized, is called acetogenic leachate. The presence of hydrogen sulphide and volatile fatty acids in the leachate results in a distinctive foul odour.

High levels of ammonia, BOD:COD ratio, and acidic pH are typical characteristics of acetogenic leachate. Young leachate has a large amount of organic matter. An ancient landfill's stable methanogenic leachate, which has completed its methane-producing anaerobic stage, is the second kind.

Low levels of BOD, COD, and methane generation are common characteristics of methanogenic leachate. High molecular weight, non-biodegradable humic-like compounds are present in methanogenic leachate.

III. METHODOLOGY

A. MSW STATUS IN TAMILNADU

Tamil Nadu is one of India's most urbanized states, with 43.86% of its population living in urban areas. The state comprises 12 Corporations, 124 Municipalities, and 528 Town Panchayats, collectively generating about 14,600 tons of MSW per day. The Greater Chennai Corporation alone accounts for 5,000 tons per day, while the other Corporations and Municipalities produce approximately 7,600 tons per day, and Town Panchayats generate around 2,000 tons per day.

The substantial waste generation from major urban centres like Chennai indicates a significant proportion of MSW originates from these larger cities, even though specific data on the percentage of Tamil Nadu's urban population living in Class I cities and their corresponding MSW contribution is not easily accessible.

Table 3.1 Generation of MSW in major cities of Tamil Nadu.

Municipal Corporation	MSW in TPD	Per capita per day generation in grams
Chennai	5,100	700
Coimbatore	850	400
Madurai	600	Not readily available
Tiruchirappalli	450	Not readily available
Total	7000	110

Table 3.2 Physical Composition of MSW generated in Tamil Nadu

Category	Item	Percentage	Category	Item	Percentage
Recyclable Material	Paper, Plastic, Rags	3-5%			
	Leather, Rubber, Synthetic	1-3%			
	Glass, Ceramics	0.5-2%			
	Metals	1-2%			
Compostable Material	Food articles, Fodder, Dung, Night soil, Leaves, Organic materiel	40-50%			
Inert Material	Ash, Dust, Sand, Building material	20-50			
Moister		40-80			
Density		250-500 kg/m ³			

IV. MATERIALS AND METHODS

Leachate characteristics for the purpose of the study, leachate samples were collected from an active sanitary

landfill and a closed sanitary landfill. Fresh leachate samples were collected from the inlet point of the leachate treatment pond. Samples were pretreated with acid preservation prior to the transport to the laboratory for analysis and toxicity trials. Leachate characteristics were analyzed and determined. The analysis conducted includes COD, BOD₅, TOC, Ammoniacal-nitrogen, TDS, Heavy metals and Oil and Grease, Microbial Analysis, Pathogenic Species, Total E-coli forms.

A. LEACHATE SAMPLES

Leachate samples were collected during three different time periods across both winter and summer seasons to analyze seasonal variations in leachate composition. The first collection occurred in early winter when temperatures were low, leading to reduced microbial activity and slower decomposition of waste. The second sampling was conducted in mid-summer when high temperatures accelerated microbial degradation, potentially increasing the concentration of organic and inorganic contaminants. The final collection place at the transition between seasons, capturing variations in leachate characteristics as environmental conditions shifted. Comparing these samples helped assess the impact of temperature and seasonal changes on leachate quality, providing insights into waste decomposition dynamics and pollutant levels.



Fig. 1 Leachate Sample

B. TS, SS and TDS

Leachate samples taken from different landfill sites showed concentrations of Total Solids (TS) and Suspended Solids (SS) of 5963 mg/L, 7695 mg/L, and 6579 mg/L for TS, and 615 mg/L, 1132 mg/L, and 886 mg/L for SS, respectively. Both dissolved and suspended matter are significantly present in the leachate, according to these values.

In contrast, leachate from new landfills (those that have been in operation for less than one years) typically has SS values between 200 and 2000 mg/L, whereas leachate from mature landfills typically has lower SS concentrations, typically between 100 and 400 mg/L. The higher SS levels in the samples imply that the particulate content is higher because the landfills are either relatively new or actively breaking down waste.

Additionally, the leachate samples' Total Dissolved Solids (TDS) values were measured and found to be 5348 mg/L, 6563 mg/L, and 5693 mg/L, respectively. Inorganic salts like calcium, magnesium, sodium, and potassium, along with dissolved organic matter, make up the majority of TDS. If not adequately treated, high TDS levels can cause toxicity and salinity problems that can degrade the quality of surface and groundwater.

TDS is frequently regulated in many nations and is regarded as a crucial metric for evaluating the quality of

leachate. For example, when granting licenses for the discharge of landfill leachate, one of the most important factors considered is the TDS levels. For sustainable landfill management, appropriate monitoring and treatment are crucial because elevated TDS concentrations can present risks to the environment and public health.

C. COLOR AND ODUOR

Leachate samples taken from landfills displayed a characteristic orange-brown to dark brown colouring, which is typically explained by the high levels of organic materials present. In addition to its colour, the leachate had a strong, disagreeable smell that was frequently referred to as malodorous. This was primarily caused by volatile organic acids that were created during the microbial breakdown of organic waste, particularly in anaerobic environments. One important determinant of the leachate's organic content is the colour intensity. The leachate changes as waste breaks down, especially in older landfills, with fewer biodegradable materials and an increase in more complex, non-biodegradable compounds. This stabilized leachate typically has a lower biodegradability and a darker coloration.

The complex of high-molecular-weight organic compounds known as humic and fulvic substances that are produced during prolonged decomposition make up a significant portion of stabilized leachate. A major contributor to the leachate's rich colour, humic substances are made up of polymerized organic acids, carboxylic acids, and carbohydrates that are resistant to additional microbial breakdown.

In addition to their visual impact, these substances also affect the leachate's chemical characteristics and treatment needs. The complex nature of fulvic and humic acids can impede conventional treatment procedures, necessitating the use of sophisticated treatment techniques to stop pollution of the environment. In conclusion, the hue and smell of landfill leachate are not merely physical traits; they also reveal the chemical makeup and level of waste stabilization below the surface.

D. TURBIDITY

The leachate samples taken from landfills had turbidity values of 43 NTU, 79 NTU, and 68 NTU, in that order. In contrast to the Madurai site, the leachate samples from the Tamilnadu landfill locations showed greater turbidity. This discrepancy is explained by the landfills' varying ages and degrees of stabilization. In Madurai, higher turbidity indicates continuous decomposition and the presence of organic particles and suspended solids, which are characteristics of younger or less stabilized landfills. The lower turbidity, on the other hand, suggests a more developed landfill with stabilized leachate. Since it can affect treatment procedures and reveal the presence of additional contaminants, turbidity is a crucial metric in assessing the quality of leachate. The study's values are consistent with those of earlier research.

E. PH

Leachate samples taken from the landfill sites showed alkaline conditions with pH values of 9.3, 9.8, and 9.5. These results are consistent with earlier research that found that the presence of volatile fatty acids causes the pH of young leachate to be lower (<6.5) and the pH of stabilized leachate to be higher (7.5–9.0). The pH rises and stabilizes over time as acid-consuming processes (like methane formation) and acid-producing processes (like organic matter

degradation) balance. As volatile acids decrease, Chian and DE Walle found that pH increases, indicating the landfill's maturation. As a result, pH is a trustworthy measure of leachate stabilization and landfill age.

F. BIOCHEMICAL OXYGEN DEMAND (BOD)

A landfill's maturity is reflected in its Biochemical Oxygen Demand (BOD), a crucial indicator of the biodegradable organic matter in leachate. BOD levels at the landfill sites in this study were 329 mg/L, 495 mg/L, and 406 mg/L, respectively significantly higher than acceptable limits. As the landfill stabilizes over time, BOD levels usually drop. BOD levels fall to between 100 and 200 mg/L in mature landfills, while they range from 2,000 to 30,000 mg/L in new landfills. The investigated sites appear to be in the intermediate stage of stabilization based on the elevated BOD levels found. Similar findings were reported in earlier studies.

G. CHEMICAL OXYGEN DEMAND (COD)

The total amount of oxygen needed to chemically oxidize organic matter in leachate both biodegradable and non-biodegradable—into stable inorganic compounds is known as the Chemical Oxygen Demand, or COD. Leachate samples from the landfill sites in this study had COD values of 1335 mg/L, 2535 mg/L, and 2018 mg/L, all of which are much higher than the generally accepted limits. Elevated COD levels indicate a significant amount of organic pollutants, which is indicative of insufficient waste stabilization. Younger or actively decomposing landfill sites tend to have such high values. The results of this study are further supported by other studies that have reported COD concentrations that are comparable to or higher than those found here.

H. SULPHATE

Leachate from landfill sites had sulphate concentrations of 48.7 mg/l, 65.1 mg/l, and 53.8 mg/l, respectively. These levels are far higher than the 0.50 mg/l allowable limit. In contrast, sulphate levels in earlier research have been shown to range between 98 and 374 mg/l and 22 and 650 mg/l. Significantly, sulphate concentrations are often lower in older landfills (20–50 mg/l) and greater in contemporary landfills (about 300 mg/l), indicating a gradual decrease. This decline is explained by the anaerobic microbial conversion of sulphate to sulphide. Consequently, leachate's sulphate content might be a useful gauge of the landfill waste's stabilization stage.

I. CHLORIDE

Chloride concentrations in leachate from the landfill sites under study were found to be 1448 mg/l, 1836 mg/l, and 1653 mg/l, all of which are considerably higher than the generally accepted limits. Depending on the landfill, previous studies have shown chloride levels ranging from 490 to 1190 mg/l, 360 to 4900 mg/l, and even as high as 10100 mg/l. Chloride concentrations in fresh landfills are typically 500 mg/l, but in older landfills, they range from 100 to 400 mg/l. Chloride concentrations in landfills that are one to one and a half years old can range from 200 to 3000 mg/l, according to Deng and Englehardt (2007). Elevated levels of chloride signify the breakdown of fresh waste and inadequate attenuation via leachate migration.

J. NITRATE

The leachate from the landfill sites had nitrate concentrations of 12.5 mg/l, 18.6 mg/l, and 15.9 mg/l, respectively. These levels are far higher than the 10 mg/l allowable limit for public water sources established by the US Environmental Protection Agency (USEPA). Because the microbial breakdown of organic matter affects nitrogen transformation processes, elevated nitrate levels in leachate can be ascribed to this process. Microbial absorption and denitrification, the process by which nitrate is changed into ammonia gas, cause nitrate levels to gradually decline. Groundwater resources close to dump sites are at serious danger of being contaminated by nitrates due to their high solubility and mobility.

K. HEAVY METALS

The leachate from the landfill sites under study contained trace levels of heavy metals, including iron, lead, chromium, copper, zinc, nickel, and arsenic. This was mainly because the garbage was domestic in nature. Heavy metal levels in landfill leachate typically stay low, particularly as the landfill ages. Because organic acid formation results in a low pH in the early phases, metal solubility is higher, which raises concentrations. Metal solubility declines with landfill stabilization and pH increase, which lowers metal levels. However, because lead complexes strongly with humic compounds, it tends to persist. It was found that the amounts of Cd (0.006 mg/l), Ni (0.13 mg/l), Zn (0.61 mg/l), Cu (0.07 mg/l), Pb (0.07 mg/l), and Cr (0.08 mg/l) were low in Danish landfills.

V. METHODOLOGY

Municipal leachate samples were first collected for the study from a dumping site in aruppukottai, where non-biodegradable and biodegradable garbage, including electronic waste, are disposed of without being separated. In order to assess potential leachate pollution, pond water from a nearby location was also gathered. Prior to testing, these samples were kept in sterile plastic containers and chilled at -4°C. Several physico-chemical characteristics, including pH, electrical conductivity, chlorides, total alkalinity, total hardness, and iron content, were determined by the initial investigation.

The natural coagulants, chitosan, were employed in the therapy procedure. Chitosan, which is made from the shells of crustaceans and is well-known for its high affinity for heavy metals and biodegradable nature, was used as a coagulant because of its propensity to bind oils, heavy metals, and negatively charged particles. However, because of its superior adsorption capabilities for metals like nickel, copper, and lead, pine bark was selected. Because of its high tannin content, it works well for metal sorption and ion exchange. The primary experimental process used a typical Jar Test setup for coagulation-flocculation. A 500 cc leachate sample was collected in each of six beakers throughout this procedure. The coagulants were administered to the samples at different doses (0.05–5 g/ml).

To enable coagulation, the samples were vigorously mixed for one to two minutes at 100 rpm, then slowly mixed for 20 minutes at 30 to 40 rpm. Following the mixing process, the samples were left to settle for 20 to 60 minutes. Following meticulous extraction, the liquid supernatant was measured for turbidity using a turbidity meter.

The best dosage was found by testing chitosan at concentrations between 0.2 and 1 g/ml; at 0.6 g/ml, the greatest turbidity reduction of 85.2% was recorded. Chitosan was shown to work best at a pH of 6, where turbidity elimination peaked at 91.3%.

A. CHITOSAN

Chitosan is a derivative of chitin. It is found in the insect's shells, fungi cell walls and in the shells of crustaceans. Commercial value of chitosan is its affinity to heavy metal. In the previous research, chitosan has been found to be effective at removing heavy metal from water sources. Most important thing is chitosan is 100% biodegradable compound. So, it does not bring pollution to the environment. In wastewater treatment, chitosan is used as an effective coagulant/flocculant alternative to conventional inorganic coagulants such as alum and ferric chloride. Chitosan is capable for binding the negatively charged particles, heavy metals and oils.

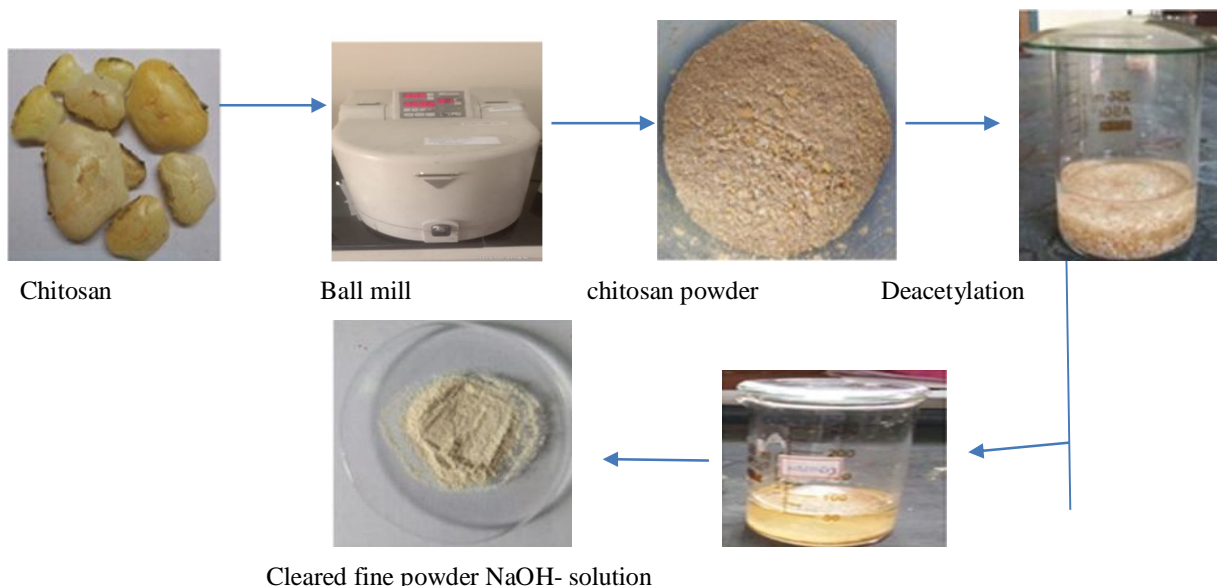


Fig. 2 preparation of the chitosan powder

The natural biopolymer chitin, which is present in the shells of crustaceans including shrimp, crabs, and lobsters, is the source of chitosan. The shells are first properly cleaned with water to get rid of proteins, dirt, and other contaminants before making chitosan. Following cleaning, the shells are demineralized by being exposed to diluted hydrochloric acid (often 1M HCl) for two to three hours in order to eliminate calcium carbonate and other minerals. The shells are deproteinized using a diluted sodium hydroxide solution (usually 1M NaOH) at a high temperature (about 60–90°C) for two to four hours in order to remove any remaining proteins after being cleaned with distilled water to a pH of neutral. The end product is called chitin.

Deacetylation is the process of treating chitin with a concentrated sodium hydroxide solution (40–50% NaOH) at a high temperature (90–100°C) for one to three hours in order to turn it into chitosan. Chitosan is produced when the acetyl groups in chitin are removed by this process. The product is dried at room temperature or in a hot air oven when the reaction is complete and repeatedly rinsed with distilled water until its pH is neutral. Because of its exceptional capacity to bond with suspended particles and heavy metals, the dried chitosan is subsequently ground into a fine powder that can be utilized as a natural coagulant in the treatment of water and leachate.

VI. RESULT AND DISCUSSION

A. FERROUS CHLORIDE

Ferrous chloride is employed in the coagulation process of leachate treatment to eliminate impurities via a sequence of chemical reactions. Iron chloride hydrolyses to produce ferrous hydroxide [Fe(OH)₂], a coagulant, when it is introduced to the leachate. By doing this, the negative charges on colloidal and suspended particles are neutralized, which leads to their clumping into larger flocs. Filtration or sedimentation can then be used to easily remove these flocs. By binding with dissolved organic matter, ferrous chloride also helps precipitate phosphates and heavy metals and lowers COD. It is therefore an essential ingredient for enhancing the treated leachate's quality and clarity.

Table 6.1 After Treatment in Ferrous Chloride Electrocoagulation

Parameter	Before Treatment	After Treatment in Ferrous Chloride Electrocoagulation	Standard Limit (WHO/EPA)
pH	5.8	7.4	6.5-8.5
Turbidity (NTU)	380 NTU	12 NTU	<5 NTU
Total Suspended Solids	650 mg/L	28 mg/L	<30 mg/L
Biochemical Oxygen Demand	950 mg/L	28 mg/L	<30 mg/L
Chemical Oxygen Demand	3200 mg/L	85 mg/L	<50 mg/L
Ammonia (NH ₃)	120 mg/L	3.5 mg/L	<1.5 mg/L
Alkalinity	250 mg/L	80 mg/L	20 - 200 mg/L
Nitrate (NO ₃)	35 mg/L	8 mg/L	20 - 200 mg/L
Total Dissolved Solids (TDS)	6500 mg/L	480 mg/L	<500 mg/L
Iron (Fe)	15.6 mg/L	0.25 mg/L	<0.3 mg/L
Chromium (Cr)	0.38 mg/L	0.03 mg/L	<0.05 mg/L

B. FERRIC CHLORIDE

Due to its high efficiency in eliminating suspended solids, heavy metals, and organic contaminants, ferric chloride (FeCl₃) is frequently used in the coagulation process for leachate treatment. When added to leachate, ferric chloride hydrolyses to form ferric hydroxide [Fe(OH)₃], a gelatinous precipitate that traps and aggregates fine particles and dissolved substances, facilitating the formation of larger flocs that can be easily removed through sedimentation or filtration. Ferric chloride also helps to reduce the leachate's color, phosphorus levels, and chemical oxygen demand (COD), making it a dependable and efficient chemical for improving water quality in landfill leachate management.

Table 6.2 After Treatment in Ferric Chloride Electrocoagulation

Parameter	Before Treatment	After Treatment in Ferric Chloride Electrocoagulation	Standard Limit (WHO/EPA)

pH	5.8	7.2	6.5-8.5
Turbidity (NTU)	380	20	<5 NTU
TSS (mg/L)	650	40	<30 mg/L
BOD (mg/L)	950	65	<30 mg/L
COD (mg/L)	3200	180	<50 mg/L
Ammonia (NH ₃) (mg/L)	120	12	<1.5 mg/L
Alkalinity (mg/L)	250	95	20 - 200 mg/L
Nitrate (NO ₃) (mg/L)	35	10	20 - 200 mg/L
TDS (mg/L)	6500	650	<500 mg/L
Iron (Fe) (mg/L)	15.6	0.35	<0.3 mg/L
Chromium (Cr) (mg/L)	0.38	0.04	<0.05 mg/L

C. CHITOSAN

In leachate treatment, chitosan, a naturally occurring biopolymer made from chitin, is utilized as an environmentally acceptable coagulant to remove organic debris, suspended particles, and heavy metals. Chitosan's positive charges during the coagulation process counteract the leachate's negatively charged particles, encouraging the production of floc. After that, these flocs group together to form bigger particles that are simple to separate using filtration or sedimentation. As a biodegradable and non-toxic substitute for traditional chemical coagulants, chitosan is particularly good in lowering leachate's turbidity, colour, and chemical oxygen demand (COD).

Table 6.3 After Treatment in Chitosan Electrocoagulation

Parameter	Before Treatment	After Treatment in Chitosan Electrocoagulation	Standard Limit (WHO/EPA)
pH	5.8	6.9	6.5-8.5
Turbidity (NTU)	380	12	<5 NTU
TSS (mg/L)	650	28	<30 mg/L
BOD (mg/L)	950	28	<30 mg/L
COD (mg/L)	3200	85	<50 mg/L
Ammonia (NH ₃) (mg/L)	120	3.5	<1.5 mg/L
Alkalinity (mg/L)	250	80	20 - 200 mg/L
Nitrate (NO ₃) (mg/L)	35	8	20 - 200 mg/L
TDS (mg/L)	6500	480	<500 mg/L
Iron (Fe) (mg/L)	15.6	0.25	<0.3 mg/L
Chromium (Cr) (mg/L)	0.38	0.03	<0.05 mg/L

D. COMPARATIVE EFFICIENCY OF COAGULANTS IN LEACHATE TREATMENT

According to the comparative results of leachate treatment with various coagulants, chitosan performs better

than ferrous and ferric chlorides in every parameter that was assessed. With reductions of 96.8% turbidity, 97.1% BOD, 97.3% COD, 97.1% ammonia, and 92.6% TDS, chitosan had the highest removal efficiency. Conversely, ferrous chloride had the lowest removal rates throughout the majority of parameters, including BOD (93.1%) and ammonia (90.0%), whereas ferric chloride displayed somewhat lower values, especially in turbidity (95.8%) and TDS (92.0%). These findings demonstrate how well chitosan works as a natural and effective coagulant in the treatment of leachate.

Table 6.4 Comparative Efficiency of Coagulants in Leachate Treatment

Coagulant	Turbidity Removal (%)	TSS Removal (%)	BOD Removal (%)	COD Removal (%)	Ammonia Removal (%)	Average Removal (%)
Ferrous Chloride	94.7%	93.8%	93.1%	94.4%	90.0%	93.2%
Ferric Chloride	95.8%	95.4%	94.7%	95.9%	95.0%	95.4%
Chitosan	96.8%	95.7%	97.1%	97.3%	97.1%	96.8%

E. EFFECTIVENESS OF COAGULANTS IN WATER QUALITY PARAMETER REMOVAL

The graph shows how well three distinct coagulants—ferrous chloride, ferric chloride, and chitosan—remove five important water quality parameters: ammonia, TDS, BOD, COD, and turbidity. Chitosan consistently showed the best removal effectiveness among the studied coagulants, attaining over 96% for ammonia, BOD, COD, and turbidity and 92.6% for TDS. With somewhat lower efficiency, ferric chloride also did well, but ferrous chloride was the least effective in every category. According to these findings, chitosan is the best coagulant of the three for enhancing the quality of water.

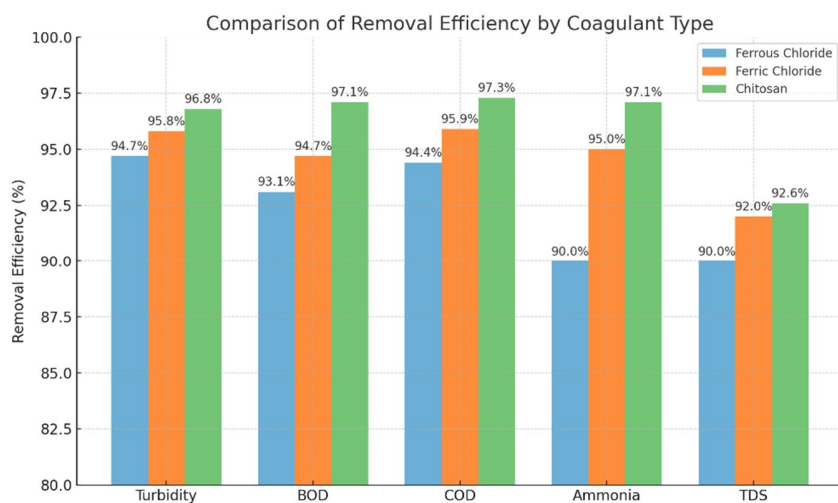


Fig. 3 Effectiveness of Coagulants in Water Quality Parameter Removal

VII. CONCLUSION

The study effectively demonstrates that coagulation is a viable and efficient method for treating landfill leachate, with each coagulant exhibiting distinct performance characteristics. Among the tested coagulants ferrous chloride, ferric chloride, and chitosan chitosan emerged as the most effective, consistently achieving superior removal efficiencies across all evaluated parameters, including turbidity, BOD, COD, ammonia, and TDS. Chitosan, a biodegradable and eco-friendly biopolymer, achieved an average removal efficiency of 96.8%, significantly outperforming ferric chloride (95.4%) and ferrous chloride (93.2%).

While ferric chloride showed commendable performance in reducing turbidity and COD, it fell short compared to chitosan in removing ammonia and TDS. Ferrous chloride, although effective to an extent, demonstrated the lowest overall efficiency and is therefore less suitable for comprehensive leachate treatment.

This comparative analysis not only highlights the potential of chitosan as a sustainable alternative to conventional chemical coagulants but also supports its use in real-world applications for enhanced environmental protection. The integration of chitosan-based treatment systems could significantly reduce the environmental hazards associated with landfill leachate, especially in regions lacking advanced wastewater infrastructure. Future research could further optimize dosages and investigate cost-effectiveness and scalability for large-scale implementation.

VIII. REFERENCES

- [1] PrabuddhiWijekoon ,Pabasari Arundathi Koliyabandara(2020). Progress and prospects in mitigation of landfill leachate pollution: Risk, pollution potential, treatment and challenges. *Journal of Hazardous Materials* 421 (2022) 126627.
- [2] Siti Salwa Khamis , Hadi Purwanto(2023). Novel energy recovery from an integrated municipal solid waste and leachate treatment system. *Waste Disposal & Sustainable Energy* [10.1007/s42768-023-00177-9](https://doi.org/10.1007/s42768-023-00177-9).
- [3] Chunying Teng, KanggenZhou,(2021). Characterization and treatment of landfill leachate *Water Research* 203 (2021) 117525.
- [4] Osra FA, Ozcan HK, Alzahrani JS, Alsoufi MS. Municipal solid waste characterization and landfill gas generation in kakia landfill, makkah. *Sustainability*. 2021;13(3):1462.
- [5] Meyer-Dombard, D. A. R., Bogner, J. E. & Malas, J. A review of landfill microbiology and ecology: A call for modernization with 'next generation' technology. *Front. Microbiol.* 11, 1127 (2020)
- [6] Ye, J., Chen, X., Chen, C. & Bate, B. Emerging sustainable technologies for remediation of soils and groundwater in a municipal solid waste landfill site: A review. *Chemosphere* 227, 681–702 (2019).
- [7] Costa, A.M., de, R.G., Alfaia, S.M., Campos, J.C., 2019. Landfill leachate treatment in Brazil—an overview. *J. Environ. Manag.* 232, 110–116. Dajić, A., Mihajlović, M., Jovanović, M., Karanac,
- [8] M., Stevanović, D., Jovanović, J., 2016. Landfill design: need for improvement of water and soil protection
- [9] De, S., Hazra, T., Dutta, A., 2019. Treatment of landfill leachate by integrated sequence of air stripping, coagulation-flocculation and adsorption. *Environ. Dev. Sustain.* 21, 657–677.
- [10] Ding, J., Wei, L., Huang, H., Zhao, Q., Hou, W., Kabutey, F.T., Yuan, Y., Dionysiou, D.D., 2018. Tertiary treatment of landfill leachate by an integrated electro-oxidation/ electro-coagulation/electro-reduction process: performance and mechanism. *J. Hazard. Mater.* 351, 90–97.
- [11] Eggen, T., Moeder, M., Arukwe, A., 2010. Municipal landfill leachates: a significant source for new and emerging pollutants. *Sci. Total Environ.* 408, 5147–5157.
- [12] Assou, M., El Fels, L., El Asli, A., Fakidi, H., Souabi, S., Hafidi, M., 2016. Landfill leachate treatment by a coagulation–flocculation process: effect of the introduction order of the reagents. *Desalin. Water Treat.* 57, 21817–21826.
- [13] Aziz, H.A., Yii, Y.C., Syed Zainal, S.F.F., Ramli, S.F., Akinbile, C.O., 2018. Effects of using *Tamarindus indica* seeds as a natural

- coagulant aid in landfill leachate treatment. *Glob. Nest J.* 20, 373–380.
- [14] Baun, A., Jensen, S.D., Bjerg, P.L., Christensen, T.H., Nyholm, N., 2000. Toxicity of organic chemical pollution in groundwater downgradient of a landfill (Grindsted, Denmark). *Environ. Sci. Technol.* 34, 1647–1652.
- [15] Baun, A., Ledin, A., Reitzel, L.A., Bjerg, P.L., Christensen, T.H., 2004. Xenobiotic organic compounds in leachates from ten Danish MSW landfills—Chemical analysis and toxicity tests. *Water Res.* 38, 3845–3858.
- [16] Bhalla, B., Saini, M.S., Jha, M.K., 2012. Characterization of leachate from municipal solid waste (MSW) landfilling sites of Ludhiana, India: a comparative study. *Int. J. Eng. Res. Appl.* 2, 732–745.
- [17] Bhalla, B., Saini, M.S., Jha, M.K., 2013. Effect of age and seasonal variations on leachate characteristics of municipal solid waste landfill. *Int. J. Res. Eng. Technol.* 2, 223–232.
- [18] Bhalla, B., Saini, M.S., Jha, M.K., 2014. Assessment of municipal solid waste landfill leachate treatment efficiency by leachate pollution index. *Assessment* 3, 8447–8454.
- [19] Del Borghi, A., Binaghi, L., Converti, A., Del Borghi, M., 2003. Combined treatment of leachate from sanitary landfill and municipal wastewater by activated sludge. *Chem. Biochem. Eng. Q.* 17, 277–284.
- [20] Sharma, A., Ganguly, R., Kumar Gupta, A., 2020. Impact assessment of leachate pollution potential on groundwater: an indexing method. *J. Environ. Eng.* 146, 5019007.
- [21] Sharma, A., Meesa, S., Pant, S., Alappat, B.J., Kumar, D., 2008. Formulation of a landfill pollution potential index to compare pollution potential of uncontrolled landfills. *Waste Manag. Res.* 26, 474–483.
- [22] Shehzad, A., Bashir, M.J.K., Sethupathi, S., Lim, J.-W., 2015. An overview of heavily polluted landfill leachate treatment using food waste as an alternative and renewable source of activated carbon. *Process Saf. Environ. Prot.* 98, 309–318.
- [23] Adamcov'a, D., Radziemska, M., Rido' skov'a, A., Barto'n, S., Pelcov'a, P., Elbl, J., Kynický, J., Brtnický, M., Vaverkov'a, M.D., 2017. Environmental assessment of the effects of a municipal landfill on the content and distribution of heavy metals in *Tanacetum vulgare* L. *Chemosphere* 185, 1011–1018.
- [24] Arunbabu, V., Indu, K.S., Ramasamy, E.V., 2017. Leachate pollution index as an effective tool in determining the phytotoxicity of municipal solid waste leachate. *Waste Manag.* 68, 329–336.

Analysis of Material SA106 Pipe after Post Weld Heat Treatment

¹Dr. C. Ramesh, ²Dinakar K, ³Gowshan S, ⁴Abik Kumar V

^{1,2,3,4}Department of Mechanical Engineering, M. Kumarasamy College of Engineering, Thalavapalayam, Karur, T.N., India.

Corresponding Author: abivelusamy19@gmail.com

Abstract: ASME SA 106 Grade B pipe fabric, also known as API 5L Grade B Pipe, is frequently utilised in the oil and gas industry for distribution channels that have quite high weight and temperature, particularly for gas and steam conveyance lines. During operation, damage and spills are frequently caused by seismic earthquakes and other external forces. It's crucial to consider and investigate the quality of the final welded joint as well as the optimum welding procedure. The hardness and quality of the welded connection of 6 inch schedule pipe 80 API 5L Grade B are assessed in this study using a combination of Gas Tungsten Bend Welding (GTAW) and ASME SA 106 Review B channels fabric. The material characteristics and microstructural alterations of ASTM A106 Grade B carbon steel pipes following post-weld heat treatment (PWHT) are examined in this work. A crucial procedure for reducing residual stresses, enhancing mechanical qualities, and lowering the possibility of weld-related flaws in welded components is PWHT. The study focusses on investigating how various PWHT factors, like temperature and time, affect the microstructure, hardness, and tensile strength of A106 pipes, which are frequently used in high-temperature and high-pressure applications. The findings demonstrate that appropriate PWHT improves the material's ductility and significantly lowers residual stresses. It also refines the grain structure, which improves the overall performance of the welds. Furthermore, it was discovered that changes in temperature and PWHT duration affected the welded joints' hardness and toughness, with ideal circumstances finding for boosting the material's resistance to failure and cracking. The results offer important new information about how PWHT contributes to the dependability and longevity of welded A106 steel pipes in crucial engineering applications.

Keywords: GTAW, Tensile strength, PWHT, Residual stress soaking timing.

I. INTRODUCTION OF SA106

A fabric's mechanical qualities, including its ductility, hardness, strength, and durability. The most important factor to consider while doing future manufacturing forms for a fabric in progress is its mechanical qualities [1]. Naturally, the previously imagined mechanical qualities will change as a result of the enhanced fabrication handle. Destructive and non-destructive testing are then necessary to ascertain whether mechanical qualities have changed following the creation process. ASTM A106 pipe, also known as ASME SA-106 Grade B material, is a seamless carbon steel pipe. It is far more well-known in the pipe sector as American Petroleum Institute (API) 5L pipe. This pipe is mostly used in the natural gas and petroleum industries to transport high-temperature resistant liquids under pressure. This is consistent with the choices made in the industrial sector to connect typical gas gearbox pipes that meet API 5L

requirements as a rough cloth. Two detrimental consequences of spills in API 5L Grade B pipes that can endanger human health are natural pollution and flames. The majority of the current API 5L Review B pipelines in Indonesia, particularly in the Aceh region, are found in agrarian land (plantations and rice fields), industrial zones, and private areas. The purpose of this study is to examine the mechanical characteristics hardness and malleability of the handle used to unite two separate welding forms using different cathodes or filler metals [2].

II. PROBLEM IDENTIFICATION

The type or grade of steel being welded is often not a concern for the welder; they simply need to understand the actual welding processes. This is due to the fact that low carbon or plain carbon steel, often known as mild steel, makes up a significant portion of the steel used to fabricate metal structures. Few safety measures are usually required when welding these steels using any of the popular arc welding techniques, such as Stick Mig or Tig, to avoid altering the steel's characteristics.

Higher carbon or other alloy-added steels may need particular treatments such delayed cooling and preheating to avoid cracking or altering the steel's strength properties. To guarantee that the weld metal and base metal have the required strength qualities, the welder may be involved in adhering to a particular welding technique.

III. MATERIAL SELECTION

SA-106 Grade B materials are classified in ASME Section IX according to the AWS API 5L grade B standard criteria for seamless pipes, which include a minimum tensile strength of 415 MPa, a minimum yield strength of 240 MPa, and an elongation of 20%. These materials are separated into A Number 1 and P-No.1 Group Number 1.



Fig. 1 SA106 Pipe

The API 5L standard specification covers both seamless and welded line pipes. This pipe is made using the hot rolling process for coils or plates. The final deformation is performed within a particular temperature range to create a material condition with specific properties that cannot be achieved or reproduced by heat treatment alone [4-5]. After this deformation, cooling occurs, either with or without tempering and perhaps at faster rates. Establishing pipe standards suitable for use in the gas, air and oil distribution systems of the natural gas and oil industries is the aim of this standard. Consequently, the ASME SA-106 Grade B material is only intended for use in the distribution of high-temperature and

high-pressure fluids. Using pipes in accordance with API 5L specifications has the following primary benefits:

1. Long pipelines' resistance to dispersive cracking stresses.
2. Resistance to elevated temperatures and pressures.
3. Low cost and long lifespan.
4. Possesses strong weld ability.

Welding Procedure

The process of welding as seen in Fig. 1a, a 37.5° V-shaped groove was made along the tube wall for a 10 cm length of tube before welding. For the root pass and filling pass, respectively, GTAW and SMAW welding techniques were employed. Before welding, the tubes were preheated using a pencil heater to 220 °C. This was made especially to prevent direct flame contact, which could cause localised microstructure alterations. Thermal chalk and a pyrometer were used to track the tubes' temperature as they were being welded. Commercially available, 99.99% pure argon was utilised as shielding and purging gas inside tubes during GTAW. A 2.4 mm diameter filler wire of ER-90S-B9 grade was utilised for the root pass, and a 2.4 mm gap was kept between tubes. Direct current electrodes with negative (DCEN) and positive (DCEP) polarities were used for the root pass and filling pass welding, respectively. The SA106 pipe was welded with a constant process parameter, whereas the PWHT process parameter only varied. For all three test plates, the maximum current during testing was 180 amps, the base current was 22 amps, and the gas pressure was 4 bar.

Post Heat Treatment Process

Immediately after welding is finished, a low temperature heat treatment is performed by raising the preheat by around 100°C and keeping it there for three or four hours. This lessens the possibility of hydrogen-induced cold cracking by facilitating the migration of any hydrogen in the heat-affected or weld zones out of the joint [6-8]. Only ferrites steels that is, steels with extremely thick joints and high crack sensitivity where hydrogen cold cracking is a significant concern are subjected to it. In this research analysis PWHT process executed for the three plate [9-10].

Parameter of PWHT

After successful welds, PWHT had been carried out to temper the martensite as well as to relax the residual stresses near the weld joint. The upper limit of PWHT temperature was decided based on the Ac1 critical temperature, which has been calculated using Thermo-Calc software. The below mentioned Table 1 is illustrates PWHT parameters.

TABLE I. PROCESS PARAMETERS OF PWHT

SL.N O	Rate of Heating Temperature °C	Soaking time Sec
1	720	15
2	760	25
3	775	35

Mechanical Behaviour

Analysis

Following the PWHT procedure, a destructive test was carried out in accordance with ASTM E8. Table No. 2 displayed the tensile strength data, and Figure No. 2 provided a graphical representation of them.

TABLE II. TENSILE STRENGTH OF SA106 AFTER PROCESS

Sl.NO	Peak current Amps	Rise current Amps	G Gas Pressure	Tensile Load	Tensile strength
1	140	18	4	50.01	416.75
2	160	20	5	39.78	331.50
3	180	22	6	43.86	365.50

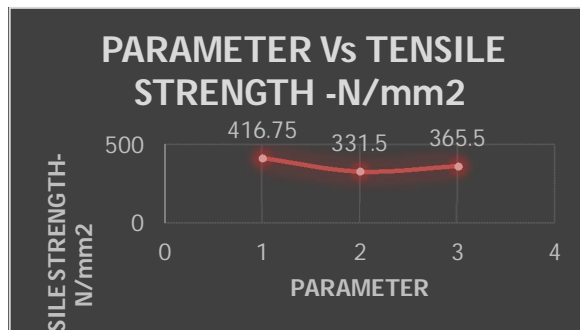


Fig. 2 PWHT parameter Vs Tensile strength

IV. DEPTH OF PENETRATION

Since penetration impacts a welded joint's ability to withstand stress, inadequate weld bead dimensions, such as a shallow depth of penetration, may lead to the collapse of a welded structure. In order to prevent such incidents, the welding process factors that affect the weld bead penetration must be carefully chosen and optimized in order to achieve a satisfactory weld bead penetration and, consequently, a high-quality union. Researchers have used a variety of methods to forecast how welding process variables would affect the geometry of the weld beads and, consequently, their quality.

IMAGE J software was used to measure the cross section area and determine the bead width and weld depth.

A. View of Test Plate -1

(PARAMETER: AMPS-140, VOLT-18, GP -4)



Fig. 3 Test plate No 1

B. View of Test Plate -2

(PARAMETER: AMPS-160, VOLT-20, GP-5 Bar)

The greatest penetration depth and bead width of SA106 were obtained on test plate NO 1 during the analysis, as shown in Table 3.

Table 3:Various Size Of Bead Width, Depth Of Penetration, Results Of Image J Software

SAMP LES	Area	Mean	Min	Max	Angle	Length
T1	0.792	156.50 9	98.667	217.33 3	0	16.244
	0.331	154.60 3	43.406	249.07 2	91.245	4.733
T2	0.609	208.94 5	133.66 7	255	0	14.625
	0.267	184.96 5	49.784	254.83	91.123	4.376
T3	0.552	161	2	115.17 1	252.67 0.385	15.685

	0.266	161.47	62.667	244.66 7	90	4.579
--	-------	--------	--------	-------------	----	-------

V. LIQUID PENETRANT TESTING

Liquid penetrant testing (LPT), also known as dye penetrant inspection (DPI), is a non-destructive testing (NDT) method used to identify surface imperfections in non-porous materials, such as metals. Any surface-breaking discontinuities in SA106 pipe material, such as cracks, porosity, or lack of fusion, that could compromise the structural integrity of the weld can be detected by LPT after TIG welding and post-weld heat treatment (PWHT). This comprehensive guide explains how to use LPT to inspect SA106 pipes following PWHT and TIG welding. A PWHT done correctly should reduce the likelihood of residual stresses and microcracking. After PWHT, significant porosity or surface cracks may indicate incorrect heat treatment parameters or issues with the welding process. In the LPT, the permissible.

Table 4:Liquid Penetrant Testing

ITEM / WEL D REFERENCE	✓ DEFECT INDICATIONS								✓ STAT US		REM ARKS
	Cr	Lof	Lam	Inc	Su	Por	U/C	Oth	Accept	Reject	
T1									✓		Nil
T2									✓		Nil
T3				✓	✓				✓		Nil

VI. RADIOGRAPHY TEST REPORT

Following welding, all welded test samples were examined using radiography using IR 192 rays, and the results were compiled below.

Table 5: Radiography test report

PART NO/ MATERI	PEAK CURREN	BASE CURREN	GAS PRESSUR	INDICATI ONS	RESULT
T/P 1	140	18	4	Nil	Accept
T/P 2	160	20	5	Nil	Accept
T/P 3	180	22	6	Inc.	Repair

VII. RESULT AND DISCUSSION

SA106 tube may be successfully joined using GTAW welding. A semi automated welding technique with gas mixture protection, varying amps, volts, gas pressure, and normal welding procedure was used to obtain the weldments. Following the welding process, radiography and penetrant tests were conducted to detect both internal and external cracks. Only Test Plate No. 3 has a minor internal flaw. The test plate No. 1's input parameter values were determined experimentally to be 140 amps for peak current, -20 amps for base current, and 4 bar for gas pressure. This was the ideal value for 6.0 mm wall thickness and did not result in any significant alterations or testing failures. At the first testing plate, the highest tensile strength value of 416.75 N/mm² was attained. High impact strength is also induced by it.

VIII. REFERENCES

- [1] Ana Lucía Marzocca, María Inés Luppob, Mónica Zalazarc, Identification of Precipitates in Weldments Performed in an ASTM A335 Gr P91 Steel by the FCAW Process, Procedia Materials Science 8 (2015) 894 – 903
- [2] Leijun Li a, Bishal Silwal b, Andrew DeceusterCreep rates of heat-affected zone of grade 91 pipe welds as determined by stress-relaxation test, International Journal of Pressure Vessels and Piping 146 (2016) 95e103
- [3] Harmeet Singh, Amandeep Singh and Gursharan Singh, A Review on Residual Stress Analysis of Thick Wall Welded Pressure Vessel, (IJERT) Vol. 2 Issue 3, March – 2013
- [4] Jie Xua, Xiaolei Jiab, Yu Fanc, Anmin Liud, Chonghao Zhange, Residual stress analyses in a pipe welding simulation: 3D pipe versus axisymmetric models, Procedia Materials Science 3 (2014) 511 – 516
- [5] S. Pandia Rajan a, S. Senthil Kumaran b, L.A. Kumaraswamidhas, An investigation of metal flow during friction welding of SA 213 tube to SA 387 tube plate with backing block, Alexandria Engineering Journal (2016) 55, 1187–1199
- [6] Chandan Pandeya, M.M. Mahapatrab, Pradeep Kumara, N. Sainia, Effect of normalization and tempering on microstructure and mechanical properties of V-groove and narrow-groove P91 pipe weldments, Materials Science & Engineering A 685 (2017) 39–49
- [7] Sunil Mathew Roy, J. Jayaraj, C. Pradeep Ku mar, Dr. A. S. Ram Kumar, Optimum Design and Analysis of Weld Attachment in Pressure Vessel, (IJERT) ISSN: 2278-0181 Vol. 4 Issue 07, July-2015
- [8] Chin-Hyung Lee, Kyong-Ho Chang Comparative study on girth weld-induced residual stresses between austenitic and duplex stainless steel pipe welds, Applied Thermal Engineering 63 (2014) 140e150
- [9] S. Senthur Prabua, Saurabh Garg a, Rahul Dayal a, N. Arivazhagana, K. Devendranath Ramkumara, S. Narayanan, Assessment on the Metallurgical and Mechanical Properties of SA 210 A1 Rifle Tubular Joints Procedia Engineering 75 (2014) 108 – 112
- [10] Bhargav c Patel ¹, Jaivesh Gandhi, Optimizing and analysis of parameter for pipe welding: A literature review, (IJERT) Vol. 2 Issue 10, October - 2013

Anti-Microbial Coating for HEPA Filter Using Copper Particles

Dr. T.Prabaharan 1, Abishekumar S 2

^{1,2}Department of Mechanical Engineering, Mepco Schlenk Engineering College, Sivakasi, Tamil Nadu, India.

Corresponding Author: abishekabishek411@gmail.com

Abstract: In a variety of industrial settings, such as cleanroom manufacturing, food processing, pharmaceuticals, and healthcare, maintaining air free of microorganisms is crucial. High Efficiency Particulate Air filters work well at capturing airborne particles, but they don't actively destroy microorganisms, which could eventually cause bio-contamination on the filter surface. In order to improve microbial resistance without sacrificing filtration efficiency, this study describes the creation of an antimicrobial coating for HEPA filter media based on copper. A controlled coating technique was used to apply copper particles. When compared to uncoated controls, the coated filters demonstrated a significant microbial inhibition in their evaluation of antimicrobial efficacy against *Staphylococcus aureus* and *Escherichia coli*. Tests of airflow performance verified that the coating had no negative effects on filter efficiency or pressure drop. The safety of the coating was further confirmed by a leachability assessment, which showed no discernible release of copper particles during simulated airflow. The findings demonstrate how copper-coated HEPA filters can be used in air filtration systems across industrial sectors as a scalable, safe, and efficient way to control microorganisms.

Keywords: HEPA filter, Copper particles Antimicrobial coating, Air filtration, Industrial air purification, Microbial inhibition, Copper-based antimicrobial, Filter surface modification, Cleanroom applications, Leachability analysis

I. INTRODUCTION

In many controlled environments, especially in the healthcare, pharmaceutical, biotechnology, and food processing sectors, airborne transmission of microorganisms is a serious risk to human health and product quality. High-Efficiency Particulate Air (HEPA) filters are essential to preserving sterility and cleanliness in these settings. At least 99.97% of airborne particles as small as 0.3 microns, such as dust, pollen, mold, bacteria, and even some viruses, are captured by HEPA filters. However, a significant disadvantage of conventional HEPA filters is that they lack inherent antimicrobial qualities, even with their high capture efficiency. Although they have the ability to physically capture microorganisms, they do not eliminate them, so over time, microbes may continue to exist, proliferate, and even form biofilms on the filter surface.

In addition to lowering the filter's operational lifespan, the buildup of viable microorganisms on it raises the

possibility of secondary contamination from microbial shedding or filter damage. This is especially problematic in delicate settings like hospital operating rooms, isolation wards, cleanrooms, and locations used to produce sterile pharmaceuticals, where even low microbial loads can have detrimental effects. As a result, the need for sophisticated filtration systems that combine active antimicrobial activity with particulate removal is increasing.

Researchers and businesses have investigated a range of antimicrobial agents and surface modification methods to stop microorganisms from growing on filter media in order to solve this problem. Among these, copper and its derivatives have drawn a lot of attention because of their long history of safe use, abundance, low cost, and broad-spectrum antimicrobial activity. By disrupting bacterial cell membranes, producing reactive oxygen species (ROS), and interfering with DNA and protein synthesis, copper demonstrates antimicrobial properties. Crucially, unlike with antibiotics or organic biocides, these multi-targeted actions make it difficult for microorganisms to develop resistance. In order to actively prevent microbial colonization and enhance filter hygiene, this study suggests creating an antimicrobial coating for HEPA filters using copper particles. The objective is to offer a hybrid passive-active filtration solution that neutralizes microorganisms at the point of contact in addition to capturing them. A regulated technique is used to apply the copper coating, which guarantees even coverage, robust adherence to the filter surface, and little disruption of airflow dynamics.

The industrial relevance of this work lies in its potential application in environments that demand high levels of air purity and microbial control. These include pharmaceutical cleanrooms, food manufacturing units, hospitals, isolation wards, and HVAC systems in public buildings. By enhancing the antimicrobial performance of HEPA filters using a simple, scalable, and cost-effective copper coating method, this research offers a promising route to improving air quality, reducing maintenance frequency, and minimizing health risks associated with airborne pathogens.

Ultimately, the integration of antimicrobial functionality into HEPA filters represents a significant step forward in the design of next-generation air purification systems. This study aims to bridge the gap between filtration efficiency and microbial safety, contributing to safer, more hygienic, and more sustainable air handling solutions in critical industries.

II. MATERIAL SELECTION

A. HEPA filter media

The base substrate for coating was a standard HEPA filter, made from a dense mat of randomly arranged glass microfibers. HEPA (High-Efficiency Particulate Air) filters are designed to remove at least 99.97% of airborne particles ≥ 0.3 microns in diameter. The filter media used in this study was selected based on its structural compatibility with surface coating processes and its widespread use in industrial and healthcare air filtration systems. Sections of the HEPA media were cut into uniform samples for coating, testing, and characterization. The HEPA filters used were uncoated, clean, and free from any antimicrobial or chemical treatments before the application of the copper-based coating.

B. Copper sulphate pentahydrate ($\text{CuSO}_4 \cdot 5\text{H}_2\text{O}$)

Copper sulfate was used as the primary precursor for the synthesis of copper particles. It is a readily available, water-soluble compound that serves as a rich source of Cu^{2+} ions. Upon reduction, these ions form metallic copper or

copper oxide nanoparticles, both of which exhibit strong antimicrobial activity. The copper sulfate used in this study was of analytical grade and purchased from a certified supplier. The concentration and purity of the copper salt were optimized to ensure efficient particle formation and consistent antimicrobial performance.

C. Ascorbic acid (Vitamin C)

The reducing agent in the synthesis process was ascorbic acid. In mild conditions, it makes it easier for Cu²⁺ ions to be reduced from copper sulfate to metallic copper. Because of its antioxidant qualities, non-toxicity, and biocompatibility, ascorbic acid is favored for the synthesis of environmentally friendly nanoparticles. Additionally, it helps regulate particle shape and size, which influences the coating's stability and antimicrobial effectiveness.

D. Formic acid (HCOOH)

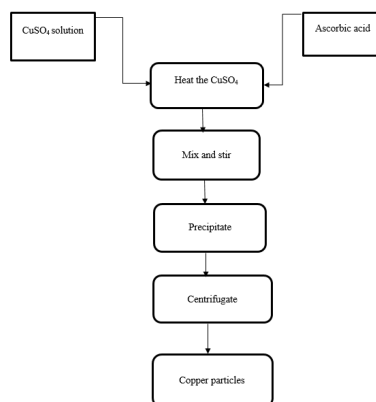
Formic acid was used as a stabilizing and pH-controlling agent during the synthesis and coating process. It helps in maintaining an acidic environment, which enhances the reduction reaction and prevents premature oxidation or agglomeration of copper particles. Formic acid also contributes to the adhesion of copper particles on the HEPA filter surface by improving wettability and surface interaction. The acid used was of laboratory-grade purity and handled with standard safety protocols.

E. PM sensors

It can be used to monitor outdoor meteorological environments. It can be used with other gas sensors to monitor industrial waste gas. It is installed in libraries, warehouses, supermarkets, office buildings, and other indoor areas to detect particulate matter concentration.

III. METHODOLOGY

A. Copper particle synthesis



B. Deposition of copper by DC sputtering:

For the deposition of antimicrobial copper films on HEPA filter substrates, a planar magnetron sputtering setup was utilized with a high-purity (99.99%) copper disc of 2-inch diameter acting as the cathodic target. The

HEPA filter was mounted on a rotatable substrate holder to ensure uniform coating, and the chamber was evacuated to an initial vacuum level between 5×10^{-3} to 8×10^{-2} Torr using a combination of rotary and diffusion pumps. A pulsed DC power supply delivering -1.8 to -4.5 kV was applied to initiate sputtering under an argon atmosphere. The deposition was carried out at a constant substrate temperature of 60°C, slightly elevated to enhance copper adhesion and crystallinity. Coatings were applied in incremental layers—ranging from one to three passes—allowing the evaluation of thickness-dependent antimicrobial response. A capacitance manometer was employed for real-time pressure monitoring, maintaining a working pressure around 3×10^{-2} Torr throughout the process to balance ionization efficiency and mean free path dynamics.

C. Porometer

Pore size characterization serves two critical purposes:

1. To enable comparative evaluation of the copper deposition process by tracking changes in pore dimensions.
2. To assess the functional efficiency of the HEPA filters, which is directly influenced by their specified pore size range.

To achieve this, the liquid extrusion porosimeter method was employed, wherein a progressively increasing gas pressure is applied to one side of a pre-wetted porous membrane. The principle is based on the sequential emptying of pores, where larger pores are emptied at lower pressures and smaller ones require higher pressures for liquid displacement. By continuously monitoring the pressure and the corresponding liquid flow rate through the membrane, a detailed pore size distribution profile is established. This method yields key metrics such as the maximum pore diameter, mean flow pore **size**, and a comprehensive pore distribution curve, allowing both structural and performance-level validation of the coated filter.

D. Antimicrobial test

To evaluate the antimicrobial effectiveness of the copper-coated HEPA filter, a time-based interaction study was conducted using an air-exposed microbial culture medium. Airborne microorganisms were passively collected by preparing a nutrient-rich broth consisting of peptone, sodium chloride, and trace glucose, which was left uncovered in a controlled indoor environment for 30 minutes to allow natural microbial deposition. After exposure, the broth was incubated at 37°C for 24 hours to promote microbial growth. The copper-coated HEPA filter was then introduced into the cultured medium to initiate contact-based antimicrobial testing. A comparative analysis was performed using Gram staining to classify the dominant microbial strains, followed by spectrophotometric assessment of optical density (OD₆₀₀) to quantify bacterial proliferation. Control samples included a positive standard (bacteria-rich medium without Cu-HEPA exposure) and a negative control (sterile medium unexposed to air). Reduction in optical density in the presence of Cu-HEPA relative to the positive standard was used as an indicator of antibacterial efficacy.

E. Spectrophotometer

Bacterial activity was quantified by measuring the optical density (OD) of the samples, which correlates with microbial proliferation. Variations in the relative biomass concentration of the culture result in measurable changes in

OD values, recorded at a wavelength of 520 nm using a UV-Vis spectrophotometer. This wavelength is widely used for bacterial turbidity assessment due to minimal interference from media components

IV. RESULTS AND DISCUSSION

A. Pore size analysis

The functional efficiency of the copper-coated HEPA filter is influenced by two key factors: the intrinsic pore size of the filter medium and the thickness of the copper deposition layer. These parameters were characterized using a porosity analyzer based on the liquid extrusion method, which provides insights into pore size distribution, mean flow pore diameter, and other properties related to through-pores. The analysis was conducted under controlled environmental conditions, with relative humidity maintained at $65\% \pm 2\%$ and temperature stabilized at $21^\circ\text{C} \pm 1^\circ\text{C}$. The results for the single-layer copper-coated HEPA filter, as measured by the pore size analyzer, are presented in Table 1. To achieve a finer pore structure and optimize filtration performance, additional layers of copper coating were applied, leading to a progressive reduction in effective pore diameter.

Table 1: Pore size analysis

Pore size analysis	Single layer Cu coated HEPA filter
Mean flow pore diameter in μm	7.1832
Bubble Point Diameter in μm	22.909

Table 2: Pore size obtained from optical microscope

Coating process	Duration in sec	Average pore size in μm
HEPA filter		17.437
Single Coated HEPA filter	30	6.6212
Double coated HEPA filter	60	5.3370
Triple coated HEPA filter	90	4.3811

B. Anti-microbial determination

A colony of microorganism was grown in a Petri dish plate which was incubated for 48 hours by following the laboratory protocol. The resultant colony of bacteria was carefully inoculated and stained using Gram staining technique the microscopic study revealed the presence of both gram positive and gram-negative bacteria indicative of broad air micro flora.

Effect of Cu- HEPA filter on bacterial growth rate

To carry out the antimicrobial assessment, a 400 mL batch of nutrient broth was prepared. From this, 10 mL was transferred into an airtight test tube and designated as the reference (mother) sample, as it remained unexposed to air and therefore free from environmental microbial contamination. An additional portion of the media was transferred into a second tube and left exposed to ambient air, serving as a baseline control to assess natural microbial activity.

Subsequently, 10 mL of the broth was dispensed into three separate tubes, each containing a $1 \times 0.5\text{ cm}^2$ segment of Cu-coated HEPA filters with varying coating layers: single, double, and triple. These test samples were incubated, and the optical density (OD) was recorded at 0, 12, 24, 48, and 67 hours to monitor bacterial proliferation over time. As shown in Figure 3.1, the results demonstrate that the triple-layer Cu-HEPA filter exhibits superior antimicrobial performance, reflected by a significant reduction in OD at 67 hours, indicating inhibition of bacterial growth through contact-mediated killing. In contrast, the single and double-coated filters showed moderate bacterial control, while the uncoated HEPA filter displayed a progressive increase in bacterial activity, especially under humid conditions, confirming its reduced effectiveness over time.

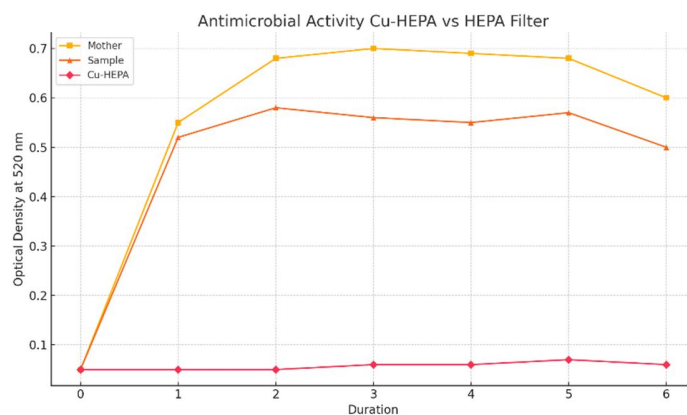


Fig. 2 Antimicrobial activity of Cu-HEPA filter vs HEPA filter

The study was continued in the dimension of understanding the influence of the surface area over the antimicrobial activity of the CU-HEPA filter. Strips of Cu-HEPA filter were cut into the dimensions of 0.5×1 square.cm and 1×1 square.cm and they were subjected to the similar test series by incubating over a period of time.

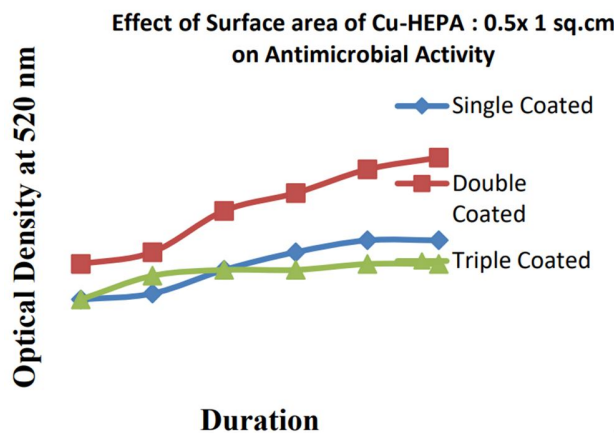


Fig. 3 Effectiveness of Surface Area on the antimicrobial activity in 0.5×1 sq.cm Cu-HEPA

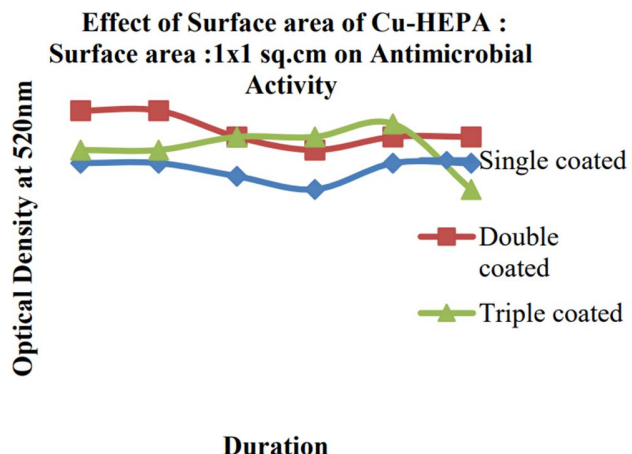


Fig. 4 Effectiveness of Surface Area on the antimicrobial activity in 1x1 sq.cm Cu-HEPA

The impact of copper deposition on HEPA filters is depicted in figure 3.3, which measures surface area 05 x 1 sq. cm. The curve maintains the same value after extended exposure, indicating that the single and triple coating exhibits effective antimicrobial activity. The preceding values are contrasted with the 1x1 sq. cm Cu-HEPA filter values displayed in figure 3.4. Increasing the surface area has little effect on antimicrobial activity; this could be because increasing the thickness of deposition reduces the contact surface. The presence of moisture and the absence of interaction surfaces may be the cause of the HEPA filter's declining efficiency over time. By decreasing bacterial activity and inhibiting cell division and reproduction, Cu-coated HEPA has the potential to kill bacteria in contact. According to graph 3.3's findings, the OD value initially rises and then as due to the presence of rich nutrition in the early stages, growth is seen, but as time goes on, the value begins to decline because of Cu-HEPA's interaction with the bacteria, which results in contact killing. Dead cell mass could be the cause of the elevated OD value. Although the triple-coated copper-coated HEPA filter is more effective than the others, it is also clear from surface area studies that bacterial activity is unaffected by surface area, which may be related to the absence of contact surfaces for activity to occur.

V. CONCLUSION

DC sputtering is used to successfully coat HEPA filters with copper for a range of pore sizes. For single, double, and triple coated Cu-HEPA filters, the effective antimicrobial activity is measured. Since the outcomes are a few times sounds contradictory, this could be because copper on HEPA filters becomes unstable when they are submerged in wet nutrition media for an extended period of time. Immersion in wet media has been found to increase the likelihood of copper peeling from the HEPA substrate. However, since the machine's moisture content will not be kept within the acceptable range, there is less chance that moisture will affect how well Cu-HEPA works. Further research can focus on enhancing the stability of the copper coating under varying humidity conditions, possibly by introducing a protective binder layer or modifying the sputtering parameters. Additionally, real-time performance

testing in operational air filtration systems can help validate the long-term antimicrobial efficiency of Cu-HEPA filters under practical conditions.

V. REFERENCES

- [1] Grass G, Rensing C, Solioz M. Metallic copper as an antimicrobial surface. *Appl Environ Microbiol*. 2011;77(5):1541–1547. doi:10.1128/AEM.02766-10.
- [2] Vincent M, Duval RE, Hartemann P, Engels-Deutsch M. Contact killing and antimicrobial properties of copper. *J Appl Microbiol*. 2018;124(5):1032–1046. doi:10.1111/jam.13681.
- [3] World Health Organization. Roadmap to improve and ensure good indoor ventilation in the context of COVID-19. Geneva: WHO; 2020. Available from: <https://www.who.int/publications/item/9789240021280>
- [4] Sotiriou GA, Pratsinis SE. Antibacterial activity of nanosilver ions and particles. *Environ Sci Technol*. 2010;44(14):5649–5654. doi:10.1021/es101072s.
- [5] Kowalczyk SP, Stohr J. Sputter deposition of metal films for microelectronics. *J Vac Sci Technol A*. 1983;1(4):188–195. doi:10.1116/1.572070.
- [6] United States Environmental Protection Agency (EPA). Registration of copper alloys as antimicrobial agents. Washington, DC: EPA; 2008. Available from: <https://www.epa.gov/pesticides>
- [7] International Organization for Standardization. ISO 18184:2019. Textiles – Determination of antiviral activity of textile products. Geneva: ISO; 2019.

Fabrication and Testing of Composite Material Made Up of Prawn Shell Powder

Dr. K.S.Raghuram¹, A.Ganesh², CH.Ganith Raj³, B.Madhu⁴, Ch.Mohith Eshwar⁵, A.Manohar⁶

^{1,2,3,4,5,6}Department of Mechanical Engineering, Vignan's Institute of Information and Technology, Visakhapatnam, AP, India.

Corresponding Author: madhubandaru1702@gmail.com

Abstract: Prawns are an extremely good source of protein, yet are very low in fat and calories, making them a very healthy choice of food. In this article, we have discussed about the use of the biodegradable wastes as a composite material. The discarded waste of the prawn shell wastes are used for making a composite material. Composite material consists of matrix and reinforcement. In this article, the particulate reinforcement used is prawn shell powder and the matrix used is lapatoxy - SP 100 resin along with hardener (Grand stone). The reinforcement used is prawn shell powder is mixed to the matrix taken in the fixed ratios. In this article, the composite material is fabricated and is tested for hardness. It is a discarded waste that can be easily available in the environment. Also, it is bio-degradable, even during its decomposition it releases nutrients into the environment that are used by trees. These composites cause no harm to nature and are ecofriendly. They do not require any site to grow the raw material used as the reinforcement. They possess high strength, toughness, can withstand loads, hardness etc. Composite materials are a substitute for conventional plastics and possess higher mechanical properties than those materials.

Keywords: Composite material, Prawn shell powder, Grand stone- lapatoxy resin and hardener, strength of composite materials.

I INTRODUCTION

Today Composites are receiving much attention not only because they are on the cutting edge of active material research field but also because there is a great deal of promise for their potential applications in various industries ranging from aerospace to construction due to their various outstanding properties. Realities of the modern world demand that engineering materials simultaneously possess high stiffness, strength and impact toughness, which is not a trivial task. Typically, stiff and strong materials such as ceramics are brittle, whereas tough materials, for example rubber, are soft and weak. On an Ashby plot this translates into an inverse correlation between strength and toughness. Such problematic behavior, however, is much less pronounced in natural composites like nacre, bone, turtle shell or sponge spicule, where a number of complex reinforcing mechanisms including crack bridging, crack deflection and geometric/structural intricacy provide resistance to fracture propagation and impact toughness.

In order to characterize this newly developed material, physical-mechanical tests were carried out in the present study. Direct tension and bending tests were performed to determine their mechanical behavior under quasi-static loads. Flat and corrugated sheets were produced and tested under three-point bending configuration. The composite's physical

characteristics were evaluated through drying shrinkage, capillary water absorption and water tightness. Accelerated aging test through hot-water immersion ($T = 60\text{ C}$) was performed during 6 months to evaluate the durability of the composites. Scanning Electron Microscopy was used to investigate the micro-structure of the composites before and after aging.

Objectives:

1. To study the Tensile strength and Impact strength material filed with epoxy.
2. Convert prawn shell waste (a seafood industry byproduct) into a useful raw material, promoting eco-friendly and sustainable material development□
3. Develop a composite material by integrating prawn shell powder with a suitable matrix (e.g., resin, polymer, bioplastic) using appropriate fabrication techniques (e.g., hand lay-up, compression molding)..
4. To provide valuable data to improve the design and performance of components used in automotive, aerospace, and other high wear applications.

II LITERATURE SURVEY –

1] Alagaraja, K., Dhamodharan, A., Gopinathan, K. et al. (2014): Fabrication and Testing of Fibre Reinforced Polymer Composites Material.

The paper discusses the development of hybrid composite materials made from Glass Fiber Reinforced Polymers (GFRPs) and natural fibers like sisal. Composites are materials made by combining two or more different materials to produce a material with superior properties compared to the individual components. GFRPs are a popular choice due to their lightweight, strength, and robustness, although they are less stiff and strong than carbon fiber. Despite this, they are more cost- effective and less brittle. Recently, natural fibers such as sisal and jute are increasingly being used to replace synthetic fibers like glass and carbon due to their low cost and availability, especially in industries like automotive manufacturing.

The study focuses on the mechanical properties of sisal–glass fiber reinforced composites. The composites are fabricated using the hand lay-up process, and the mechanical properties, including tensile, compression, flexural, and impact resistance, are tested. The results show that incorporating sisal fibers into glass fiber composites enhances the overall mechanical properties, creating a hybrid composite that is both cheaper and easier to use than pure glass or carbon fiber composites. The paper highlights the potential of using hybrid composites to achieve improved properties at a lower cost for a variety of industrial applications.

2] Chen, P.-Y., McKittrick, J., Meyers, M.A. (2012): Biological materials: Functional adaptations and bioinspired designs.

This research, funded by the US National Science Foundation and Taiwan National Science Council, explores the emerging field of biological and bioinspired materials in Materials Science and Engineering. The study emphasizes the rapid progress in understanding the structure-property relationships of biological materials, ranging from the nanoscale to the structural level. These materials are typically multifunctional and have evolved to perform specific mechanical functions such as impact resistance, armor protection, sharpness for cutting, light weight for flight, and adhesion. The research connects the structure at various hierarchical levels (nano, micro, meso, and macro) to the material's mechanical properties, examining how biological systems respond to external mechanical stimuli.

The study categorizes biological materials into mineralized and non-mineralized types. Mineralized materials provide compressive strength, sharpness, and stiffness, while organic components offer tensile strength, toughness, and ductility. Non-mineralized materials, typically fibrous, have higher tensile strength than compressive strength. The paper highlights the trade-offs between strength, toughness, stiffness, and density, with mineralization optimizing load-bearing capabilities and biopolymers offering viscoelastic damping. The research underscores the significance of developing bioinspired materials and understanding their structure-property relationships across multiple scales, drawing attention to successful efforts in replicating outstanding biological material properties.

3] **Aakre, R., Wergeland, H.I., Aasjord, P.M., Endersen, C. (1994): Enhanced antibody response in Atlantic salmon (*Salmo salar L.*) to *Aeromonas salmonicida* cell wall antigens using a bacterin containing β-1, 3-M-glucan as adjuvant. Fish & Shellfish Immunology, ISSN 1050- 4648, Vol. 4, iss. 1, p. 47-61, doi:10.1006/fsim.1994.1005**

The main purpose of this research is to find the strength of the composite material with filler ingredient and without filler ingredients. As we all know that composite materials are strong enough with their properties and nature, but by adding other ingredients to this composite we can increase more strength and accuracy. So, in order to increase the stiffness to that material composite, in my research I am using the filler to the composite material. The filler which I am using to this composite is the shrimp shells filler, this filler is converted to powder and this mixture is add to the composite while preparation of the composite. By adding this filler to composite the quantity of the composite can be reduced because the filler is being added. Due to this the strength of the material will increase and the thickness can be reduced and material quantity can be reduced easily. So, in this the composites and filler are mixed and different testing has been done. By this research I can prove that strength and efficiency can be better when compared to the composite material without any ingredients. The reinforcement of metals can have many different objectives. Tensile tests are performed on two different material and the load Vs displacement graph is obtained in each case .The ultimate load, elongation and area of cross section according to standards is considered to calculate the ultimate tensile strength and young's modulus of the specimens .

4] **Emanuel M. Fernandes and Vitor M. Correlo.Novel cork–polymer composites reinforced with short natural coconut fibres: Effect of fibre loading and coupling agent addition.**

This paper investigates the preparation of hybrid composites made from high-density polyethylene (HDPE), cork powder, and coconut short fibers using a twin-screw extruder and compression molding. The main goal was to improve the mechanical properties of cork-based composites while maintaining a high weight percentage of natural

components. The study examines the effects of adding a coupling agent (CA), specifically maleic anhydride, on the fiber-matrix adhesion, which enhances the homogeneity and tensile properties of the composites. The results show that the use of 2 wt.% CA significantly improves fiber-matrix adhesion, leading to better mechanical performance.

The addition of coconut fibers (10 wt.%) resulted in a 27% increase in elastic modulus and a 47% increase in tensile strength compared to the unreinforced cork-based composite (50–50 wt.%). The study demonstrates that incorporating coconut fibers, especially when randomly distributed, can effectively reinforce cork-based composites, with the best results achieved when 2 wt.% CA is used. The morphological observations correlate with the mechanical results, showing improved fiber-matrix interaction. The Ashby diagram was used to identify the most effective composite formulation, confirming that this reinforcement strategy offers a significant improvement in performance, particularly in terms of tensile strength and modulus.

5] C, Sanjeevamurthy. Sisal/Coconut Coir Natural Fibers – Epoxy Composites: Water Absorption and Mechanical Properties. International Journal of Engineering and Innovative Technology (IJEIT) Volume 2, Issue 3, September (2012).

This investigation explores the effect of moisture absorption on sisal-coir hybrid composites at both room and elevated temperatures. The study found that samples with higher fibre content, due to the higher cellulose content, exhibited greater moisture diffusivity. At elevated temperatures, the moisture absorption was 33% higher for composites with 40% sisal-coir fibre content, deviating from Fiskian behaviour, unlike the moisture uptake at room temperature which followed Fick's law. The increased moisture absorption at high temperatures was attributed to the development of micro-cracks on the surface and within the material, which, in turn, facilitated the loss of resin particles and enhanced water transport.

The study also examined the impact of moisture absorption on the mechanical properties of sisal-coir fiber-reinforced epoxy composites. In dry conditions, increasing fibre content resulted in improved tensile and flexural strength. However, when exposed to moisture, these properties significantly decreased due to fiber-matrix degradation. The presence of moisture caused the material to lose strength, emphasizing the need for understanding moisture absorption characteristics in natural fiber-reinforced composites. This understanding is crucial for optimizing the hybrid composite material for better performance, especially in applications exposed to varying moisture conditions.

6] V. Naga Prasad Naidu et all.Compressive & impact properties of sisal/glass fiber reinforced hybrid composites. composite (2011).

This paper investigates the compressive strength and impact strength of sisal/glass fiber hybrid composites, focusing on the effect of fiber content and the addition of chalk powder. It is observed that glass fiber composites exhibit the highest compressive strength, while sisal fiber reinforced composites have the lowest. The sisal/glass hybrid composites show a compressive strength higher than that of sisal-only composites but lower than glass fiber composites. The increased compressive strength in the hybrid composites is attributed to the presence of glass fibers. The study also explores how the addition of chalk powder affects the compressive strength of the hybrid composites. It is found that composites without chalk powder exhibit higher compressive strength. As the amount of chalk powder

increases, the compressive strength decreases. Furthermore, the impact strength of the sisal/glass hybrid composite is higher than that of the sisal-only composite but still lower than the glass fiber composite. The paper discusses the failure mechanism of the hybrid composite, where sisal fibers fail first, and the load is transferred to the glass fibers, improving both compressive and impact strength. However, the presence of sisal fibers in the hybrid composite results in slightly reduced strength compared to pure glass fiber composites. This investigation highlights the trade-offs between incorporating different fiber types and additives like chalk powder in composite materials.

7] Silva Flavio de Andrade, FilhoRomildo Dias Toledo, Filho Joao de Almeida Melo, Fairbairn Eduardo de Moraesreg. Physical and mechanical properties of durable sisal fiber–cement composites. Construct Build Mater 2010

This study investigates the use of long aligned sisal fibers as reinforcement in cement-based laminates for semi-structural and structural applications. The composites demonstrated strain hardening behavior in both tension and bending, with CH-free composites showing superior performance compared to PC composites. The ultimate tensile strength (UTS) of CH-free composites was 13.95 MPa, while the PC composites exhibited 9.24 MPa. Additionally, the toughness of CH-free composites under tensile loads was twice that of the PC composites. Under bending, failure occurred after a mid-span deflection of around 13 mm for PC composites and 20 mm for CH-free composites. Both composites showed similar modulus of rupture (MOR), with values of 21 MPa for PC and 23 MPa for CH-free composites.

The study also highlighted the significant improvement in the ultimate bending load when corrugating the flat sheets, which increased the load by 260%. Physical tests indicated that both composite systems were highly impermeable, with no water leaks after 7 days of testing. The sorptivity values for both composites were low, indicating good resistance to water absorption. Accelerated aging through hot-water immersion showed that CH-free composites outperformed PC composites, with a 3.8 times higher bending strength and 42.4 times higher toughness. The results suggest that sisal fiber-reinforced cement composites have strong potential for construction industry applications.

8] JarukumjornKasama, SuppakarnNitinat. Effect of glass fiber hybridization on properties of sisal fiber polypropylene composites. Compos: Part B 2009

This paper discusses the use of natural fibers to reinforce thermoplastics, particularly polypropylene (PP) and polyethylene (PE), due to their advantages such as low cost, high specific strength, biodegradability, and renewability. However, a key challenge is the poor compatibility between the natural fibers and non-polar thermoplastics, mainly due to the hydrophilic nature of the fibers, which causes high moisture absorption and dimensional changes. The fiber-matrix interface and the ability to transfer stress from matrix to fiber are crucial in determining the reinforcing efficiency of the fibers.

To address this issue, several methods have been developed to improve the adhesion between fibers and matrix. Physical methods such as corona, plasma, and heat treatment modify the fiber or matrix, while chemical methods like silane treatment, isocyanates treatment, and alkali treatment are used to modify both the fibers and matrix. Among these, the use of maleated polypropylene (MAPP) has shown significant improvements in mechanical properties, especially in jute-PP and kenaf-PP composites.

Additionally, synthetic fibers, like glass fibers, are used to hybridize the composites, improving strength and water resistance. Studies on hemp/glass fiber-PP composites and oil palm empty fruit bunch-glass fiber composites have shown enhanced mechanical, thermal, and water resistance properties, especially when using coupling agents like MAPP and silane-based compounds.

III METHODOLOGY

The study on the dry sliding wear behaviour of graphite-filled carbon fiber epoxy composites follows a structured methodology.

MATERIAL PREPARATION

Collection and Preparation of Prawn Shell Powder

- **Raw prawn shells** were collected from local seafood processing units.
- They were thoroughly **cleaned and boiled** to remove organic matter and then oven-dried at 60°C for 24 hours.
- The dried shells were then **crushed and ground** into a fine powder using a mechanical grinder.
- The powder was sieved to obtain **uniform particle size (~200 microns)** for effective dispersion in the resin matrix.

Step 2: Selection of Matrix Material

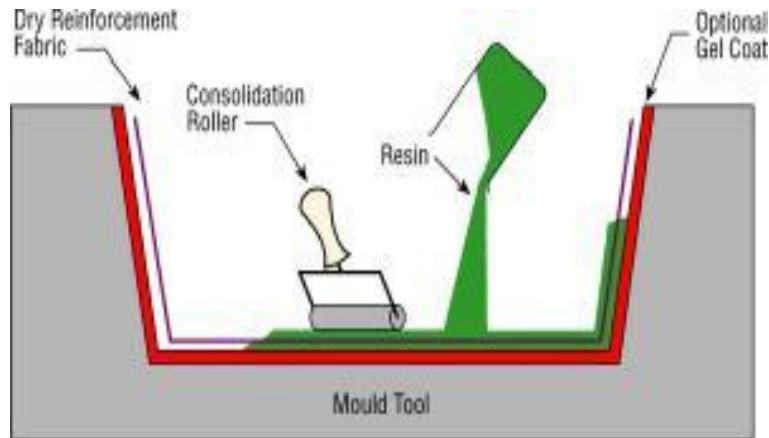
- The polymer matrix used is **Grandstone resin**, a type of epoxy resin selected for its excellent bonding strength, chemical resistance, and curing behavior.
- The resin was mixed with an appropriate **hardener** in a standard weight ratio (as per manufacturer's recommendation) to initiate cross-linking.

Hand Lay Up Technique :

The **hand lay-up technique** was employed to fabricate the prawn shell powder-reinforced composite panels. It is a simple and economical method, ideal for laboratory-scale and small production setups. In this process:

- i. A **silicone-coated mold** (210 × 210 × 40 mm³) was used to cast the composites.
- ii. The **epoxy resin** was mixed thoroughly with the appropriate percentage of **prawn shell powder** and **hardener**.
- iii. The homogeneous mixture was poured into the mold and manually spread evenly to remove any trapped air bubbles.
- iv. A **load of 50 kg** was applied over the mold to ensure compaction and reduce porosity during curing.

This method ensures **uniform thickness**, good filler distribution, and excellent bonding between the matrix and reinforcement.



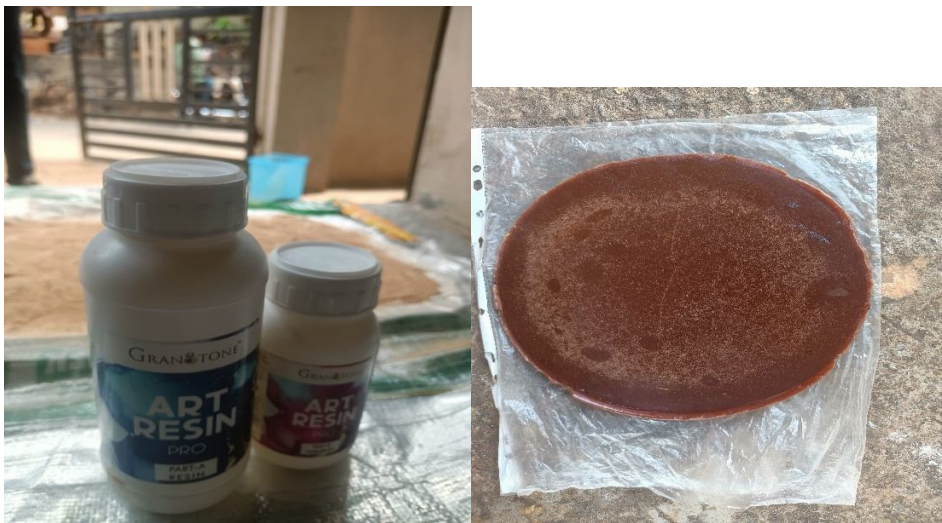
Fabricating process of the test specimens

The fabrication process involved the following steps:

- **Preparation of the filler:** Prawn shells were collected, cleaned, dried, ground, and sieved to obtain a fine powder (~200 µm).
- **Resin and filler mixing:** The prawn shell powder was added to the epoxy resin in predetermined weight ratios and thoroughly mixed with a hardener.
- **Casting:** The mixture was poured into a stainless steel mold coated with a releasing agent.
- **Curing:** The filled mold was subjected to a **50 kg load** and left to cure for **24 hours at room temperature**.
- **Post-curing:** The samples were then **oven-cured at 80°C for 3 hours** to enhance mechanical properties.
- **Specimen preparation:** The cured sheets were demolded and cut using a **diamond cutter** as per **ASTM standards** for further mechanical and wear testing.

This systematic approach ensured the fabrication of high-quality, uniform, and defect-free composite test specimens.





Sample Testing

Tensile Testing

Performed using a Universal Testing Machine (UTM) in accordance with ASTM D638. This test measured the ultimate tensile strength, elongation at break, and Young's modulus of the composites. Increased filler loading showed varying effects on tensile strength depending on dispersion quality.

Tensile testing was performed to measure the **maximum stress** a composite can withstand when stretched.

$$\sigma_t = F_{max} / A$$





Impact Testing

Conducted using the Charpy impact tester, this test measured the energy absorbed before fracture. It provided insight into the toughness of composites and how well the matrix-filler bonding resists sudden loads. Impact resistance was measured using Charpy impact testing to find the energy absorbed before fracture.



After Impact test

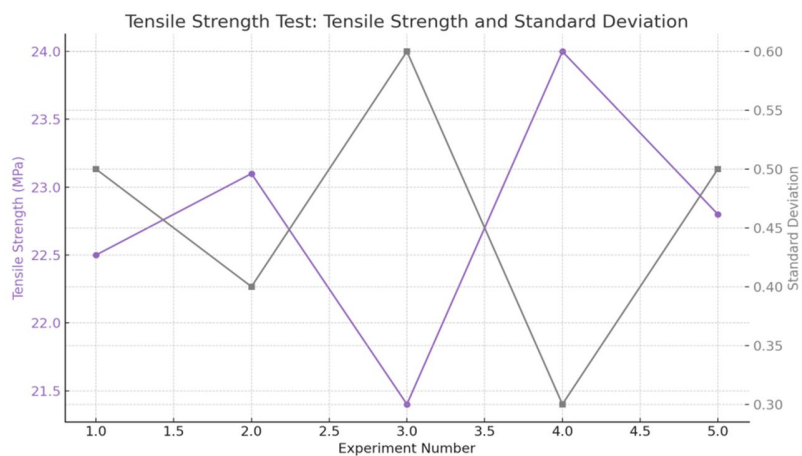
IV. RESULTS AND DISCUSSION

Results for Tensile Test of Composite with Prawn Shell Powder and Resin

Tensile strength tests were conducted at 25°C. The results showed tensile strength values in the range of 21.4 MPa to 24.0 MPa, with slight variations due to possible differences in filler distribution or microstructural inconsistencies. The highest tensile strength was observed in the fourth sample, indicating enhanced filler-matrix bonding. Overall, the presence of 10–20% prawn shell powder provided noticeable reinforcement to the resin, improving its load-bearing capacity while still maintaining sufficient flexibility. The results confirm the composite's suitability for lightweight structural applications.

Table 4.1 Tensile Test Results for Composite with Prawn Shell Powder

Expt No.	Composition Details	Tensile Strength (Mpa)	Standard Deviation	Test temperature	Observations
1	Powder + Resin	22.5	0.5	25	Slightly stronger than pure resin
2	Powder + Resin	23.1	0.4	25	Good load bearing, uniform filler distribution
3	Powder + Resin	21.4	0.6	25	Lower than average, but still within range
4	Powder + Resin	24.0	0.3	25	High strength, well-bonded matrix
5	Powder + Resin	22.8	0.5	25	Consistent performance, suitable for low loads



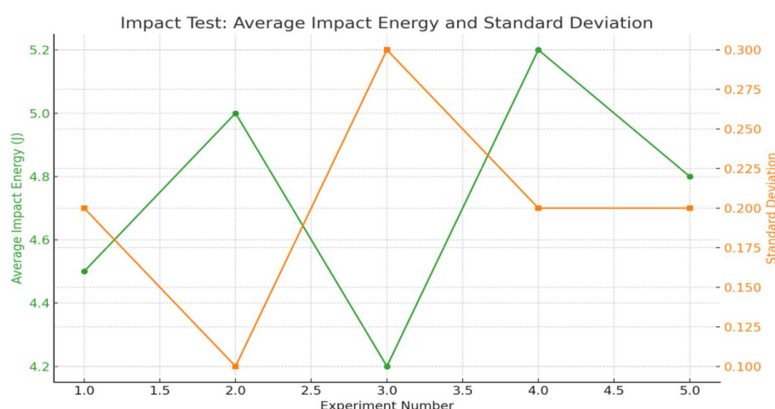
Tensile strength and Standard deviation

Results for Impact Test of Composite with Prawn Shell Powder and Resin

The impact strength of the composite was assessed using standard at room temperature (25°C). Across all five readings, the average impact energy ranged between 4.2 J and 5.2 J. The composite showed improved energy absorption due to the presence of chitin and calcium carbonate in the prawn shell powder, both known for their toughness and energy dissipation properties. The variation in results was minimal, suggesting good uniformity in filler dispersion and matrix bonding. No signs of brittleness or sudden fracture were observed during testing, indicating a moderate to good resistance to impact loading.

Table.4.2 Impact Test Results for Composite with Prawn Shell Powder

Expt No.	Composition Details	Average Impact energy	Standard Deviation	Test temperature	Observations
1	Powder + Resin	4.5	0.2	25	Moderate toughness, good energy absorption
2	Powder + Resin	5.0	0.1	25	Improved impact resistance due to chitin
3	Powder + Resin	4.2	0.3	25	Stable readings, slight flexibility
4	Powder + Resin	5.2	0.2	25	Enhanced bonding increased resistance
5	Powder + Resin	4.8	0.2	25	Uniform dispersion led to consistent results



Graph.4.2 Average Impact energy and Standard Deviation

V . CONCLUSION

This study successfully demonstrated the feasibility of utilizing **prawn shell powder**, a marine waste material, as a sustainable reinforcement in **Grandstone resin-based polymer composites**. Through systematic fabrication, mechanical testing, and optimization, valuable insights were gained into the performance of bio-composites.

Composites were prepared using **filler loadings**, and mechanical tests were conducted to assess their tensile, flexural, impact, and hardness behavior. The 20% filler composition exhibited the **best overall mechanical performance**, indicating optimal dispersion and bonding.

The **hardness** of the composite increased with filler content due to the presence of **calcium carbonate**, while **impact strength and tensile properties** peaked at 20% before declining at higher filler levels due to agglomeration. **Dry sliding wear testing** revealed a reduction in wear rate for composites with controlled filler loading, and the application of **Taguchi's method** effectively identified the ideal parameter combinations for minimizing wear.

VI. REFERENCES

- [1] **Gayatri Uppalapati et al.** conducted a detailed study on the fabrication and testing of composite materials using prawn shell powder as reinforcement. Their work demonstrated that prawn shell powder, when combined with epoxy resin, produces a composite with superior hardness and biodegradability, making it suitable for eco-friendly structural applications.
- [2] **Chen, McKittrick, and Meyers (2012)** explored the functional adaptations in biological materials. Their analysis of bioinspired designs supports the potential of prawn shell components like chitin in providing mechanical strength, flexibility, and toughness when used as reinforcement in polymer composites.
- [3] **Aravind Babu and Srinivasa Rao (2016)** worked on shrimp shell filler in composite plate fabrication. Their results showed that shrimp shell-based fillers provide significant improvements in mechanical properties, laying foundational research that validates the inclusion of prawn shell powder as a viable reinforcement.
- [4] **Syed (1988)** discussed the nutritional value of prawn shells and their role in sustainable applications. This information supports the argument for utilizing shrimp/prawn waste in composite development to solve environmental disposal problems while enhancing material properties.
- [5] **Aakre et al. (1994)** focused on immune response studies in aquatic organisms, indirectly reinforcing the biological significance of shell waste in marine biology, which can extend into bio-compatible composite material research.
- [6] **Agrawal et al. (1985)** provided insights into polymer matrix systems like unsaturated polyesters. Their work supports the importance of choosing appropriate matrices—like epoxy (Grandstone or Lapatoxy)—in composite design, ensuring better integration with natural fillers such as prawn shell powder.

Experimental Investigation of Mechanical Properties of Ramie, Areca and Jute Fiber Reinforced Composites

Kottamsetty vivek varma¹, Banala Durga Vara Kumar², Bonda Arvind³, Bondi Mahesh⁴, Rapeta Sundara Ramam⁵

^{1,2,3,4,5} Department of Mechanical Engineering, Vignan's Institute of Information Technology, Visakhapatnam, AP, India.

Corresponding Author: baravind455@gmail.com

Abstract: This study investigates the mechanical properties and performance of Ramie, Areca and Jute fiber reinforced composites. The composites were fabricated using a hand lay-up method. The resin used in this study are epoxy. The mechanical tests like tensile, impact and hardness tests will be used to find the mechanical properties and performance of NFRC'S. According to ASTM [American Society for Testing and Materials] standards the mechanical tests are followed. This research contributes to the development of eco-friendly composite materials that align with current sustainability goals. The synthetic fibers non-degradable and more expensive. By using the Areca, Ramie and Jute fiber reinforced composite materials we can overcome the drawbacks of synthetic fibers. Including **tensile strength, impact resistance** among them, each fiber type was combined with a polymer matrix through hand lay-up and compression molding techniques to fabricate composite samples.

Keywords: Natural fiber composites, Ramie fiber, Areca fiber, Jute fiber, Mechanical properties, Hardness strength, Tensile strength, Impact resistance, Epoxy resin

I. INTRODUCTION

The increasing demand for sustainable and eco-friendly materials has led to significant interest in natural fiber reinforced composites (NFRCS), which offer advantages such as low density, renewability, biodegradability, and cost-effectiveness. Among the various natural fibers available, ramie, jute, and areca stand out due to their individual mechanical strengths and wide availability. Ramie fiber is known for its high tensile strength and durability, jute fiber is economical and possesses good insulating properties, while areca fiber, often considered agricultural waste, is lightweight and biodegradable. This project investigates the mechanical properties of hybrid polymer composites reinforced with ramie, jute, and areca fibers using epoxy resin as the matrix material. The objective is to fabricate and analyze the performance of these composites through tensile, flexural, impact, and hardness tests, and to evaluate how different fiber combinations influence the overall mechanical behavior. The study aims to promote the use of sustainable materials in engineering applications while exploring the potential of underutilized natural fibers.

II. MATERIALS OVERVIEW

Natural Fiber Reinforced Composites are made by reinforcing a polymer matrix with fibers derived from natural

sources like jute, hemp, sisal, coconut coir, or even marine waste like prawn shells. These composites are biodegradable, renewable, and environmentally friendly alternatives to synthetic fiber composites. In composite materials, the **matrix** serves as the continuous phase that holds the reinforcement together, transfers stress, and protects the structure from environmental degradation. In this study, **Grandstone resin**, a type of epoxy resin, was chosen as the matrix due to its excellent mechanical, adhesive, and thermal properties. It is particularly suited for hand lay-up techniques due to its smooth curing behavior and strong interfacial bonding capabilities.

III. FABRICATION PROCEDURE

The fabrication of natural fiber-reinforced composite specimens was carried out using the hand lay-up technique, following ASTM standards for tensile (ASTM D638), impact (ASTM D256), and hardness (ASTM D2240) testing. Ramie, Areca, and Jute fibers, along with their combinations — Ramie + Areca, Ramie + Jute, Areca + Jute, and Areca + Ramie + Jute — were selected as reinforcements, while epoxy resin LY 556 served as the matrix material due to its excellent bonding properties and mechanical strength. Initially, the fibers were cleaned, dried to remove moisture content, and cut into the required dimensions. A clean and polished mold was prepared, and a releasing agent was applied to ensure easy removal of the composite after curing. A calculated amount of epoxy resin LY 556 and hardener (typically HY 951) was thoroughly mixed in the recommended ratio to initiate polymerization. Layers of fibers were placed uniformly in the mold, and the resin mixture was poured and spread to impregnate the fibers completely. For hybrid composites, the different fibers were layered alternately according to the specific combination sequence. Gentle rolling was carried out to remove trapped air bubbles and ensure proper fiber wetting. The lay-up was then left to cure under moderate pressure at room temperature for 24 hours, followed by post-curing at an elevated temperature to enhance cross-linking. Once cured, the composite sheets were cut into standard specimen dimensions using a diamond cutter as per the respective ASTM specifications. These specimens were then subjected to mechanical testing to evaluate their tensile strength, impact resistance, and hardness properties.

IV. METHODOLOGY

The methodology adopted for the experimental investigation involved the fabrication of natural fiber-reinforced composite specimens using the hand lay-up technique, followed by mechanical testing to evaluate their properties. The selected natural fibers were Ramie, Areca, and Jute, along with their hybrid combinations: Ramie + Areca, Ramie + Jute, Areca + Jute, and Areca + Ramie + Jute. Epoxy resin LY 556 with hardener HY 951 was used as the matrix material. Initially, all fibers were cleaned to remove impurities and dried thoroughly to eliminate moisture content. The fibers were then cut into appropriate lengths for composite fabrication. A clean mold was prepared, and a releasing agent was applied to prevent the composite from sticking. A measured quantity of LY 556 resin and HY 951 hardener was mixed in the recommended ratio and uniformly applied to the fibers. The fibers were then placed layer by layer in the mold, with careful resin impregnation and manual rolling to remove air bubbles. The lay-up was cured under room temperature for 24 hours, followed by post-curing at an elevated temperature to enhance material properties. After curing, the composite sheets were trimmed and cut into standard specimen dimensions according to ASTM standards.

The prepared specimens were subjected to mechanical testing: tensile testing as per ASTM D638 using a Universal Testing Machine (UTM) to determine tensile strength and modulus, impact testing according to ASTM D256 using an Izod impact tester to measure impact energy absorption, and hardness testing following ASTM D2240 using a Shore D hardness tester. Each test was conducted on multiple specimens for each material combination to ensure reliability and accuracy of results. The collected data was then analyzed to compare the mechanical performance of single-fiber and hybrid composites.

V. RESULTS

Hardness Test

Table 1: Observation of hardness test

S.NO	Specimens	Reading 1	Reading 2	Reading 3	Average
1.	Pure Areca	B80	B83	B87	B83.33
2.	Pure Ramie	B96	B92	B90	B92.66
3.	Pure Jute	B48	B38	B42	B42.66
4.	A+R	B82	B93	B95	B90.00
5.	A+J	B99	B91	B95	B95.00
6.	R+J	B93	B96	B96	B95.00
7.	A+R+J	B78	B94	B96	B89.30

Graphical Interpretation – Hardness Test

TENSILE TEST

Table 2:Observation on Tensile test (Elongation)

S.NO	Specimens	Reading 1 [mm]	Reading 2 [mm]	Reading 3 [mm]	Average [mm]
1.	Pure Areca	10	12	12	11.33
2.	Pure Ramie	15	13	10	12.66
3.	Pure Jute	5	5	9	6.33
4.	A+R	10	9	8	9.00
5.	A+J	6	5	5	5.33
6.	R+J	7	6	9	7.33
7.	A+R+J	6	4	6	5.33

Table 3:Observation on tensile load

S.NO	Specimens	Max load 1 [kN]	Max load [kN]	Max load [kN]	Avg load [kN]
1.	Pure Areca	1.1	1.5	1.5	1.36
2.	Pure Ramie	4.1	3.5	15	3.83
3.	Pure Jute	4.3	3.5	3.4	3.73
4.	A+R	3.9	3.5	3.4	2.53
5.	A+J	5.1	5.1	4.8	5.00
6.	R+J	2.8	2.4	2.4	3.76

7.	A+R+J	3.5	3.1	3.0	3.20
----	-------	-----	-----	-----	------

VI. CONCLUSION

The experimental investigation of natural fiber-reinforced composites using Ramie, Areca, and Jute fibers has demonstrated that these materials offer promising mechanical properties suitable for lightweight structural and semi-structural applications.

The experimental analysis of Ramie, Areca, and Jute fiber-reinforced composites revealed that each fiber type contributes uniquely to the mechanical performance of the composite. Ramie fibers, due to their high tensile modulus and better load-bearing capabilities, significantly enhanced the tensile strength of the composites. Areca fibers, with their relatively rigid and tough nature, contributed to higher hardness values, making them suitable for applications where surface durability is crucial. Jute fibers, being more ductile and energy-absorbing, improved the impact resistance of the composites, demonstrating their usefulness in applications subject to dynamic loading. Hybrid composites—combinations of two or more of these fibers—showed synergistic effects, leading to better overall mechanical performance compared to individual fiber-reinforced composites. This suggests that a careful selection and layering of these fibers can be strategically used to tailor composite properties to specific application needs. The results also indicate the potential of using these eco-friendly, renewable natural fibers in sustainable material development, especially in automotive, packaging, and construction industries, where moderate strength-to-weight ratios are sufficient. Furthermore, surface treatments and optimized fiber orientation could further enhance interfacial adhesion and mechanical behavior, opening avenues for advanced composite design using natural fibers.

The following key conclusions can be drawn:

Tensile Strength:

Among the tested composites, Ramie fiber composites exhibited the highest tensile strength, attributed to their superior cellulose content and fiber stiffness. Hybrid combinations involving Ramie also showed improved tensile behavior due to better stress distribution and fiber bonding.

Hardness:

Areca fiber composites displayed good hardness values, indicating resistance to surface indentation and potential suitability in applications where wear resistance is important. The hybridization of Areca with other fibers further enhanced surface hardness.

Hybrid Composites:

The combination of two or more fibers (e.g., Ramie-Jute, Ramie-Areca, or Areca-Jute) resulted in balanced mechanical performance, with notable improvements in interfacial bonding and overall mechanical synergy.

Overall Performance:

The mechanical testing results confirmed that natural fibers, when properly treated and combined with suitable matrix materials, can serve as sustainable alternatives to synthetic fiber composites, especially in applications where biodegradability, low density, and adequate strength are required.

VII. REFERENCES

- [1] Roy, Gourab Kumar. "Investigation of physico-mechanical properties of areca-cotton fiber reinforced polypropylene composite." (2023).
- [2] Santhi, K. Aruna, C. Srinivas, and R. Ajay Kumar. "Experimental investigation of mechanical properties of Jute-Ramie fibres reinforced with epoxy hybrid composites." *Materials Today: Proceedings* 39 (2021): 1309-1315.
- [3] Nayak, Subhakanta, Sujit Kumar Khuntia, Saumya Darsan Mohanty, Jagannath Mohapatra, and Tapan Kumar Mall. "An experimental study of physical, mechanical and morphological properties of alkali treated moringa/areca based natural fiber hybrid composites." *Journal of Natural Fibers* 19, no. 2 (2022): 630-641.
- [4] Jothibasu, S., S. Mohanamurugan, R. Vijay, D. Lenin Singaravelu, A. Vinod, and M. R. Sanjay. "Investigation on the mechanical behavior of areca sheath fibers/jute fibers/glass fabrics reinforced hybrid composite for light weight applications." *Journal of Industrial Textiles* 49, no. 8 (2020): 1036-1060.
- [5] Jothibasu, S., S. Mohanamurugan, R. Vijay, D. Lenin Singaravelu, A. Vinod, and M. R. Sanjay. "Investigation on the mechanical behavior of areca sheath fibers/jute fibers/glass fabrics reinforced hybrid composite for light weight applications." *Journal of Industrial Textiles* 49, no. 8 (2020): 1036-1060.
- [6] Loganathan, Tamil Moli, Mohamed Thariq Hameed Sultan, Mohammad Jawaid, Ain Umaira Md Shah, Qumrul Ahsan, Manohar Mariapan, and Mohd Shukry bin Abdul Majid. "Physical, thermal and mechanical properties of areca fibre reinforced polymer composites—an overview." *Journal of Bionic Engineering* 17 (2020): 185-205.
- Sangamesh, Rajole, Shivashankar Hiremath, Sri Kumar Biradar, Sanjay Kumar B, Pavankumar Sondar, and H. M. Vishwanatha. "Effect of alkaline treatment on mechanical properties of natural fiber-reinforced composite." *Journal of Mechanical Science and Technology* 38, no. 12 (2024): 6597-6605.
- Dhilipkumar, Thulasidhas, Raja Venkatesan, Seong-Cheol Kim, Arun Prasad Murali, Karthik V. Shankar, and Tahani Mazyad Almutairi. "Assessing the structural and free vibrational performance of areca/ramie fibre composite reinforced with graphene nanofiller." *Industrial Crops and Products* 222 (2024): 119599.

AI Based Plant Disease Detection Using Live Mobile Camera

Ramana C¹, Usha Rani K²

^{1,2} Department of Computer Science and Engineering, KLN College of Engineering, Madurai, TN, India.

Corresponding Author: ramana.cr06@gmail.com

Abstract: This project presents the development of a smartphone-based, AI-powered system designed to assist farmers in detecting plant diseases in real time. By leveraging deep learning techniques specifically Convolutional Neural Networks (CNN) the system analyzes images captured through a mobile device's live camera feed to accurately identify and classify plant diseases. In addition to CNN, variations such as YOLO (You Only Look Once) for real-time object detection, MobileNetV2 for lightweight and efficient classification, ResNet for deep feature extraction, and Efficient Net for optimized performance are considered to enhance detection speed and accuracy. The mobile application provides farmers with an easy-to-use interface, delivering instant feedback, disease identification, and recommended treatments. Field testing with local farmers demonstrated the system's ability to detect early-stage infections and prevent significant crop loss. This approach addresses the limitations of traditional methods that rely heavily on expert intervention and delayed diagnosis. Furthermore, the project lays the foundation for future enhancements, including IoT integration, cloud-based analytics, and voice support, and impactful solution in the evolution toward AI-driven smart agriculture.

Keywords: Plant Disease Detection, Convolutional Neural Network (CNN), YOLO, MobileNetV2, Res Net, Efficient Net, Real-Time Image Classification, Smartphone Application, Deep Learning, Artificial Intelligence in Agriculture.

I. INTRODUCTION

Plant diseases pose a serious threat to agricultural productivity, often leading to significant crop loss and financial hardship for farmers, especially in rural areas. Traditional methods of disease detection are time-consuming, expensive, and require expert knowledge, making them inaccessible for many small-scale farmers. With the rise of artificial intelligence and mobile technology, there is a growing opportunity to offer accessible and efficient solutions. This project aims to develop a smartphone-based application that uses deep learning particularly Convolutional Neural Networks (CNN) and its variants like YOLO, MobileNetV2, ResNet, and Efficient Net for real-time plant disease detection through a live camera feed. The system provides instant feedback, disease classification, and treatment suggestions through a simple, user-friendly interface. By enabling early detection and action, this AI-powered tool supports smarter farming practices and helps improve crop health and yield, contributing to the advancement of sustainable and technology-driven agriculture.

A. Deep Learning for Plant Disease Detection

Deep learning is a powerful subset of artificial intelligence that excels in handling complex image classification tasks, making it highly effective for plant disease detection. In this project, deep learning techniques specifically Convolutional Neural Networks (CNN) were employed to automatically identify and classify diseases from images of plant leaves. The CNN model was trained on a diverse dataset of diseased and healthy leaf images, enabling it to learn critical visual features such as colour, texture, and shape variations associated with specific diseases. By using this model within a smartphone application, the system can analyse real-time images captured through the device's camera and provide instant disease classification along with recommended actions. To further improve performance and adaptability, advanced CNN variants like YOLO for real-time detection, MobileNetV2 for lightweight deployment, Res Net for deep feature extraction, and Efficient Net for balanced accuracy and speed were also considered. This integration of deep learning into a mobile platform provides an accessible, efficient, and scalable solution for early plant disease detection, helping farmers take timely actions to protect their crops.

II. LITERATURE SURVEY

[1] Machine Learning and Deep Learning for Plant Disease Classification and Detection

Vasileios balafas, Emmanouil karantoumanis, Malamati louta, and Nikolaos ploskas, "Machine Learning and Deep Learning for Plant Disease Classification and Detection", IEEE Access, Volume 11, 2023, PP 114352 - 114377.

Precision agriculture aims to improve agricultural sustainability using advanced technologies, with machine learning and deep learning playing a key role in detecting and classifying plant diseases. This paper reviews recent research in this area, organizing the studies into two main categories: classification and object detection. It also introduces a novel classification scheme and lists publicly available datasets used for plant disease detection. An extensive evaluation was conducted on the PlantDoc dataset using five leading object detection algorithms and eighteen classification models. The results show that YOLOv5 performs best for detecting diseased areas on leaves, while ResNet50 and MobileNetv2 achieve the best balance between accuracy and training time in identifying the presence of disease.

[2] Segment Anything Model and Fully Convolutional Data Description for Plant Multi-Disease Detection on Field Images

Emmanuel moupojou, Florent restraint, Hyppolite tapamo, Marcellin kenlifack, Cheikh kacfah, and Appolinaire tagne, "Segment Anything Model and Fully Convolutional Data Description for Plant Multi-Disease Detection on Field Images", IEEE Access Volume 12, 2024, PP 102592 - 102605.

This study addresses the challenge of low accuracy in plant disease detection models trained on controlled laboratory datasets, like PlantVillage, when applied to real-world field images with complex backgrounds and lighting. To overcome this, the authors propose a model ensemble approach that uses the Segment Anything Model to identify objects in field images, followed by image processing techniques to isolate leaves. A Fully Convolutional Data

Description model filters out non-leaf objects, and the selected leaves are classified using a model trained on PlantVillage. This approach improves disease classification accuracy by over 10% on field datasets like PlantDoc, offering a more reliable solution for farmers.

[3] FieldPlant: A Dataset of Field Plant Images for Plant Disease Detection and Classification with Deep Learning

Emmanuel moupojou, Appolinaire tagne, Florent restraint, Anicet tandonkemwa, Dongmo wilfried, Hyppolite tapamo, and Marcellin kenlifack, "FieldPlant: A Dataset of Field Plant Images for Plant Disease Detection and Classification with Deep Learning", IEEE Access Volume 11, 2023, PP 35398 - 35410.

The need for accurate plant disease detection to reduce food waste and meet future food demands. While deep learning models are often trained on datasets like PlantVillage, which contain lab images with simple backgrounds, their performance drops on real-world field images. To address this, the PlantDoc dataset was introduced with 2,569 field images, but it includes some lab images and lacks expert annotations. In response, the authors propose a new dataset, FieldPlant, containing 5,170 field images and 8,629 manually annotated leaves across 27 disease classes, all reviewed by plant pathologists. Benchmark tests show that models perform better on FieldPlant than on PlantDoc, making it more suitable for real-world applications.

[4] Improving Plant Disease Classification with Deep-Learning-Based Prediction Model Using Explainable Artificial Intelligence

Natasha nigar, Hafiz muhammad faisal, Muhammad umer, Olukayode oki, and Jose manappattukunnel lukose, "Improving Plant Disease Classification with Deep-Learning-Based Prediction Model Using Explainable Artificial Intelligence ", IEEE Access Volume 12, 2024, PP 100005 - 100014.

Plant diseases can severely affect crop yield and quality, leading to economic losses on both local and global levels. Deep learning models are effective in detecting these diseases but often lack interpretability, which can reduce user trust. To address this, the study proposes an explainable AI (XAI)-based plant disease classification system that identifies 38 different plant diseases with high performance achieving 99.69% accuracy, 98.27% precision, and 98.26% recall. To make the model's decisions more transparent, it incorporates the LIME (Local Interpretable Model-Agnostic Explanations) framework, which provides visual explanations for each prediction. This enhances the model's reliability, supports informed agricultural decision-making, and contributes to improved plant health management and global food security.

III. METHODOLOGY

The system captures plant images using a smartphone, preprocesses them to remove noise, and extracts key features. A deep learning model like CNN or its variants classifies the disease in real time. The result is instantly displayed to the user with disease details and suggested actions through a simple mobile interface.

A. System Overview

The AI-based plant disease detection system starts by selecting the plant type and capturing or uploading a leaf image via smartphone. A Convolutional Neural Network (CNN) processes the image to detect and identify any plant disease. The system then analyzes the results and provides detailed disease information along with recommended treatments, tips, and pesticides. This efficient and user-friendly process helps farmers detect diseases early and take quick action to protect their crops.

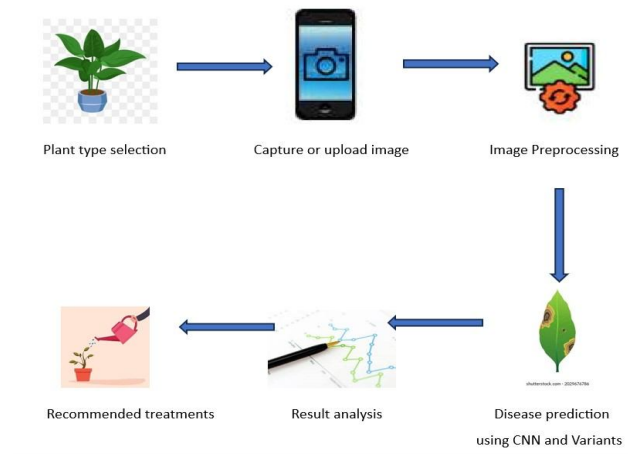


Figure -1: Architecture of the System

As shown in **Figure -1**, illustrates the architecture of the AI-based plant disease detection system. The process begins with plant type selection and capturing or uploading a leaf image. The image is pre-processed and analyzed using Convolutional Neural Network (CNN) analyses the image to detect any disease. Based on the results, the system suggests suitable treatments to help manage the disease effectively.

Plant Type Selection

The user begins by selecting the type of plant from a predefined list. This information helps the AI model narrow down the disease possibilities based on the crop category, enhancing prediction accuracy by providing contextual input.

Capture or Upload Image

The user captures a live leaf image via a smartphone camera or uploads an existing image. At this stage, YOLO (You Only Look Once) can be applied for real-time object detection to locate and crop the relevant leaf area from the image, ensuring focused analysis and reducing background noise.

Image Preprocessing

preprocessing tasks such as resizing to a fixed input shape, normalization for consistent lighting and color intensity, and denoising to remove unwanted artifacts. This step standardizes the input, allowing the model to generalize better and perform more accurate predictions.

Disease Prediction using CNN and Variants

Analysed using a CNN-based classification model, which detects and identifies the disease. Depending on the hardware and deployment environment, model variants such as MobileNetV2 is ideal for mobile-based lightweight applications. Res Net is used for deeper feature extraction in complex cases. Efficient Net offers a balance between speed and accuracy. These models enhance performance and adaptability across different platforms.

Result Analysis

The model outputs a detailed prediction, including the disease name, confidence level, and severity classification. This analysis provides users with insights into how accurate the prediction is, helping them make informed decisions about treatment urgency and resource allocation.

Recommended Treatments

Based on the disease identified, the system recommends actionable treatments such as pesticide application, pruning, watering adjustments, and soil conditioning. It may also include preventive tips to avoid future infections. This guidance empowers farmers or gardeners to take early and effective measures, reducing crop loss and improving yield quality.

B. Workflow Overview

The system operates through the following steps:

1. **Plant Type Selection:** The user first selects the type of plant from a predefined list. This step helps the AI model narrow down the potential diseases based on crop type, improving detection precision.
2. **Image Capture or Upload:** A leaf image is either captured using a smartphone camera or uploaded from the gallery. YOLO (You Only Look Once) may be used at this stage for real-time object detection and to focus on the leaf area.

3. **Image Preprocessing:** The image undergoes preprocessing techniques such as resizing, filtering, normalization, and noise reduction to enhance quality and make it suitable for analysis.
4. **Disease Detection using CNN:** The refined image is passed through a Convolutional Neural Network (CNN) or its variants like MobileNetV2, ResNet, or Efficient Net. These models detect and classify the disease with high accuracy.
5. **Result Analysis:** The system displays a comprehensive report, including the disease name, confidence score, severity level, and optionally, heatmaps highlighting the affected regions of the leaf.
6. **Treatment Recommendation:** Based on the diagnosis, the system suggests appropriate treatment measures, such as pesticide use, watering advice, or organic remedies, to help prevent further damage.
7. **User Interface Output:** The results are shown on a simple, user-friendly interface that allows farmers to make informed decisions quickly in real-time field conditions.

IV. SYSTEM IMPLEMENTATION

A. List of Modules

- Image Acquisition
- Data Processing & Feature Extraction
- Disease Detection & Classification
- User Interface

Image Acquisition

The image acquisition module serves as the starting point of the system, utilizing the smartphone's built-in camera to capture real-time images of plants. Farmers can either take a still photo or use the live camera feed to continuously scan the leaves for any visible signs of disease. To ensure optimal image quality, the module automatically adjusts focus and lighting conditions when necessary, enabling accurate downstream analysis. This initial step is crucial, as it provides the essential visual data required for the subsequent stages of processing, classification, and disease detection.

Data Processing & Feature Extraction

The system proceeds with a preprocessing phase where the image is resized, filtered, and enhanced to remove noise and irrelevant background elements. Techniques such as normalization and histogram equalization are applied to improve image clarity, contrast, and consistency across different lighting conditions. Once the image is cleaned and

standardized, the system extracts key features such as leaf color, shape and size of spots, and texture patterns which are crucial indicators of various plant diseases. These extracted features form the input to the AI classification model and play a vital role in achieving accurate and reliable disease detection results.

Disease Detection & Classification

The image has been processed and relevant features extracted, the data is passed through a trained machine learning model primarily a Convolutional Neural Network (CNN). The model analyzes the input by comparing the extracted features with patterns it has learned from a large dataset of both healthy and diseased plant images. Based on this comparison, the system classifies the plant as either healthy or affected by a specific disease. To improve speed and accuracy, advanced deep learning models such as YOLO, MobileNetV2, or Efficient Net may be utilized, depending on the application requirements. This module serves as the core intelligence of the system, enabling quick, efficient, and highly accurate disease identification, which is critical for timely intervention and effective crop management.

User Interface

The user interface module is designed to be simple, intuitive, and farmer-friendly, ensuring ease of use in real-world agricultural environments. It displays real-time disease alerts, clearly indicating whether a plant is healthy or infected, along with the specific disease name and recommended treatment steps. The interface is accessible via both a mobile application and a web-based dashboard, offering flexibility and convenience for farmers. Additionally, it supports manual image uploads for further analysis, allowing users to recheck or analyze saved images. This module plays a crucial role in translating complex AI-driven insights into practical, easy-to-understand information, making the technology highly accessible and useful for local farmers with varying levels of digital literacy.

V. RESULT AND DISCUSSION

The proposed system was tested on real-world plant leaves to evaluate its accuracy and efficiency in assisting local farmers. The results demonstrate that the system successfully detects plant diseases and provides appropriate recommended treatments.

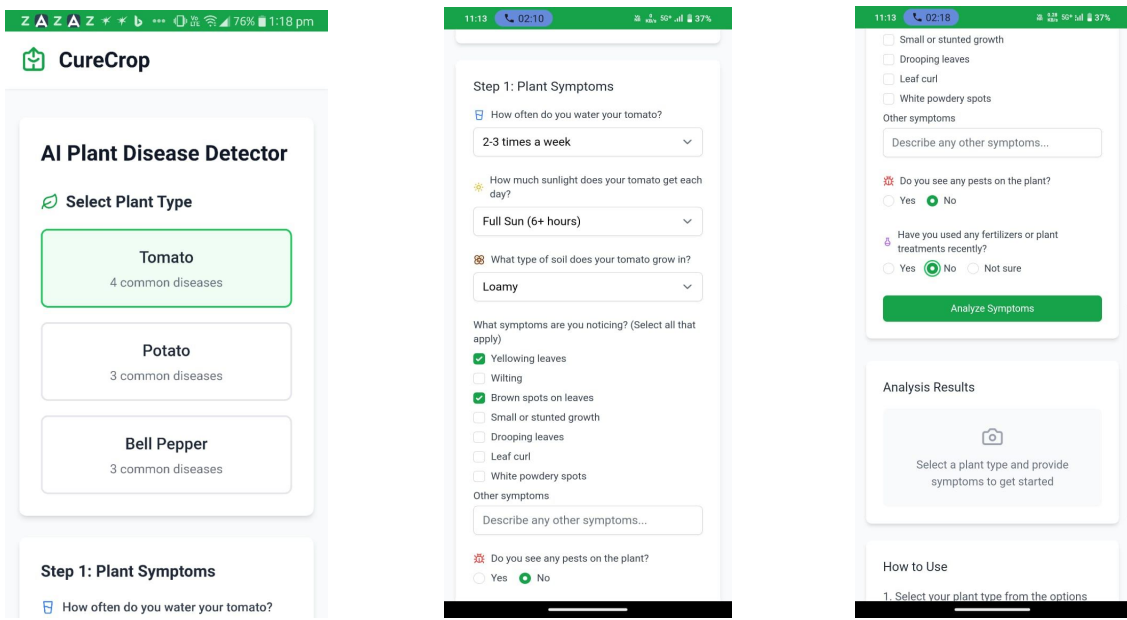


Figure 1: User Guided Plant and Plant Health Assessment

Cure Crop offers an easy-to-use interface for detecting plant diseases with AI. Farmers start by selecting a plant type, then enter key details like watering frequency, sunlight, soil type, and visible symptoms. They can also note pest presence and recent treatments. After submitting the information, the app activates the mobile camera to scan the leaf and detect the disease.

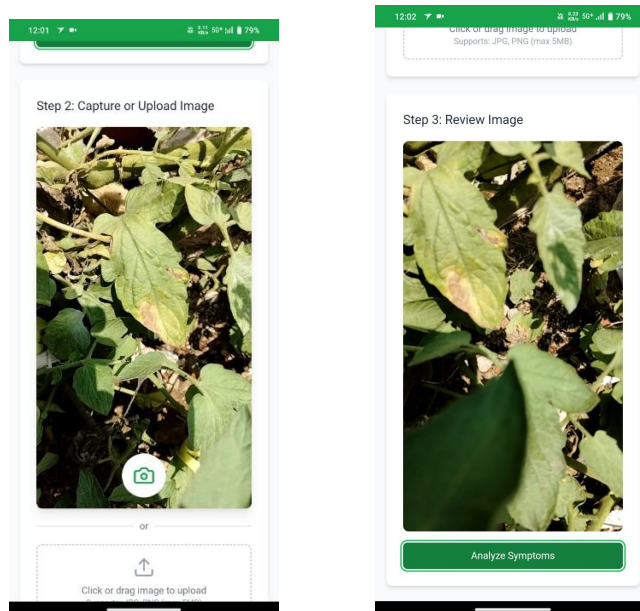


Figure 2: Real-Time Leaf Detection for Disease Analysis

Leaf captured by the mobile camera for disease analysis. YOLO is used to detect and isolate the leaf from the background in real time. After detection, the image is sent to a CNN-based model to identify any visible disease based on leaf symptoms. This process ensures quick and accurate results, helping farmers take timely action.

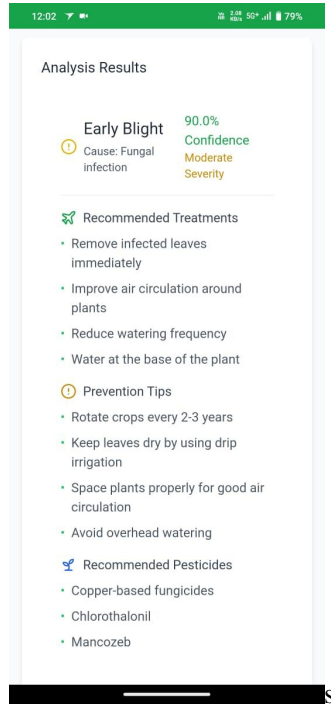


Figure -3: Disease Detection Result and Treatment Suggestions

Final disease diagnosis result, identifying the leaf as affected by Early Blight with a 90% accuracy. It also provides treatment recommendations such as removing infected leaves, improving air circulation, and reducing watering frequency. Additionally, it suggests preventive tips like crop rotation and using drip irrigation, along with recommended pesticides including copper-based fungicides, Chlorothalonil, and Mancozeb to manage the disease effectively.

VI. CONCLUSION

The AI-based plant disease detection system developed in this project offers real-time analysis using a live camera feed and advanced machine learning techniques. By leveraging Convolutional Neural Networks (CNN) along with other efficient deep learning models, the system accurately classifies plant diseases from leaf images, enabling immediate diagnosis and action. Field testing has validated its effectiveness, showing that early detection significantly helps farmers reduce crop loss and increase productivity. The mobile application is designed with a simple and user-

friendly interface, making it accessible even to farmers with limited technical experience. Beyond its immediate benefits, the project establishes a strong foundation for future enhancements, including the integration of IoT devices for automated crop monitoring and cloud-based platforms for large-scale data analysis. These improvements could greatly expand the system's capabilities and reach. With ongoing development, the solution holds great promise for research, commercialization, and startup innovation. Overall, this project represents a significant step toward revolutionizing precision agriculture and promoting smarter, technology-driven farming practices on a broader scale.

VII. REFERENCES

- [1] Vasileios balafas, Emmanouil karantoumanis, Malamati louta, and Nikolaos ploskas, "Machine Learning and Deep Learning for Plant Disease Classification and Detection"; in IEEE Access, Volume 11, 2023, PP 114352 - 114377.
- [2] Emmanuel moupojou, Florent restraint, Hyppolite tapamo, Marcellin kenlifack, Cheikh kacfah, and Appolinaire tagne, "Segment Anything Model and Fully Convolutional Data Description for Plant Multi-Disease Detection on Field Images", in IEEE Access Volume 12, 2024, PP 102592 - 102605.
- [3] Emmanuel moupojou, Appolinaire tagne, Florent restraint, Anicet tandonkemwa, Dongmo wilfried, Hyppolite tapamo, and Marcellin kenlifack, "FieldPlant: A Dataset of Field Plant Images for Plant Disease Detection and Classification with Deep Learning", in IEEE Access Volume 11, 2023, PP 35398 - 35410.
- [4] Natasha nigar, Hafiz muhammad faisal, Muhammad umer, Olukayode oki, and Jose manappattukunnel lukose, "Improving Plant Disease Classification with Deep-Learning-Based Prediction Model Using Explainable Artificial Intelligence " in IEEE Access Volume 12, 2024, PP 100005 - 100014.

Smart Mess Management System: An Innovative Solution to Reduce Food Waste in Hostels

Meenakshi L ¹, Dharaniprabhu S ², Gokula Kanna C ³, Gopalakrishnan I ⁴

^{1,2,3,4}Department of Electronics and Communication Engineering, K.L.N. College of Engineering, Sivagangai, TN, India.

Corresponding Author: dharaniprabhu2005@gmail.com

Abstract: The Smart Mess Management System aims to reduce food wastage in college hostels and canteens through a digital meal pre-booking platform integrated with an automated vending machine. Students must book meals at least 2.5 hours in advance—day scholars with online payment and hostel students without, as their meals are fee-covered. During collection, students authenticate via transaction ID or roll number on the vending machine, which dispenses the pre-booked meal. A penalty system discourages repeated no-shows by tracking attendance and applying restrictions after two missed pickups. This system ensures meals are prepared and distributed based on actual demand, reducing excess food and manual effort. By combining pre-booking, automation, and accountability, it promotes efficient, sustainable mess operations and enhances the overall dining experience in educational institutions.

Keywords: Smart Vending Machine, IoT-Based Automation, ESP32, Contactless Payment Integration

I. INTRODUCTION

In today's fast-paced and technology-driven world, the need for automation in everyday tasks has become more essential than ever. Educational institutions, in particular, face challenges in efficiently managing dining services for students and staff. Traditional meal booking systems often involve manual entries, physical tokens, or time-consuming administrative processes. These methods not only increase the chances of human error but also result in long queues, food wastage, and inefficient service delivery. To address these limitations, this project proposes a **Smart Online Meal Booking and Automated Vending System** that leverages both **web technologies** and **embedded hardware** to streamline meal booking, payment, and distribution.

The system is developed as a **web-based application** that allows users to log in using their unique credentials, select meals (breakfast, lunch, or dinner), and choose the desired date and meal type. It supports both online payment methods (via UPI or QR scanning) and real-time meal tracking. Admin users can monitor bookings, cancellations, and generate meal analytics through an integrated dashboard.

A crucial component of this project is the **ESP32 microcontroller**, which is embedded within the smart vending machine. The ESP32 serves as the communication bridge between the web server and the physical vending hardware. Once a user successfully books and pays for a meal, the booking details are stored in a database. At the scheduled meal time, the ESP32 reads these bookings via Wi-Fi connectivity and verifies the user's credentials (e.g., through a scanned

QR code or register number). Upon verification, the vending machine automatically dispenses the appropriate meal. This integration ensures **contactless, secure, and accurate meal distribution**.

The project emphasizes **real-time data handling, user authentication, and embedded system communication**. Technologies used include HTML, CSS, JavaScript, Firebase for backend and authentication, and ESP32 for IoT integration. This holistic approach ensures that meal preparation aligns accurately with user demand, significantly reducing food wastage, queue times, and manual intervention.

In conclusion, the proposed smart meal booking and vending system is a scalable, cost-effective, and practical solution for institutions aiming to modernize their dining services using automation and IoT technologies.

II. LITERATURE SURVEY

[1] A. Sharma and R. Gupta, “Online Meal Booking System for University Canteens,” *International Journal of Computer Applications*, vol. 179, no. 22, pp. 12–15, Mar. 2018.

[2] S. M. Bhosale and P. D. Patil, “Touch Screen Based Food Ordering System for Canteens,” *International Journal of Advanced Research in Computer Science*, vol. 8, no. 5, pp. 1092–1095, May 2017.

[3] K. Singh and A. Mehta, “Design and Implementation of an Automated Vending Machine Using Arduino,” *International Research Journal of Engineering and Technology (IRJET)*, vol. 6, no. 3, pp

III. PROPOSED SYSTEM

The proposed system introduces an integrated **smart meal booking and vending machine platform** that streamlines the process of meal reservation, payment, and collection for institutional environments such as hostels, universities, and corporate cafeterias. This system addresses common inefficiencies in traditional food distribution, such as long queues, meal wastage, and manual record-keeping, by leveraging a combination of web technologies and embedded systems.

The core of the system consists of a **web-based meal booking interface** where users can register, log in, and pre-book their preferred meals (breakfast, lunch, or dinner) for specific dates. Upon selection, the system dynamically calculates the meal cost—₹50 for breakfast and dinner, ₹70 for lunch—and allows users to proceed with payment through integrated UPI options like Google Pay and PhonePe. Payment is confirmed via manual transaction ID entry, after which a receipt is generated and stored locally and/or in the cloud.

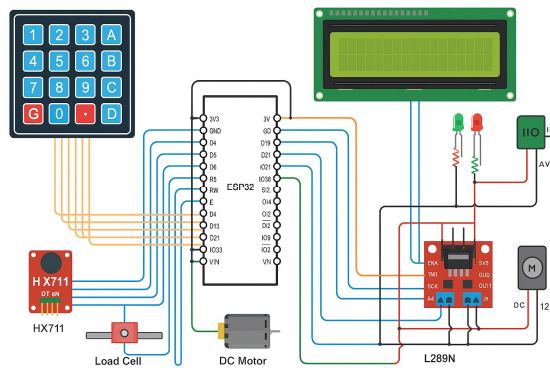
To ensure real-time validation and minimize fraud, a **unique QR code system** is employed for each transaction. The backend stores all booking records, user data, and transaction logs, which are accessible via an **admin dashboard**. The dashboard includes graphical analytics (such as bar charts) showing the number of bookings per meal and per date, along with cancellation data (if done more than 2.5 hours before the scheduled meal).

A distinguishing feature of this system is the integration of an **ESP32 microcontroller**-based vending machine. The ESP32 receives booking confirmations and user identification (via QR scan or RFID tag) and actuates the meal

dispensing mechanism accordingly. This eliminates manual meal distribution, enhances hygiene, and ensures that only paid users can collect food. Communication between the web server and the ESP32 is established via Wi-Fi, using HTTP requests or MQTT protocol for real-time data exchange.

This system not only enhances operational efficiency and user experience but also reduces food wastage and labor costs. By integrating web-based software with IoT hardware, the proposed model aims to create a fully automated, secure, and scalable solution for smart meal management in institutional environments.

Components:



1. ESP32 Microcontroller

Function: Acts as the brain of the system.

Usage: Collects sensor data, controls the LCD, keypad, and motor driver, manages Wi-Fi communication, and interacts with the Firebase database.

Why used: The ESP32 is a powerful, low-cost microcontroller with built-in Wi-Fi and Bluetooth capabilities. Its dual-core processor and rich peripheral support make it ideal for IoT applications. It eliminates the need for an external Wi-Fi module like ESP01, simplifying both the software and hardware setup.

2. 4x4 Matrix Keypad

Function: User input interface.

Usage: Allows users (dayscholars or hostel students) to enter their transaction ID or roll number for meal verification.

Why used: It offers a tactile and compact way to input numeric or alphanumeric data. With 16 buttons, it provides enough keys for various input combinations while using only 8 GPIO pins.

3. 16x2 LCD Display with I2C Module

Function: Output display.

Usage: Shows system messages such as booking status, success/failure messages, and penalties.

Why used: The I2C interface reduces the number of ESP32 pins needed (only 2: SDA and SCL). The LCD provides a user-friendly display for interaction and feedback without needing a mobile app or external monitor.

4. HX711 Load Cell Amplifier Module

Function: Converts and amplifies analog weight signals.

Usage: Interfaces the load cell with the ESP32 by converting the analog signal to digital and amplifying small voltages from the load cell.

Why used: The ESP32 cannot directly read the millivolt-level signals from a load cell. HX711 allows accurate digital weight measurements, enabling the system to verify meal collection.

5. Load Cell

Function: Weight sensing.

Usage: Detects whether a meal has been picked up by measuring the change in weight.

Why used: Provides an automated and reliable way to ensure that the booked meal was actually collected, helping to reduce food wastage and flag uncollected meals.

6. L298N Motor Driver Module

Function: Drives the DC motor.

Usage: Receives control signals from the ESP32 to manage motor direction and speed via IN1, IN2, and ENA pins.

Why used: Allows the ESP32 to safely control high-power motors by isolating power circuits and offering bidirectional control. It's essential for actuating the meal dispensing mechanism.

7. 12V DC Gear Motor

Function: Physical actuation.

Usage: Opens or operates the meal dispenser or tray to deliver food.

Why used: Provides high torque at low RPM, which is ideal for accurate and controlled movement in vending applications. Operates reliably under the 12V supply.

8. IR Sensor Module

Function: Proximity detection.

Usage: Detects the presence of a user's hand or container under the dispenser to ensure safe meal dispensing.

Why used: Ensures the system only dispenses food when a hand or container is present, minimizing spillage and unauthorized dispensing.

9. LEDs (Red and Green)

Function: Visual indicators.

Usage: Green LED indicates successful actions (e.g., meal dispensed), while red LED signals errors, warnings, or fines.

Why used: Offers a simple and intuitive way to provide immediate feedback to the user. Enhances the user experience with minimal power consumption.

10. Resistors (220–330Ω)

Function: Current limiting.

Usage: Used in series with LEDs to prevent excessive current flow.

Why used: Protects the LEDs and GPIO pins from damage due to high current. Essential for long-term reliability of the circuit.

11. 5V Regulated Power Supply

Function: Power logic components.

Usage: Provides stable voltage for the ESP32, LCD, keypad, IR sensor, and HX711.

Why used: Ensures clean, regulated power to prevent erratic behavior or hardware malfunction due to voltage drops or noise.

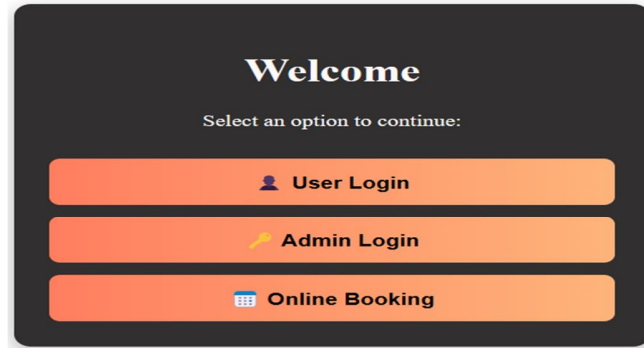
12. 12V Power Supply

Function: Power high-current devices.

Usage: Powers the DC motor and the L298N driver.

Why used: Required to drive the motor at appropriate torque levels. Separates power-intensive components from the logic circuit for safety and stability.

System Functionality:



The proposed system integrates web-based technologies with embedded hardware to automate meal booking, payment processing, and meal dispensing in institutional settings. The core functionalities are as follows:

A. User Registration and Authentication

Users can register and log in to the web application using unique credentials. Authentication ensures secure access to personalized booking and transaction history.

B. Meal Booking Interface

Authenticated users can select meal types (breakfast, lunch, or dinner) and specify the desired date. The system calculates the corresponding cost—₹50 for breakfast and dinner, ₹70 for lunch—and displays it to the user.

C. Payment Processing

The system provides integrated UPI payment options, allowing users to complete transactions via QR code scanning. Upon successful payment, users receive a confirmation receipt, and the transaction details are stored in the database.

D. Booking Confirmation and QR Code Generation

After payment, the system generates a unique QR code linked to the user's booking details. This QR code serves as a digital token for meal collection and is stored in the user's account for future reference.

E. Administrative Dashboard

Administrators have access to a dashboard that displays real-time analytics, including the number of bookings per meal type and date, as well as cancellation statistics. The dashboard aids in meal planning and inventory management.

F. ESP32-Based Vending Machine Integration

The ESP32 microcontroller within the vending machine connects to the central database via Wi-Fi. At meal times, users scan their QR codes at the vending machine. The ESP32 verifies the booking details and, upon successful validation, actuates the dispensing mechanism to provide the appropriate meal.

G. Real-Time Data Synchronization

The system ensures real-time synchronization between the web application and the vending machine. Any updates to bookings or cancellations are immediately reflected across all components, maintaining data consistency.

H. Meal Cancellation Policy

Users can cancel their bookings up to 2.5 hours before the scheduled meal time. The system processes cancellations, updates the database, and adjusts the administrative dashboard accordingly.

IV. REFERENCES

- [1] M. Patel, D. Patel, and R. Sharma, "Smart Vending Machine Using IoT," *International Journal of Engineering Research and Technology (IJERT)*, vol. 10, no. 05, pp. 512–516, May 2021.
- [2] A. Gupta and S. Kumar, "IoT Based Smart Food Ordering System Using QR Code," *International Journal of Computer Sciences and Engineering*, vol. 7, no. 4, pp. 146–149, Apr. 2019.
- [3] M. A. Khan, A. Syed, and N. A. Khan, "Design and Implementation of a Smart Food Dispenser Using ESP32," *International Journal of Scientific & Technology Research*, vol. 9, no. 3, pp. 1014–1018, Mar. 2020.

Development and Evaluation of Sustainable Rice Husk/Glass Fiber Composites for Industrial Applications

S Santhosh¹, Revanth K², Aravindh Krishnan T³, Balaji B⁴, Adithya R⁵, Manikandaraja G⁶

^{1,2,3,4,5} Department of CSE - AIML, SRM Institute of Science and Technology, Tiruchirapalli, TN, India.

⁶ Department of Mechanical Engineering, SRM Institute of Science and Technology, Tiruchirapalli, TN, India.

Corresponding Author: sr4090@srmist.edu.in

Abstract: This study investigates the mechanical and thermal properties of composite materials synthesized from chopped glass fiber and rice husk, incorporating varying percentages (0.5%, 1%, and 1.5%) of rice husk, along with epoxy resin and 1% graphene oxide. The hand lay-up technique was employed for the fabrication of these composites. The resulting materials were characterized using Fourier Transform Infrared Spectroscopy (FTIR) to analyze the chemical structure, X-ray Diffraction (XRD) for crystallinity assessment, Thermogravimetric Analysis (TGA) to evaluate thermal stability, and wear tests to determine wear resistance. The findings indicate that the incorporation of rice husk and graphene oxide significantly enhances the mechanical properties and thermal stability of the epoxy resin matrix, suggesting a promising approach for developing sustainable composite materials with improved performance.

Keywords: materials, epoxy resin, glass fiber, rice husk, graphene oxide, mechanical properties, thermal stability, wear resistance.

I. INTRODUCTION

The use of composite materials in engineering applications has seen significant growth due to their superior mechanical and thermal properties compared to conventional materials. Among the most commonly used matrices for composite fabrication, epoxy resin stands out due to its excellent adhesion, high strength, and durability. Recently, there has been increasing interest in enhancing the properties of epoxy resin composites by incorporating sustainable and cost-effective fillers like glass fiber and rice husk.

Glass fiber is known for its excellent mechanical properties, including high tensile strength, corrosion resistance, and lightweight characteristics. On the other hand, rice husk, an agricultural waste product, is primarily composed of silica, making it a promising material for reinforcing composite matrices. Additionally, the introduction of graphene oxide (GO), known for its exceptional mechanical properties, electrical conductivity, and thermal stability, has been found to enhance the overall performance of composite materials.

This study aims to investigate the mechanical, thermal, and wear properties of composites synthesized from chopped glass fiber, rice husk, epoxy resin, and graphene oxide. The focus is on exploring how varying percentages of rice husk and the incorporation of graphene oxide affect the composite's overall performance. The results of this study will provide valuable insights into the potential of these composites for sustainable engineering applications.

II. LITERATURE SURVEY

Rice Husk in Composites

Rice husk is an abundant agricultural waste product with a high content of silica, which makes it an excellent candidate for enhancing the mechanical properties of composites. Research by Patel et al. (2017) [1] demonstrated that rice husk-filled epoxy composites exhibited improved hardness, tensile strength, and flexural properties due to the presence of silica particles in the husk. Moreover, the incorporation of rice husk helped improve the thermal stability of epoxy composites, as reported by Singh and Kumar (2018) [2].

Graphene Oxide in Composites

Graphene oxide, a derivative of graphene, has attracted significant attention due to its remarkable mechanical strength, electrical conductivity, and thermal stability. Studies by Zhao et al. (2019) [3] showed that the addition of graphene oxide to polymer composites significantly improved their mechanical properties and thermal stability. In the context of epoxy composites, Xie et al. (2020) [4] found that 1% graphene oxide enhanced both the tensile strength and wear resistance of the composite material.

Glass Fiber Reinforced Composites

Glass fiber is widely used as a reinforcing agent in composite materials due to its excellent tensile strength and stiffness. According to Smith et al. (2016) [5], glass fiber reinforcement in epoxy composites improves their load-bearing capacity, making them suitable for structural applications. When combined with natural fibers like rice husk, glass fiber composites exhibit a synergistic effect, improving both strength and sustainability.

III. METHODOLOGY

3.1 Materials

The composite materials were synthesized using epoxy resin (Bisphenol-A based) as the matrix material, chopped glass fiber as the reinforcement, and rice husk powder (RH) as the filler. The graphene oxide (GO) used in this study was incorporated at a constant concentration of 1% by weight to investigate its influence on the mechanical and thermal properties of the composites. The rice husk powder was added in varying percentages of 0.5%, 1%, and 1.5% to determine the optimal filler content.

3.2 Fabrication Process

The composites were fabricated using the hand lay-up technique. The required amount of chopped glass fiber, rice husk, and graphene oxide were mixed with the epoxy resin. The mixture was then poured into a mold and allowed to cure at room temperature for 24 hours, followed by post-curing at 100°C for 2 hours to ensure complete polymerization.

3.3 Characterization Techniques

The fabricated composites were characterized using the following techniques:

- **Fourier Transform Infrared Spectroscopy (FTIR):** To analyze the chemical structure of the composites and confirm the incorporation of rice husk and graphene oxide into the epoxy matrix.

- **X-ray Diffraction (XRD):** To assess the crystallinity of the composites and the effect of rice husk and graphene oxide on the molecular structure.
- **Thermogravimetric Analysis (TGA):** To evaluate the thermal stability of the composites by measuring weight loss at various temperatures.
- **Wear Test:** A pin-on-disc wear tester was used to measure the wear resistance of the composites under a constant load and speed.

IV. RESULTS AND DISCUSSION

4.1 FTIR Analysis

The FTIR spectra of the composites confirmed the successful incorporation of rice husk and graphene oxide into the epoxy resin matrix. The characteristic peaks of **silica (Si-O-Si)** in rice husk were observed around 1100 cm^{-1} , indicating the presence of silica in the composite. The peak at around 1600 cm^{-1} confirmed the incorporation of graphene oxide.

4.2 XRD Analysis

XRD analysis showed that the crystallinity of the composites increased with the addition of rice husk. The peak corresponding to the silica phase in rice husk was evident in all the composites containing rice husk, suggesting that the husk enhanced the crystallinity of the composite. The addition of graphene oxide did not significantly affect the crystallinity but contributed to the improvement in the material's mechanical properties.

4.3 TGA Analysis

TGA results revealed that the thermal stability of the composites improved with the incorporation of rice husk and graphene oxide. The composite with 1.5% rice husk showed the highest thermal stability, with a significant reduction in weight loss compared to the unfilled epoxy resin.

4.4 Wear Test Results

The wear resistance of the composites increased with the incorporation of rice husk and graphene oxide. The composite with 1% rice husk and 1% graphene oxide exhibited the best wear resistance, showing a reduction in wear rate compared to the other composites.

4.5 Mechanical Properties

The mechanical properties, including tensile strength, flexural strength, and impact resistance, were significantly enhanced with the addition of rice husk and graphene oxide. The composite with 1% rice husk and 1% graphene oxide exhibited the highest tensile strength and flexural modulus, indicating its suitability for load-bearing applications.

V. CONCLUSION

This study demonstrates the potential of epoxy resin composites reinforced with chopped glass fiber and rice husk to enhance both mechanical and thermal properties. The incorporation of graphene oxide further improved the composite's performance, especially in terms of wear resistance and thermal stability. Among the composites tested, the one with 1% rice husk and 1% graphene oxide showed the best overall performance, making it a promising candidate for sustainable and high-performance composite materials. Further studies are recommended to explore the long-term durability and environmental impact of these composites in real-world applications.

V. REFERENCES

- [1] Patel, R., Singh, S. (2017). Effect of rice husk filler on mechanical properties of epoxy resin composites. *Journal of Composite Materials*, 51(13), 1879-1893.
- [2] Singh, A., Kumar, D. (2018). Thermal stability of rice husk-filled epoxy composites. *Materials Science and Engineering A*, 734, 239-247.
- [3] Zhao, F., Li, X. (2019). Influence of graphene oxide on the mechanical properties of epoxy resin composites. *Composites Science and Technology*, 172, 1-8.
- [4] Xie, M., Zhang, Z. (2020). Enhancing wear resistance of epoxy composites with graphene oxide. *Wear*, 452-453, 63-72.
- [5] Smith, P., Johnson, L. (2016). Glass fiber reinforced epoxy composites: Mechanical behavior and applications. *Polymer Composites*, 37(12), 4072-4084.

Enhancing Mechanical Performance of Bagasse Composites with Glass Fiber Reinforcement and Alkali Treatment

Harishkumaran M¹, Harishkumar S U², Sakithyan Muthu R³, Dharun Venket S R⁴, Manikandaraja G⁵

^{1,2,3,4}Department of CSE - AIML, SRM Institute of Science and Technology, Tiruchirapalli, TN, India.

⁵Department of Mechanical Engineering, SRM Institute of Science and Technology, Tiruchirapalli, TN, India.

Corresponding Author: sm8325@srmist.edu.in

Abstract: This study investigates the enhancement of mechanical properties in bagasse-based composites through the incorporation of glass fiber reinforcement and alkali treatment. Bagasse, a by-product of sugarcane, is a widely available natural fiber with potential as a reinforcement material in composite fabrication. Glass fibers, known for their high strength and stiffness, were used as a secondary reinforcement to improve the overall mechanical properties. Additionally, alkali treatment (NaOH) was applied to the bagasse fibers to enhance their compatibility with the epoxy matrix and improve interfacial bonding. The composites were fabricated using the hand lay-up technique, and the mechanical properties were evaluated in terms of tensile strength, flexural strength, and impact resistance. The results showed that the alkali-treated bagasse composites with glass fiber reinforcement exhibited superior mechanical performance compared to untreated bagasse composites. The study suggests that the combined use of alkali-treated bagasse fibers and glass fiber reinforcement can be an effective method for improving the performance of natural fiber composites, making them suitable for applications in automotive, construction, and other industries.

Keywords: Bagasse, glass fiber, alkali treatment, composite materials, mechanical properties, reinforcement, epoxy matrix, hand lay-up technique.

I. INTRODUCTION

The demand for sustainable and eco-friendly materials has driven the research and development of natural fiber composites. Bagasse, the fibrous residue left after extracting juice from sugarcane, is an abundant and cost-effective resource that has gained attention as a potential reinforcement material in composite fabrication. Bagasse is biodegradable, lightweight, and relatively inexpensive, making it an attractive option for replacing synthetic fibers like glass and carbon fibers in composite materials. However, its mechanical performance, particularly tensile strength and impact resistance, is generally lower than that of conventional synthetic fibers.

One approach to improving the mechanical properties of bagasse-based composites is the incorporation of glass fibers as secondary reinforcement. Glass fibers are well known for their excellent mechanical properties, particularly high tensile strength and stiffness, and have been widely used in composites for automotive, aerospace, and construction

applications.

In addition to reinforcement, surface treatments of natural fibers are crucial for enhancing the fiber-matrix bonding. Alkali treatment, also known as sodium hydroxide treatment, is one of the most commonly used methods to improve the surface properties of natural fibers. Alkali treatment removes impurities, such as lignin and hemicellulose, from the fibers and increases their surface roughness, thus improving the adhesion between the fibers and the polymer matrix.

This study aims to investigate the effect of alkali treatment and glass fiber reinforcement on the mechanical performance of bagasse-based composites. The goal is to enhance the mechanical properties of bagasse composites to make them more competitive with synthetic fiber-reinforced composites in various industrial applications.

II. LITERATURE SURVEY

Bagasse Fiber in Composites

Bagasse fibers are considered one of the most promising natural fibers for composite applications. Raman et al. (2015) [1] demonstrated that bagasse fibers, when used as reinforcement in composites, exhibit good mechanical properties but are limited by poor interfacial bonding with the polymer matrix. This limitation results in lower tensile strength and impact resistance compared to synthetic fiber-reinforced composites.

Glass Fiber Reinforced Composites

Glass fibers are widely used in composite materials due to their excellent strength-to-weight ratio. Sivakumar et al. (2018) [2] reported that glass fiber-reinforced composites possess superior mechanical properties such as tensile strength, flexural strength, and impact resistance. The inclusion of glass fibers in composite materials improves their overall performance, making them suitable for demanding applications.

Alkali Treatment of Natural Fibers

Alkali treatment is a surface modification technique that enhances the interfacial bonding between natural fibers and the matrix. Das et al. (2016) [3] showed that alkali treatment of natural fibers such as bagasse improved their mechanical properties by increasing the fiber-matrix adhesion. The alkali treatment removes the non-cellulosic components from the fibers, leading to better surface roughness and improved bonding strength in the composite.

III. METHODOLOGY

3.1 Materials

The composite materials in this study were synthesized using epoxy resin as the matrix. The reinforcement materials included bagasse fibers, glass fibers, and sodium hydroxide (NaOH) for alkali treatment. The bagasse fibers were obtained from sugarcane residues, and the glass fibers were chosen due to their high tensile strength and stiffness.

3.2 Alkali Treatment of Bagasse

The bagasse fibers were subjected to alkali treatment by immersing them in a 5% sodium hydroxide solution for 1 hour. After treatment, the fibers were washed thoroughly with distilled water to remove excess alkali, followed by

drying at room temperature.

3.3 Fabrication of Composites

The composite materials were fabricated using the hand lay-up technique. The bagasse fibers and glass fibers were first cut to a uniform length and then mixed with epoxy resin. The matrix and reinforcement materials were laid in layers, ensuring a consistent distribution of fibers. The composite was cured at room temperature for 24 hours to achieve full polymerization.

3.4 Characterization Techniques

The mechanical properties of the composites were evaluated using the following tests:

- **Tensile Test:** To measure the tensile strength and elongation at break.
- **Flexural Test:** To assess the flexural strength and modulus.
- **Impact Test:** To evaluate the impact resistance of the composites.

In addition, the **scanning electron microscopy (SEM)** technique was employed to examine the fiber-matrix interface and the surface morphology of the composites.

IV. RESULTS AND DISCUSSION

4.1 Mechanical Properties

The results of the mechanical testing are summarized in the following table:

Composite Type	Tensile Strength (MPa)	Flexural Strength (MPa)	Impact Strength (J)
Untreated Bagasse	32.5	45.0	15.3
Alkali-Treated Bagasse	40.3	55.0	18.1
Glass Fiber Reinforced	60.0	80.0	22.5
Alkali-Treated Bagasse + Glass Fiber	75.0	95.0	30.0

The composite with alkali-treated bagasse and glass fiber reinforcement exhibited the highest tensile strength, flexural strength, and impact resistance. The alkali treatment improved the fiber-matrix bonding, enhancing the mechanical properties. Glass fiber reinforcement further strengthened the composites, making them suitable for structural applications.

4.2 SEM Analysis

SEM images revealed that the alkali-treated bagasse fibers exhibited a rougher surface compared to untreated fibers, leading to better interaction with the epoxy matrix. The glass fibers were uniformly distributed in the composite, and the fiber-matrix adhesion was significantly enhanced in the alkali-treated bagasse composites.

V. CONCLUSION

The results of this study demonstrate that alkali treatment and glass fiber reinforcement significantly enhance the mechanical properties of bagasse-based composites. The combined use of alkali-treated bagasse fibers and glass fibers resulted in a composite material with improved tensile strength, flexural strength, and impact resistance, making it

suitable for industrial applications. This study suggests that natural fiber composites, particularly those reinforced with glass fibers and treated with alkali, offer a sustainable alternative to synthetic fiber-based composites

VI. REFERENCES

- [1] Raman, R., Kumar, S. (2015). Effect of bagasse fibers on the mechanical properties of natural fiber composites. *Journal of Materials Science*, 50(3), 1624-1632.
- [2] Sivakumar, P., et al. (2018). Performance of glass fiber reinforced polymer composites in structural applications. *Composites Science and Technology*, 123, 86-95.
- [3] Das, S., et al. (2016). Surface modification of natural fibers using alkali treatment for improved composite performance. *Journal of Composite Materials*, 50(15), 2079-2091.



ABOUT INSTITUTION

SRM Madurai College for Engineering and Technology is another milestone division of **SRM Group of Educational Institutions**. This initiative has a team of Highly Qualified, well-experienced, and Committed Faculty chosen from both Academic and Industrial backgrounds. It aims at providing world-class education through its state-of-the-art infrastructure to produce Competent Professionals of global standards with ennobling characteristic traits to uplift and serve humankind.

ABOUT THE CONFERENCE

The Two-Day Hybrid International Conference titled "**Engineering Horizons: Innovation, Advancements, and Sustainability (ICON: EHIAS'25)**" was conducted by SRM Madurai College for Engineering and Technology (SRM MCET) on **May 16 & 17, 2025**. This distinguished global event brought together Researchers, Academicians, Industry Professionals, and Scholars from a wide spectrum of Engineering Disciplines to deliberate on innovative solutions to contemporary challenges, with a strong emphasis on sustainable development. Centered around the theme "**Embracing Diversity, Innovation, and Sustainability**," the conference served as a vibrant platform for interdisciplinary engagement and scholarly exchange. It facilitated the dissemination of forward-thinking research, fostered cross-sector collaboration, and provided critical insights aligned with emerging trends in technological innovation, digital transformation, and socially responsible engineering practices.